Key Engineering Materials
ISSN: 1662-9795, Vol. 1062, pp 81-132
doi:10.4028/p-O5VgC0
© 2026 Trans Tech Publications Ltd, All Rights Reserved
Submitted: 2025-11-06
Revised: 2026-04-02
Accepted: 2026-04-17
Online: 2026-08-14

From the Maxwell's Equations of Lattice Deformations to the Description of the Universe by a «Crystalline Ether»

Gérard Gremaud

EPFL, IPHYS, Station 3, CH-1015 Lausanne, Switzerland

gerard.gremaud@epfl.ch

Keywords: Crystalline Ether; Maxwell's equations; Special and General relativity; Quantum Physics; Cosmology; Standard Model; Theory of Everything

Abstract. Using Eulerian coordinates to describe solid lattice deformations, it has been shown that the set of equations known as *Maxwell's equations* — typically applied to electromagnetic phenomena in vacuum or matter — can also describe the elastic, anelastic, and plastic deformations of isotropic solid lattices containing topological defects such as dislocations and disclinations, under conditions of constant and homogeneous expansion. The analogy between the two physical systems is complete: it extends beyond one of the two Maxwell equation pairs in vacuum to both pairs, and includes analogues to dielectric polarization, magnetization, electric charges, and currents.
In the Eulerian approach, Maxwell's equations emerge as a special case derived from a tensor theory of lattice deformation, reducible to a vector formulation only for constant and homogeneous expansion. When dynamic and non-homogeneous expansions are considered, the tensor nature of the theory becomes essential. This generalization naturally leads to a new conceptual framework for the Universe based on the existence of a *crystalline ether*. This framework offers a simple, unified, and coherent description of all major theories of modern physics, including electromagnetism, relativity, gravitation, quantum physics, cosmology, and the Standard Model of particle physics.

The Quest for a Theory of Everything

Modern physics is built on mathematical formalisms designed to reproduce experimental observations, but these formalisms are often postulated rather than derived from transparent first principles. Maxwell's equations, for example, accurately describe electromagnetism without providing a clear physical picture of what electric and magnetic fields *are*, what electric charge fundamentally represents, or how electromagnetic waves propagate through a vacuum.

Similarly, special relativity rests on Lorentz transformations, yet offers no mechanistic explanation for why time dilates and lengths contract, or with respect to which "absolute" frame such effects occur. General relativity relates the curvature of space-time to mass-energy via Einstein's celebrated field equation, but without clarifying why matter curves space-time or what space-time itself physically constitutes. Quantum mechanics is formulated around Schrödinger's equation, but the nature of the wavefunction, the origin of quantum probabilities, and the boundary between classical and quantum regimes (quantum decoherence) remain open questions.

In cosmology, general relativity is extended with additional hypotheses such as *dark matter* and *dark energy*, terms which denote unexplained phenomena inserted to reconcile theory with observation. Likewise, the Standard Model of particle physics accurately catalogs elementary particles and their interactions, but offers no intrinsic explanation for the real nature of the particles, the existence of three particle families, the values of their masses and charges, the origin of spin, or the deep nature of the weak and strong forces.

These theories, despite their empirical success, have no common derivation from a unified foundation. The search for a *Theory of Everything* — a framework capable of explaining the nature of space-time, matter, and their interactions — remains one of the central challenges of modern physics.

Historically, physicists have pursued various unification strategies:
- *Grand Unified Theories (GUTs)* merge the electromagnetic, weak, and strong forces [1],
- *Quantum Gravity* and *Loop Quantum Gravity* aim to quantize gravity [2],
- *Supersymmetry* extends space-time symmetries to connect bosons and fermions [3],
- *String and Superstring Theories* replace point particles with one-dimensional strings whose vibrational modes correspond to different particles [4],
- *M-Theory* attempts to unify five versions of string theory, requiring additional spatial dimensions for mathematical consistency [5].

Yet none of these approaches simultaneously and coherently explains electromagnetism, relativity, gravitation, quantum physics, and the structure of elementary particles. Even the much-discussed eleven-dimensional M-Theory lacks predictive power for measurable quantities such as particle masses. Experimental searches for new particles, including dark matter candidates, have so far yielded no decisive results.

Since the 1980s, progress toward unification appears to have stagnated. Thousands of theoretical papers — often emphasizing increasingly abstract mathematical structures — have failed to resolve the core mysteries of physics. This pursuit of "mathematical beauty" has at times drifted away from physical reality, consuming vast resources in the construction of ever more complex experiments while delivering little new insight. Prominent voices, including Unzicker and Jones [6], Smolin [7], Woit [8], and Hossenfelder [9], have raised strong critiques of this trend.

The Crystalline Ether

In contrast, the approach of a *Theory of Everything* developed in this work takes a radically different path. Rather than assembling an intricate hybrid of existing theories, it begins from the simplest classical principles — Newton's equation of motion, the first and second laws of thermodynamics — and applies them within an original geometric framework based on Euler coordinates. The result is a model of the Universe as a finite, massive, elastic solid lattice — a *cosmological lattice* or *crystalline ether* — embedded in an infinite, absolute vacuum, and in which matter consists of topological singularities (dislocations, disclinations, dispirations) [10,11].

The description of solid lattice deformations using Maxwell's equations in an Eulerian framework [12,13] — for the case of constant and homogeneous expansion [14,15] — is striking for a simple reason: it begins with the assumption that the lattice obeys a purely Newtonian dynamic law in the absolute reference frame of an external observer, equipped with orthonormal rulers and a universal clock. Yet, the topological singularities within the lattice — dislocations and disclinations with their associated charges — follow relativistic dynamics inside the lattice, as dictated by the Maxwellian equations governing shear forces in the medium. From this viewpoint, the relativistic dynamics of these singularities emerge directly from the classical Newtonian dynamics of the elastic lattice in the observer's frame.

The analogy between the eulerian theory of deformable lattices and classical electromagnetism is sufficiently precise and far-reaching to merit detailed investigation. Beyond its mathematical elegance, it suggests an underlying structural correspondence between the mechanical properties of a lattice and the field properties of space. By introducing specific elastic properties — volume expansion, shear, and rotation — expressed as free energy per unit volume, one can construct a hypothetical lattice obeying a modified Newton's equation. This equation includes an additional force term directly linked to the energy-impulsion of the singularities (dislocation and disclination loops) within the lattice. Remarkably, such a model provides a coherent basis for a new interpretation of the Universe [16-18], conceptualized as a *crystalline ether*.

In this framework, the Universe behaves as a finite, massive, and elastic three-dimensional lattice embedded in an absolute vacuum, with topological singularities corresponding to matter. This approach, developed and expanded in recent works [10,11], yields natural analogues for the key phenomena described by electromagnetism, special and general relativity, gravitation, quantum physics, cosmology, and the Standard Model. It also offers physical interpretations for phenomena currently treated as axiomatic, such as the invariance of the speed of light, gravitational interaction, quantum decoherence, and the emergence of particle properties.

Storytelling of the theory

The question *"What if the Universe were a crystal?"* emerged gradually over forty years ago, while I was preparing a course for fourth-year physics students. At that time — holding a degree in physics-engineering and a doctorate in physics — I was conducting research on dislocation dynamics at the Swiss Federal Institute of Technology in Lausanne (EPFL). My experimental work focused on mechanical spectroscopy and ultrasonic attenuation, but my academic duties also included teaching.

One of the courses I taught, *Physics of Dislocations*, was closely tied to my research. Dislocations — defects in the arrangement of atoms in crystalline solids — play a central role in determining macroscopic deformation properties. Their motion explains much of the elasticity, anelasticity, and plasticity of crystalline materials. Over years of teaching and refining the course, I began noticing intriguing analogies between the theory of dislocations and other branches of physics.

The first analogy to emerge was with Maxwell's theory of electromagnetism. Initially, the resemblance seemed surprising and perhaps superficial. Yet, as the years passed, the analogy grew more precise: it was not confined to one of Maxwell's two equation pairs in a vacuum but extended to both, including phenomena such as dielectric polarization, magnetization, electric charge, and electric current.

Drawing inspiration from the literature, I demonstrated that it is possible to compute the rest energy E_0 of dislocations, corresponding to the elastic deformation energy stored in the lattice, as well as their kinetic energy E_{def}, associated with the motion of lattice particles mobilized during dislocation movement. From these results, one can define a *virtual inertial mass* M_0 that satisfies relations strikingly similar to Einstein's famous equation $E_0 = M_0 c^2$, yet obtained here through purely classical means, without invoking a principle of relativity. Furthermore, at high velocities, dislocation dynamics conform to the principles of special relativity and Lorentz transformations.

This led to a paradoxical conclusion: the relativistic behavior of dislocations is not fundamental but emerges as a consequence of the purely Newtonian dynamics of the elastic lattice in the laboratory frame. This realization deepened the analogy between solid-state deformation theory and the theories of electromagnetism and relativity.

These analogies — unexpected and yet remarkably consistent — prompted me to explore them systematically. Over the following decades, I developed two complementary lines of theoretical work. The first, published in *Eulerian Theory of Newtonian Deformable Lattices* [12,13], reformulates the mechanics of deformable solids using Euler coordinates rather than the traditional Lagrangian approach. The second, expanded in *The Theory of the Crystalline Ether* [10], proposes a radically different picture of the Universe: a finite, elastic, massive lattice embedded in an absolute vacuum, whose topological singularities correspond to matter.

Yet, despite the simplicity of its principles, the full development is mathematically demanding. The formalism involves advanced tensor and vector calculus, making it more accessible to physicists familiar with solid-state physics. To reach a broader audience, I later wrote a more accessible exposition, *The Crystalline Ether* [11], presenting the essential ideas with minimal mathematics while retaining the logical structure.

The formulation of the deformation of a solid lattice in Euler coordinates

The mechanical behavior of deformable solids is most commonly described using *Lagrangian coordinates*, where material points are tracked from their initial positions through deformation. In this framework, various differential geometries are employed to model the topological defects — such as dislocations and disclinations — that occur within the material.

However, the Lagrangian description presents intrinsic limitations. From a mathematical standpoint, the tensors describing the deformation of a continuous solid in Lagrangian coordinates are of higher order in the spatial derivatives of the displacement field, leading to cumbersome formalisms when large distortions (both deformations and rotations) are present. Physically, the Lagrangian system becomes impractical when describing the time evolution of a lattice's microscopic structure (e.g., during phase transitions) or when incorporating structural defects (point defects, dislocations, disclinations, grain boundaries) and additional physical properties (thermal, electrical, magnetic, or chemical fields).

The application of *differential geometry* to solid defects began with Nye (1953) [19], who established the relationship between the dislocation density tensor and lattice curvature. Independently, Kondo (1952) [20] and Bilby (1954) [21] demonstrated that dislocations can be interpreted as crystalline analogues of Cartan's (1922) [22] continuum torsion. This approach was formalized in detail by Kröner (1960) [23]. While geometrically elegant, such methods inherit the complexity of the general relativity formalism, making the resulting field equations difficult to manipulate and interpret. Additional complications arise when introducing defect types beyond dislocations. For example, Kröner (1980) [24] proposed that extrinsic point defects could be associated with matter in the Universe, requiring the introduction of Einstein's equations in a purely Riemannian geometry, while intrinsic point defects might require non-metric affine connections. Disclinations, in turn, may require still more elaborate geometries, such as those of Finsler or Kawaguchi.

The net effect is that both the Lagrangian coordinate system and differential geometric treatments often require a heavy "mathematical artillery" (metric tensors, Christoffel symbols, and local infinitesimal reference frames), as seen, for example, in Zorawski's theory of dislocations (1967) [25].

Motivated by these challenges, I sought a simpler yet equally rigorous formulation of deformable solids, by using an Eulerian coordinate system (Fig. 1). This led to the *Eulerian theory of Newtonian deformable lattices* [12,13], originally published in French (2013) and then in English (2016).

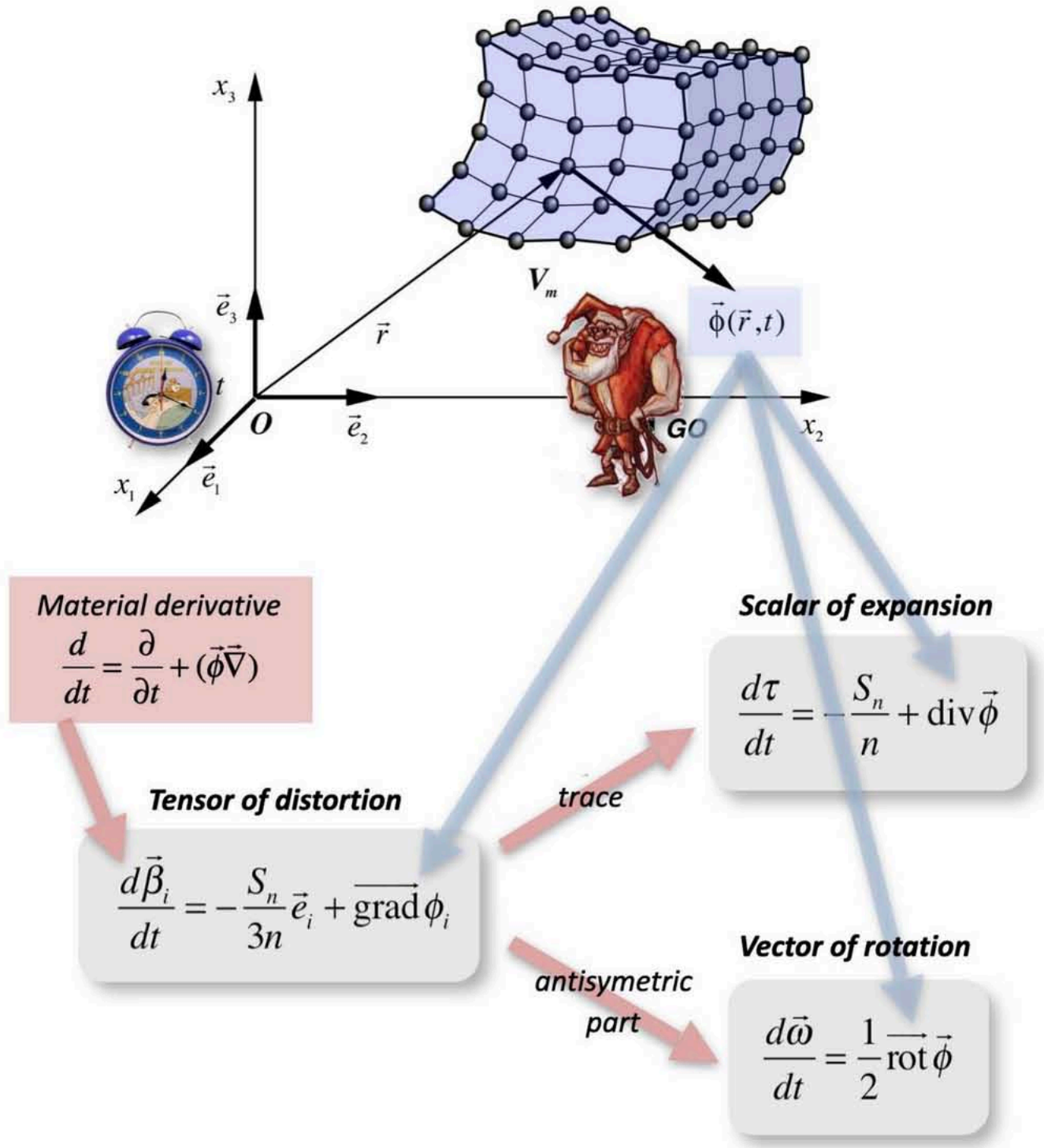


Fig. 1. Euler's coordinates and the geometro-kinetic equations

In this framework of eulerian coordinates, lattice deformation is characterized by two primary classes of geometric changes (Fig. 2): *the distortions*, changes involving deformation and rotation, and *the contortions*, changes involving bending and torsion.

The Eulerian approach employs a *vector representation of tensors*, offering significant advantages over a purely tensor description. Vector analysis provides a powerful and compact formalism for deriving *the geometro-kinetic equations* in Fig. 1, which govern the kinetics of deformation, and *the geometro-compatibility equations* in Fig. 2, which ensure the structural integrity of the lattice.

Once this topological description is established, the physics — *Newtonian dynamics* and *Eulerian thermokinetics* — is introduced. With these ingredients, one can write the complete set of evolution equations for a lattice in Euler coordinates, capturing elastic, anelastic, plastic, and self-diffusion behaviors.

This formulation enables the derivation of state functions and equations of state for isotropic solids, the analysis of elastic and thermal responses, the study of wave propagation and thermoelastic relaxation phenomena, the modeling of mass transport and inertial relaxations, and the prediction of anelastic and plastic responses. It also describes the structural transitions of both second and first order in solid lattices.

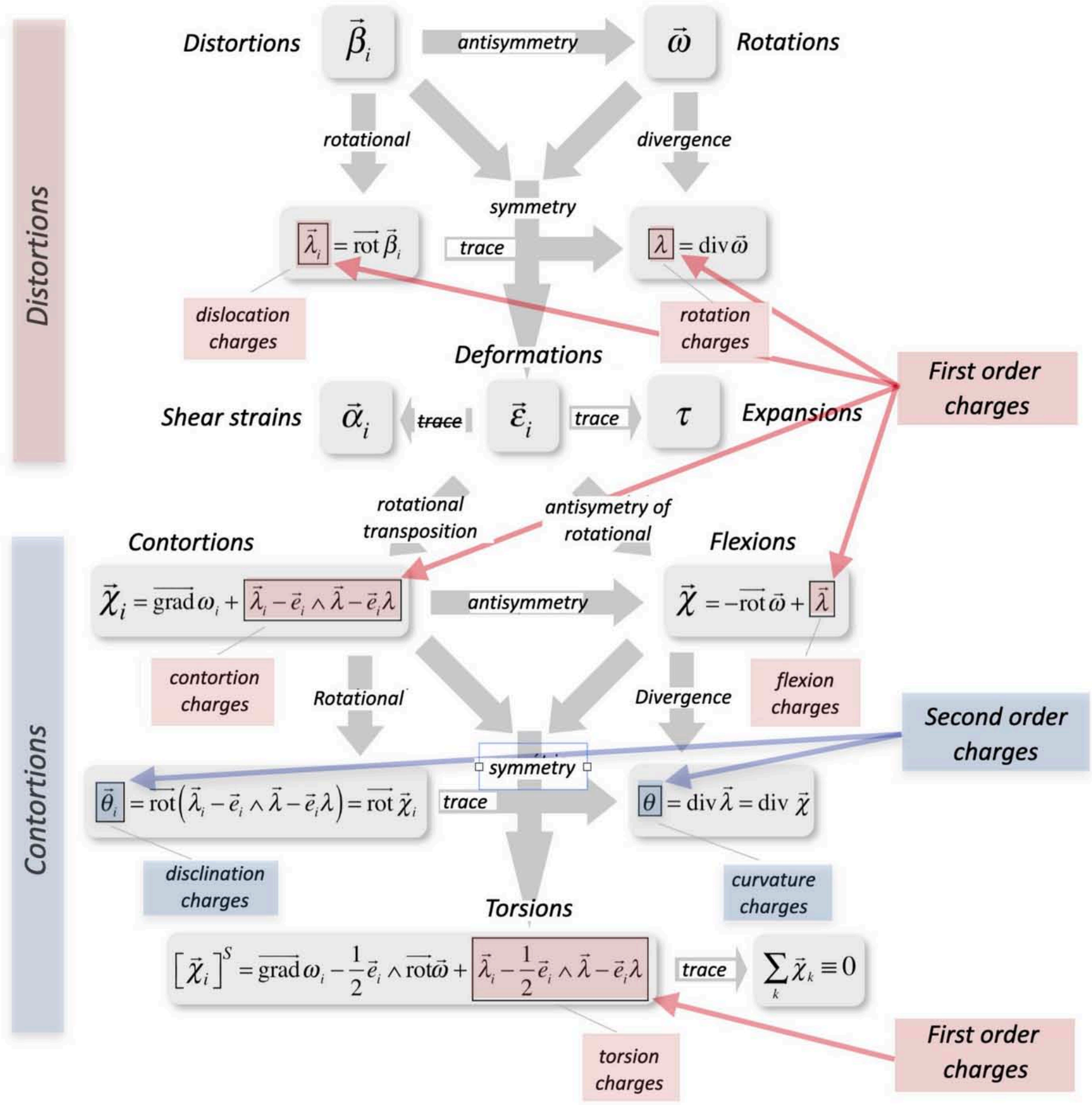


Fig. 2. The system of distortions and contortions in the presence of plastic charges and the geometro-compatibility equations

The concepts of dislocation and disclination charges in lattices

The study of *topological singularities* — defects such as dislocations (Fig. 3 and Fig. 4) and disclinations (Fig. 5 and Fig. 6) — has been a central theme in solid-state physics for over a century as well explained by the Brief History of Dislocation Theory of Hirth [26].

The conceptual foundation was laid by Volterra (1907) [27], who introduced the idea of *macroscopic defects* in elastic bodies. The modern theory of lattice dislocations began in 1934 with the independent works of Orowan [28], Polanyi [29], and Taylor [30], who described the *edge dislocation*. Burgers (1939) [31] extended the theory to *screw* and *mixed* dislocations. And by 1956, the first direct observations of dislocations, using transmission electron microscopy, were reported by Hirsch, Horne, and Whelan [32], and by Bollmann [33]. Disclinations were first observed by Lehmann (1904) [34] in molecular crystals, and later described physically by Friedel (1922) [35].

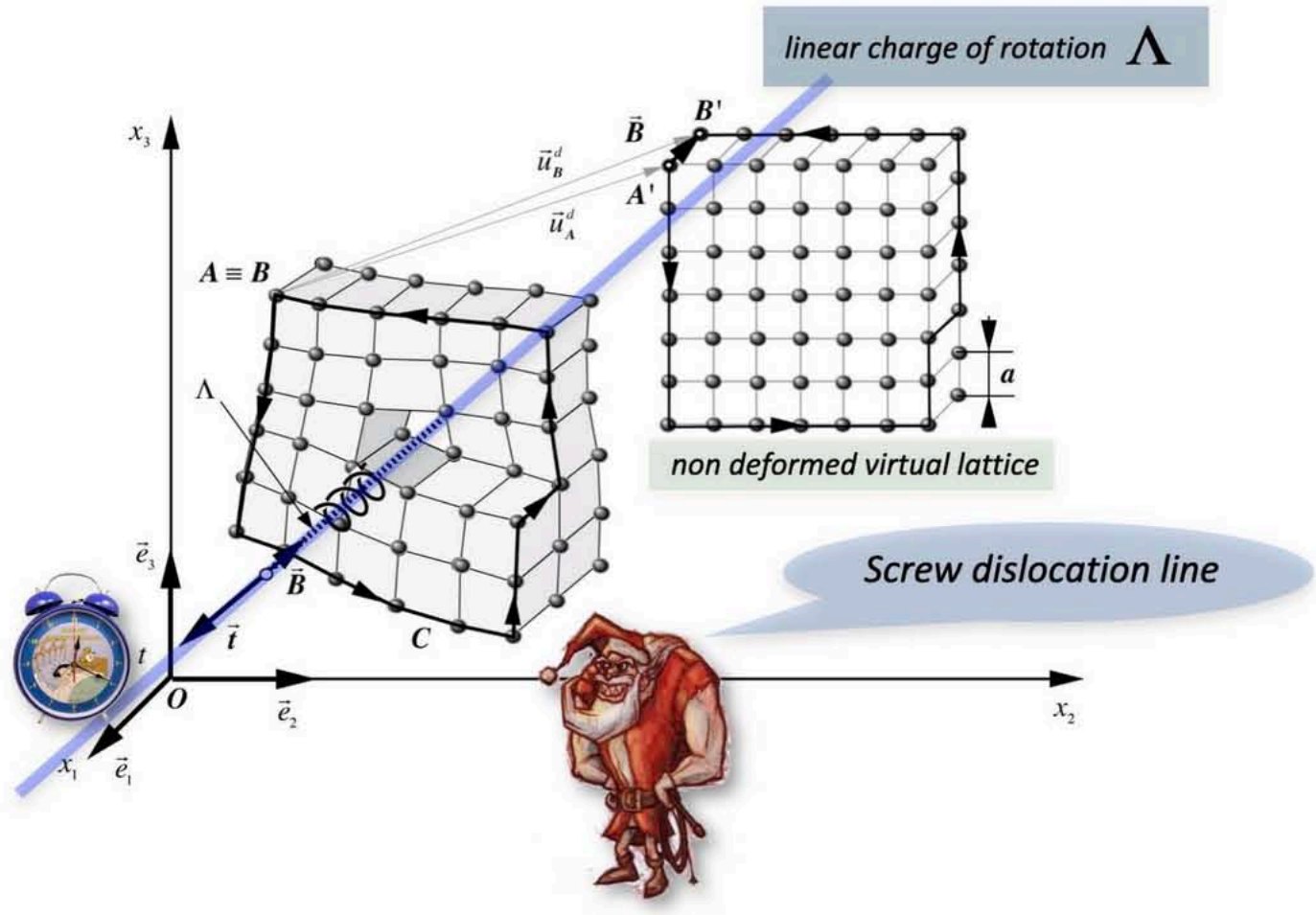


Fig. 3. Screw dislocation line quantified in a cubic lattice

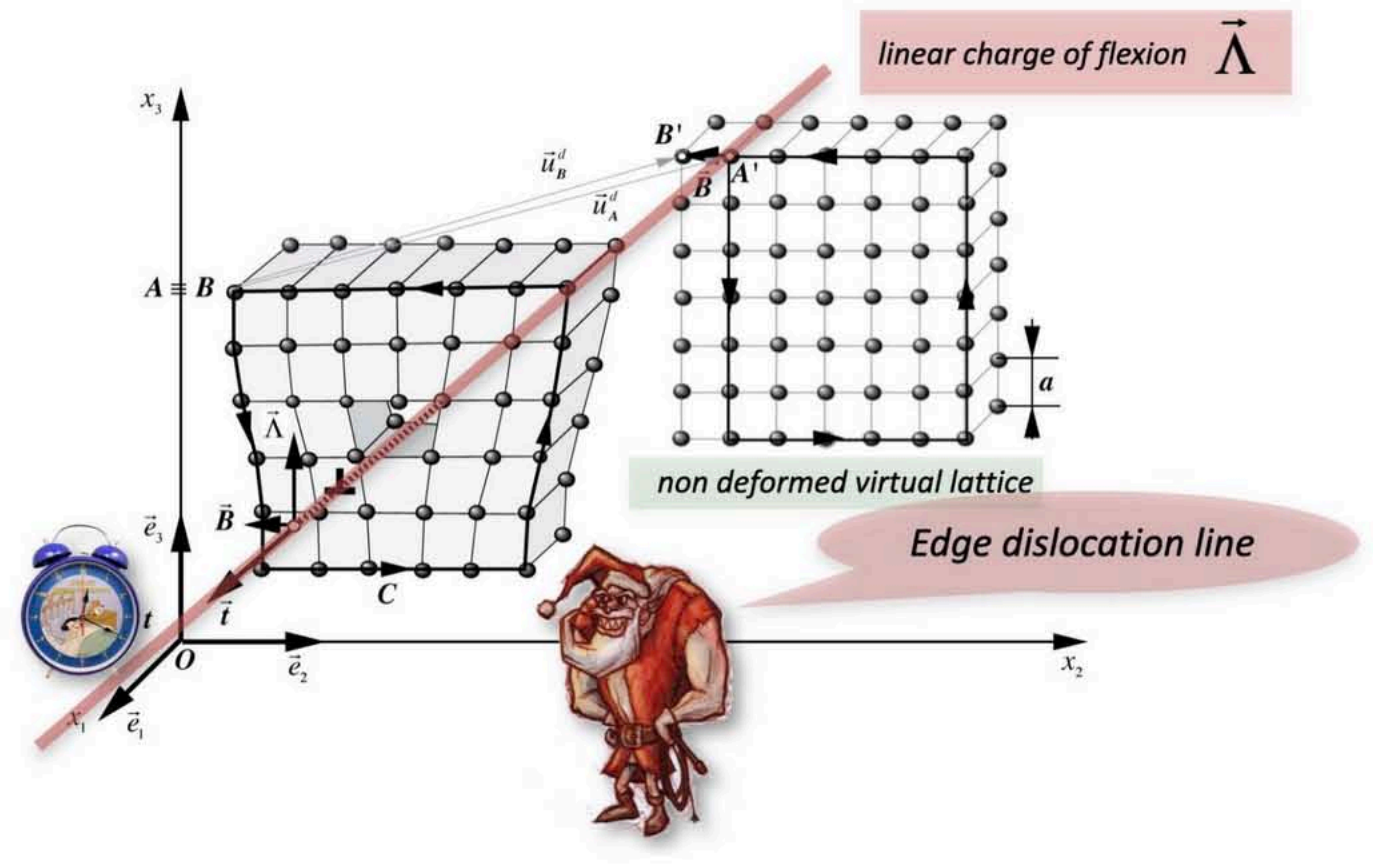


Fig. 4. Edge dislocation line quantified in a cubic lattice

In the *Eulerian theory* [12,13], these defects are approached via the *concept of charges* — an analogy to electric charge — using Volterra's "cut-and-glue" constructions as a guiding intuition. In Euler coordinates *charge density* appears in the geometrocompatibility equations, and *charge flux* appears in the geometrokinetic equations.

This formulation introduces two primary classes of charges (Fig. 2):

- *the tensor density* $\vec{\lambda}_i$ *of dislocation charge, the vector density* $\vec{\lambda}$ *of flexion charge and the scalar density* $\boldsymbol{\lambda}$ *of rotation charge* — first-order charges associated with *plastic distortions* (plastic deformation and rotation), and

- *the tensor density* $\vec{\theta}_i$ *of disclination charge* and *the scalar density* $\boldsymbol{\theta}$ *of curvature charge* — second-order charges associated with *plastic contortions* (plastic bending and torsion).

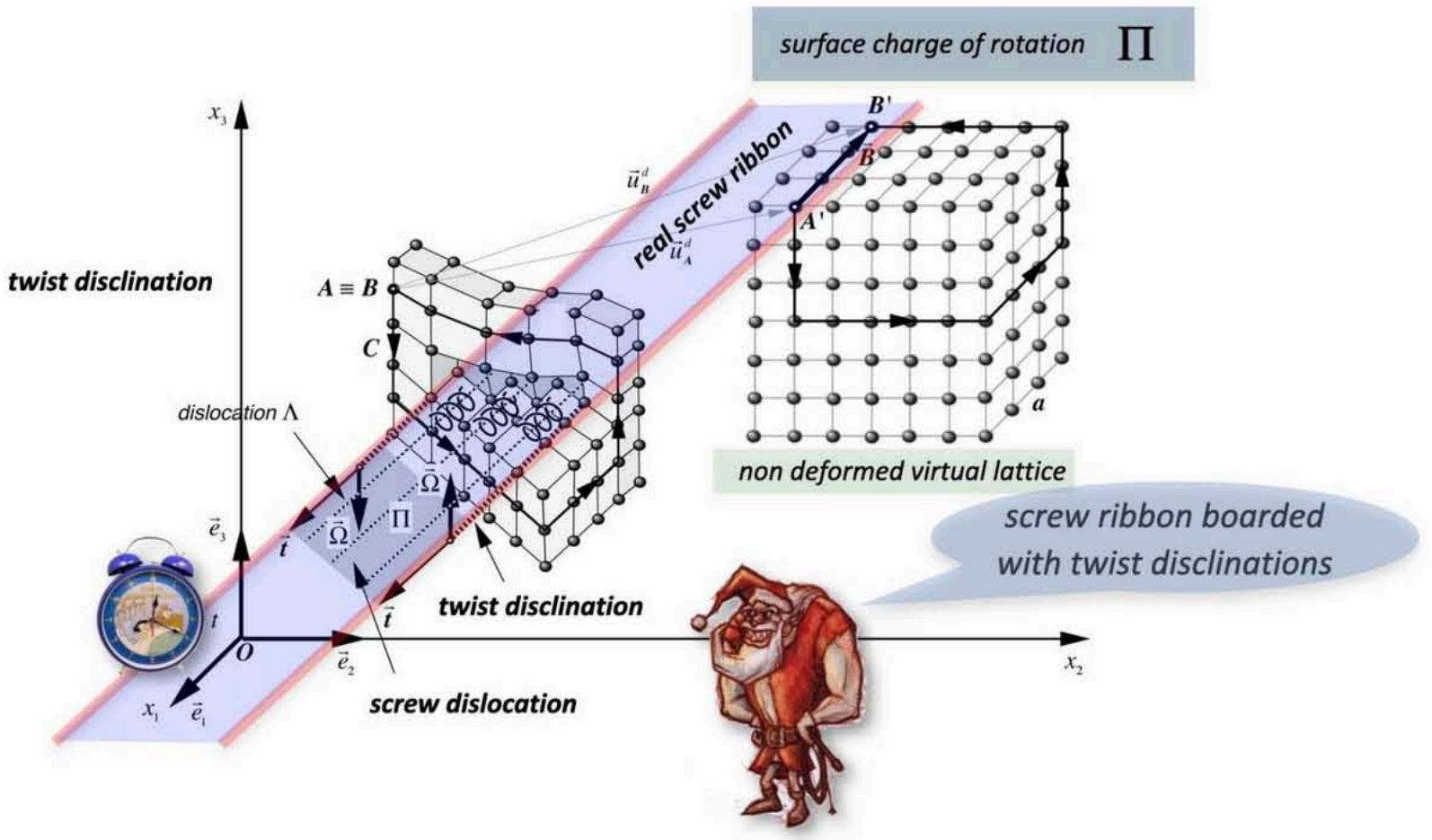


Fig. 5. Quantized two-dimensional dislocation ribbon composed of three screw lattice dislocations, with the formation of two virtual twist disclination lines

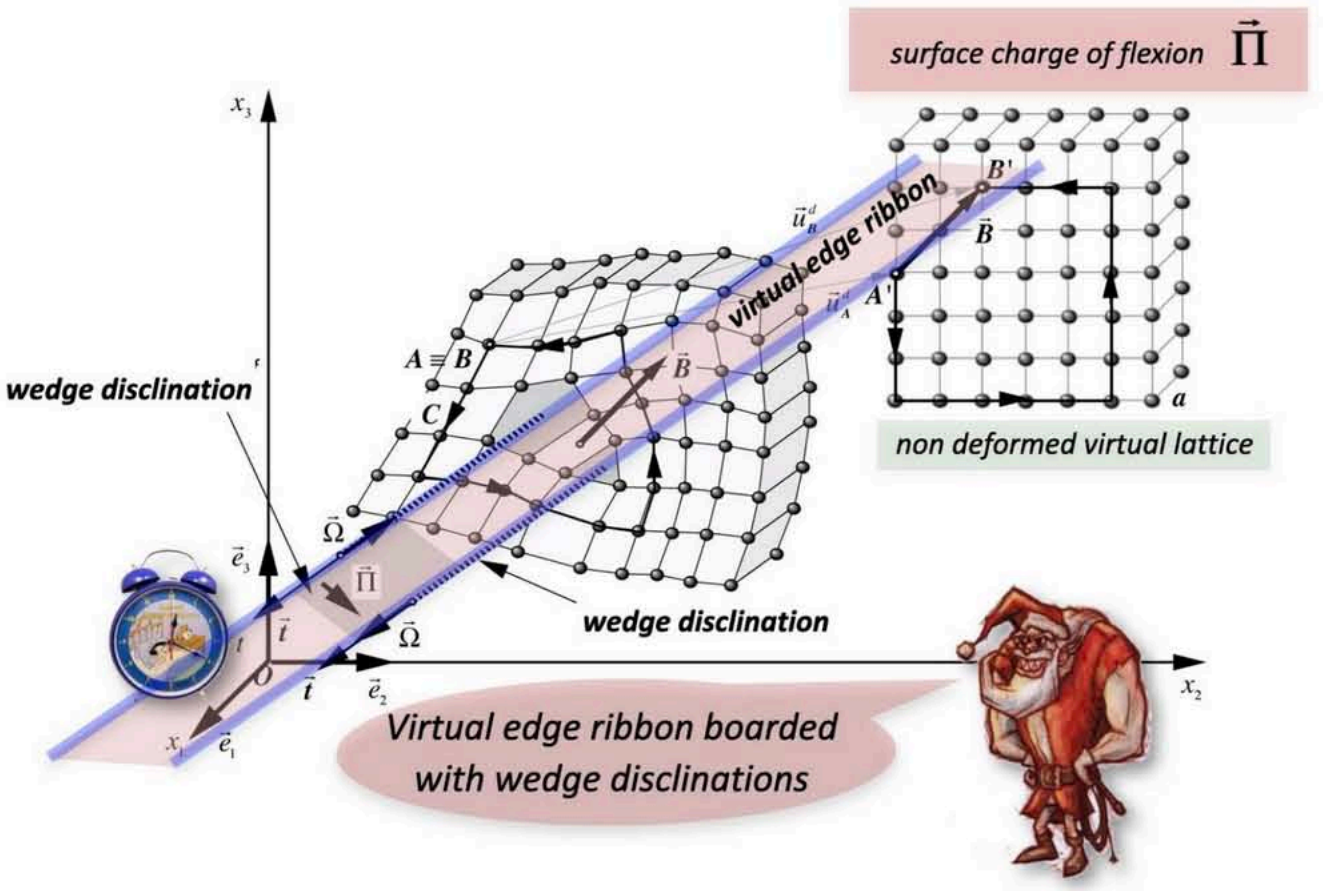


Fig. 6. Doublet of quantified wedge disclinations with the formation of a virtual edge dislocation ribbon

Dislocation and disclination lines and membranes. These charges are *quantized* within the lattice and can be topologically localized only along *strings*, 1D line defects such as dislocation or disclination lines (Fig. 3 and Fig. 4), or *membranes*, 2D defect surfaces such as grain boundaries or twin planes (Fig. 5 and Fig. 6). *A tensor linear density* $\vec{\Lambda}_i$ *of dislocation charge* can be defined, from which *a scalar linear density* $\Lambda = -\vec{B}\cdot\vec{t}$ *of rotation charge* (associated with the screw component) and *a vector linear density* $\vec{\Lambda} = \vec{B}\wedge\vec{t}$ *of bending charge* (associated with the edge component) are derived, where $\vec{B}$ is the Burgers vector of the dislocation and $\vec{t}$ is the unit vector tangent to the dislocation line.

Dislocation and disclination loops. These charges can also appear as *topological loop singularities* of the lattice. Two of them will play a central role in the particle analogy:

- *Twist Disclination Loop,* constructed by making a circular cut of radius R_{BV} in the lattice, rotating the two sides relative to each other with an angle Ω_{BV}, and reattaching them. It possesses a *rotation charge* q_λ such as $|q_\lambda| = \pi R_{BV}^2 |\Omega_{BV}|$, generating a divergent rotation vector field $\vec{\omega}$ such as $q_\lambda = \mathrm{div}\,\vec{\omega}$. The rotation charge is analogous to an *electric charge* with its divergent electric field.
- *Edge Dislocation Loop*, formed by inserting (interstitial type) or removing (vacancy type) n planes of lattice parameter a along a circular cut of radius R_{BC}, then rejoining the material. It possesses a *curvature charge* q_θ such as $|q_\theta| = 2\pi n |a|$, generating a divergent curvature vector field $\vec{\chi}$ such as $q_\theta = \mathrm{div}\,\vec{\chi}$. The curvature charge presents some analogy with a *gravitational mass*.

Long-range fields of localized clusters of charges. In Euler coordinates, when one considers a *localized cluster* of topological singularities — e.g., one or more dislocation loops or disclination loops — the short-range tensor nature of the distortion fields becomes negligible at *large distances*. The lattice perturbations can then be described by

- *a divergent vector rotation field* $\vec{\omega}$ associated with the *total scalar rotation charge* $Q_\lambda = \mathrm{div}\,\vec{\omega}$ of the cluster (analogous to the electric charge). and
- *a divergent vector curvature field* $\vec{\chi}$ associated with the *total scalar curvature charge* $Q_\theta = \mathrm{div}\,\vec{\chi}$ of the cluster (analogous, in some respects, to a gravitational mass).

The advantages of the Eulerian charge formalism. It reproduces the main results of classical dislocation theory while adding new rigor and generality. The evolution of the charges and the associated deformation fields can be treated exactly, even under strong volume expansions or contractions of the lattice.

By introducing also charge fluxes analytically, one can describe the macroscopic and microscopic defect structures associated with dislocation and disclination charges, the motion of dislocation charges through *Orowan's relation*, and the *Peach–Koehler force* acting on dislocations.

This leads to a *complete set of evolution equations* for a lattice in Euler coordinates, explicitly accounting for the presence of topological singularities. The framework enables the calculation of fields and energies for screw, edge and mixed dislocations in isotropic lattices, their mutual interactions, and the modeling by *dislocation strings*—a fundamental tool for explaining the macroscopic anelastic and plastic behaviors of crystalline solids.

The premises for describing the Universe by a «Crystalline Ether»

The rest energy and the Lorentz transformation. Within the Eulerian framework for solid lattices, it is possible to calculate the *rest energy* E_0 of dislocations, corresponding to the elastic deformation energy stored in the lattice, as well as their *kinetic energy* E_{cin}, which is the kinetic energy of lattice particles mobilized during defect motion. This allows the definition of a *virtual inertial mass* for the defect that—remarkably—satisfies a relation of the form $E_0 = M_0 c^2$, obtained entirely from classical mechanics, without invoking the principle of relativity.

At high velocities, dislocation dynamics also obey the principles of *special relativity*, including *Lorentz transformations*. This relativistic behavior emerges naturally from the Newtonian lattice dynamics described in Euler coordinates.

The analogy with Maxwell's equations: furthermore, in the case of an *isotropic solid* undergoing a *homogeneous and constant volume expansion* (so that deformation occurs purely through shear), a complete and exact analogy with *Maxwell's equations* appears. This is achieved by replacing the shear tensor with the rotation vector. The existence of analogies between electromagnetism and incompressible continuous media was noted in earlier works (see Whittaker,

1951 [36]), but the Eulerian approach extends this to *the both pairs of Maxwell equations*, and the analogues of *dielectric polarization, magnetization, electric charges*, and *currents*.

Physically, this implies that a *cosmological lattice* could serve as a real medium supporting electromagnetic fields, providing tangible interpretations for the field quantities of electromagnetism.

This analogy is striking because the initial assumption is that the lattice obeys simple Newtonian dynamics in the *absolute reference frame* of a *"Great Observer"* ***GO***, equipped with orthonormal rulers and a universal clock. Yet the *topological singularities*—dislocations and disclinations with their associated charges—are governed internally by relativistic dynamics due to the Maxwell-like equations that describe the shear forces. From this perspective, the relativistic behavior of singularities is simply a consequence of the Newtonian dynamics of the lattice as seen by the ***GO***.

The new curvature charge: it has no equivalent in standard physics, but will play a central role in the subsequent parts of this theory.

While analogies between defect mechanics and field theories (electromagnetism, relativity, gravitation) had been explored before—most notably by Kröner [23,24], and reviewed by Whittaker [36] and Unzicker [37]—none reached the level of completeness afforded by the Eulerian lattice approach. The richness of these analogies, combined with features such as the absence of magnetic-monopole analogues and possible resolutions of long-standing paradoxes (e.g., the electron's self-energy problem), strongly motivated further investigation.

This progression ultimately led to the development of the *crystalline ether hypothesis*, as presented in my later works [10,11]: a finite, elastic, massive lattice embedded in an absolute vacuum, in which topological singularities represent matter, and whose mechanical laws reproduce—and often clarify—the known laws of physics.

The «Crystalline Ether » and its Newton's Equation

The first main conjecture necessary to describe a cosmological lattice consists in expressing the internal deformation free energy $\boldsymbol{F^{def}}$ of the lattice per volume unit, as a first order term in the *volume expansion* $\boldsymbol{\tau}$ and a second order development $\boldsymbol{F^{dist}}$ in the distortion tensors—namely *volume expansion* $\boldsymbol{\tau}$, *elastic and anelastic shears* $\vec{\alpha}_i^{\,el}$ and $\vec{\alpha}_i^{\,an}$, and especially *elastic and anelastic rotations* $\vec{\omega}^{\,el}$ and $\vec{\omega}^{\,an}$ (Fig. 7). The first order term in the *volume expansion* $\boldsymbol{\tau}$ reflects the energy related to the expansion of the lattice, when the second order terms reflect the energy related to the elastic and anelastic distortions of the lattice.

From the free energy $\boldsymbol{F^{def}}$ of the lattice per volume unit, we get the state equations of elasticity and anelasticity, which allow to obtain the *Newton's equation* describing the local momentum $\vec{p}$ of the lattice, in which $\boldsymbol{C_I}$ and $\boldsymbol{C_L}$ are respectively *the atomic concentrations of self-interstitials and vacancies*, and $\vec{\lambda}$ is *the vector flexion charge.*

This Newton's equation contains an *additional force term* $\overrightarrow{\mathrm{grad}}\left(F^{dist}\right)$ directly related to the *local distortion energy which can be due to the topological singularities contained in the lattice*. In the cosmological interpretation, these singularities correspond to *matter*. This additional term will then play a fundamental role in establishing analogies not only with *gravitation,* but also with *quantum physics*.

Main conjecture: free energy of the cosmological lattice

$$F^{def} = nf^{def} = -K_0\tau + \underbrace{\left(K_1\tau^2 + K_2\sum_i (\vec{\alpha}_i^{\,el})^2 + 2K_3(\vec{\omega}^{\,el})^2 + K_1^{an}\sum_i (\vec{\alpha}_i^{\,an})^2 + 2K_2^{an}(\vec{\omega}^{\,an})^2 \right)}_{=F^{dist}}$$

State equations of elasticity

$$\begin{cases} p = -n\dfrac{\partial f^{def}}{\partial \tau} = K_0 + \left(K_0 - 2K_1\right)\tau - F^{dist} \\ \vec{s}_i = n\dfrac{\partial f^{def}}{\partial \alpha_{ik}^{el}}\vec{e}_k = 2K_2\vec{\alpha}_i^{el} \\ \vec{m} = n\dfrac{\partial f^{def}}{\partial \omega_i^{el}}\vec{e}_i = 4K_3\vec{\omega}^{el} \end{cases}$$

State equations of anelasticity

$$\begin{cases} \vec{s}_i^{cons} = n\dfrac{\partial f^{def}}{\partial \alpha_{ik}^{an}}\vec{e}_k = 2K_1^{an}\vec{\alpha}_i^{an} \\ \vec{m}^{cons} = n\dfrac{\partial f^{def}}{\partial \omega_i^{an}}\vec{e}_i = 4K_2^{an}\vec{\omega}_i^{an} \end{cases}$$

Newton's equation of the cosmological lattice

$$n\frac{d\vec{p}}{dt} = -2\left(K_2 + K_3\right)\overrightarrow{\mathrm{rot}}\,\vec{\omega}^{\,el} + \left(\frac{4}{3}K_2 + 2K_1 - K_0\right)\overrightarrow{\mathrm{grad}}\,\tau + 2K_2\vec{\lambda} + nm\vec{\phi}_I\frac{dC_I}{dt} - nm\vec{\phi}_L\frac{dC_L}{dt}$$
$$+ \overrightarrow{\mathrm{grad}}\underbrace{\left(K_1\tau^2 + K_2\sum_i (\vec{\alpha}_i^{\,el})^2 + 2K_3(\vec{\omega}^{\,el})^2 + K_1^{an}\sum_i (\vec{\alpha}_i^{\,an})^2 + 2K_2^{an}(\vec{\omega}^{\,an})^2 \right)}_{=F^{dist}}$$

Fig. 7. The main conjecture which leads to the cosmological lattice and its Newton's equation

Pure transverse waves with circular polarization

$$\vec{\omega}(x_j,t) = \omega_{i0}^{(p)}\exp\left[i\left(k_t x_j - \omega t\right)\right]\vec{e}_i \pm i\omega_{i0}^{(p)}\exp\left[i\left(k_t x_j - \omega t\right)\right]\vec{e}_k \qquad \text{with} \qquad c_t = \frac{\omega}{k_t} = \sqrt{\frac{K_2 + K_3}{mn}}$$

Transverse perturbations

Transverse waves with linear polarization necessarily coupled to longitudinal wavelets

$$\omega_i^{(p)}(x_j,t) \cong \omega_{i0}^{(p)}\exp\left[i\left(k_t x_j - \omega t\right)\right] \qquad \text{with} \qquad c_t = \frac{\omega}{k_t} = \sqrt{\frac{K_2 + K_3}{mn}}$$

$$\tau^{(p)}(x_j,t) \cong \tau_0^{(p)}\exp\left[i\left(2k_t x_j - 2\omega t\right)\right] \qquad \tau_0^{(p)} \cong -\frac{K_2 + K_3}{K_2/3 + 2K_1\left(1+\tau_0\right) - K_0 - K_3}\left(\omega_{i0}^{(p)}\right)^2$$

Pure longitudinal waves if $4K_2/3 + 2K_1\left(1+\tau_0\right) - K_0 > 0$

Longitudinal perturbations

$$\underline{\tau}^{(p)} = \tau_0^{(p)}\exp\left[i\left(k_l x_j - \omega t\right)\right] \qquad \text{with} \qquad c_l = \frac{\omega}{k_l} \cong \sqrt{\frac{1}{mn}\left[\frac{4}{3}K_2 + 2K_1\left(1+\tau_0\right) - K_0\right]}$$

Eigen modes of longitudinal localized vibrations if $4K_2/3 + 2K_1\left(1+\tau_0\right) - K_0 < 0$

$$\underline{\tau}^{(p)} = \tau_0^{(p)}\exp\left[-x_j/\delta\right]\exp\left[-i\omega t\right] \qquad \text{with} \qquad \delta = \frac{1}{\omega}\sqrt{\frac{1}{mn}\left|\frac{4}{3}K_2 + 2K_1\left(1+\tau_0\right) - K_0\right|}$$

Fig. 8. Transverse and longitudinal perturbations in the cosmological lattice

Wave Propagation and Nature of Photons and Quantum Wave Functions. In this cosmological lattice, transverse and longitudinal wave propagation exhibits surprising features (Fig. 8):
- *pure transverse waves* can only be realized as *circularly polarized waves*, a property that connects directly to the behavior of photons in quantum electrodynamics,
- *linearly polarized transverse waves* are always accompanied by longitudinal wavelets,
- *longitudinal waves* may vanish entirely (as in general relativity's treatment of gravity), but only under certain conditions, specifically when the lattice's volume expansion drops below a critical threshold, and
- *localized longitudinal vibration modes* appear in this case. These modes will have a direct link to the quantum wave function in quantum mechanics,
- in all cases of wave propagation, we observe that *the propagation speed depends heavily on the local expansion state* τ *of the lattice*, as determined by the lattice's site density $n = n_0 \exp(-\tau)$.

Black hole in the vicinity of an expansion singularity. Since the wave celerity $c = c_0 \exp(\tau/2)$ depends on the local expansion τ of the lattice, it is possible to calculate the curvature of wave trajectories in the vicinity of a singularity in the volume expansion field τ, and to determine the conditions under which *a "lattice trap"* or *"sphere of perturbations"* forms for transverse waves. Such traps correspond to *black holes* in the astrophysical analogy: regions from which no transverse wave (light) can escape (Fig. 9).

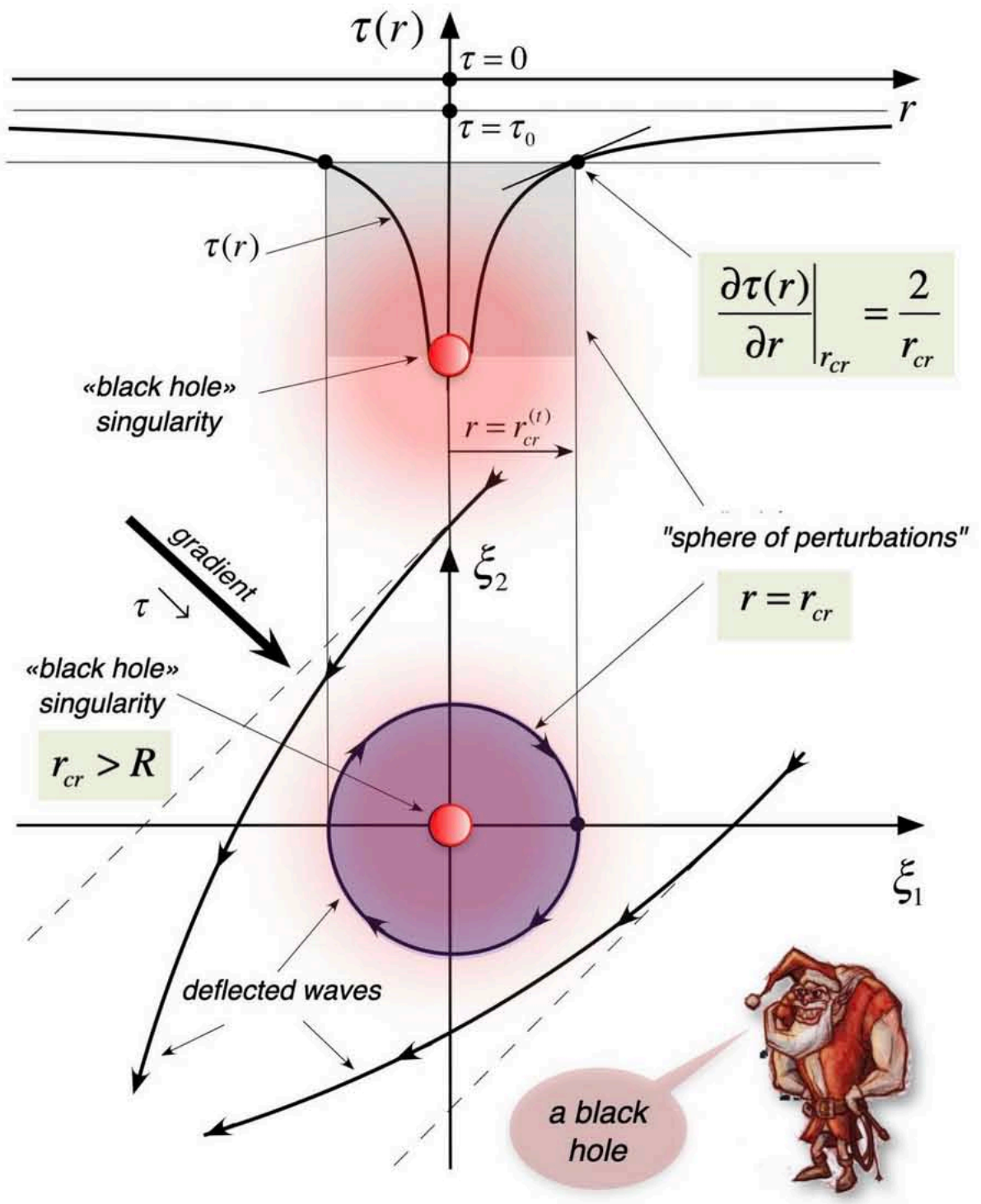


Fig. 9. The "sphere of perturbations", a real "black hole" in the vicinity of a negative singularity of expansion τ

Cosmological Expansion, Dark Energy, and Cyclic Scenarios. A finite cosmological lattice in absolute space can undergo dynamic volume expansion or contraction, driven by *a kinetic energy* T^{cin} *of expansion* (Fig. 10).

Depending on the signs and magnitudes of the elastic moduli, several expansion scenarios emerge: *Big Bang–like expansion*, with a rapid inflation, then a deceleration and possibly followed by a re-acceleration of expansion, and *Big Crunch–like contraction*, as shown in Fig. 10 for various values of *the total energy* $E = F^{def} + T^{cin}$, a trend that can lead to *Big Bounce cycles.*

In this context, the *acceleration of cosmic expansion*, currently attributed to a mysterious *dark energy*, is in fact a natural consequence of *an energy stored in the lattice — namely, the total energy* $E = F^{def} + T^{cin}$ *— if that energy exceeds a certain threshold.*

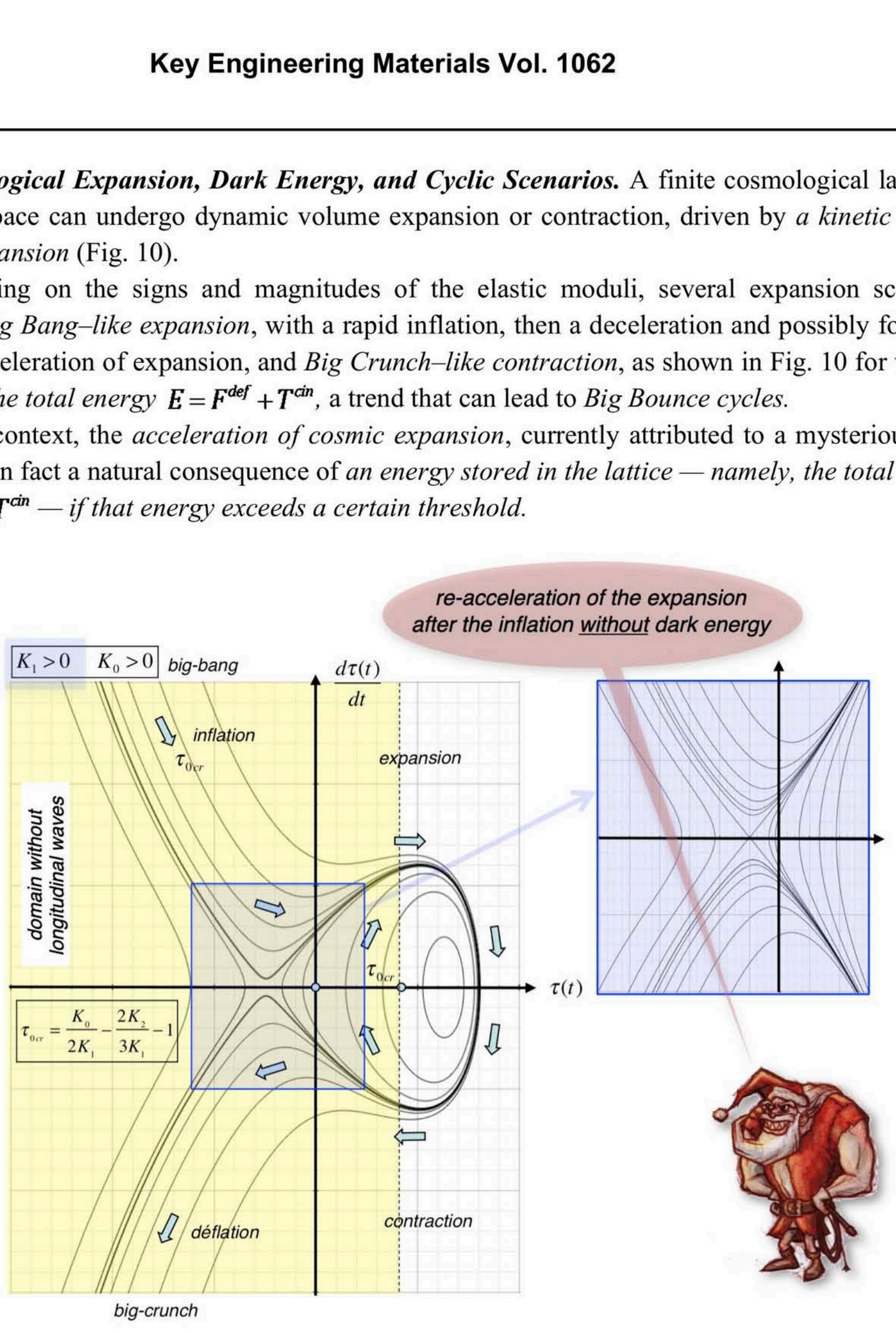


Fig. 10. «Cosmological behavior» of the speed of cosmological expansion $d\tau/dt$ as a function of the expansion τ of a cosmological lattice with $K_1 > 0$

Electromagnetic Field Analogy and Maxwell's equations

Newton's equation (Fig. 7) for the cosmological lattice can be decomposed into *a rotational part*, associated with shear deformations and local rotations, and yielding equations for the macroscopic local rotation field identical to *Maxwell's equations* of electromagnetism, and *a divergent part*, associated with the scalar expansion field, responsible for *gravitational and quantum phenomena*.

This separation is possible under the assumption that the concentrations of point defects—vacancies and self-interstitials—are spatially homogeneous and constant in time. In such a case, the velocity fields of the lattice and its defects can be split into rotational components (index "rot") and divergent components (index "div"), leading to two coupled but distinct subsystems of equations.

geometro - kinetic equation

$$-\frac{\partial(2\vec{\omega}^{el})}{\partial t}+\overrightarrow{\mathrm{rot}}\,\vec{\phi}^{rot}\cong(2\vec{J})$$

geometro - compatibility equation

$$\mathrm{div}\,(2\vec{\omega}^{el})=(2\lambda)$$

Newton's equation

$$\frac{\partial(n\vec{p}^{rot})}{\partial t}\cong-\overrightarrow{\mathrm{rot}}\left(\frac{\vec{m}}{2}\right)+2K_2\vec{\lambda}^{rot}$$

mass density conservation equation

$$\mathrm{div}(n\vec{p}^{rot})=0$$

phenomenology of elasticity and anelasticity

$$(2\vec{\omega}^{el})=\frac{1}{\left(K_2+K_3\right)}\left(\frac{\vec{m}}{2}\right)+(2\vec{\omega}^{an})+\left(2\vec{\omega}_0(t)\right)$$

phenomenology of mass transport

$$(n\vec{p}^{rot})=(nm)\left[\vec{\phi}^{rot}+\left(C_I-C_L\right)\vec{\phi}^{rot}+\left(\frac{1}{n}\left(\vec{J}_I^{rot}-\vec{J}_L^{rot}\right)\right)\right]$$

rotation charges continuity

$$\frac{\partial(2\lambda)}{\partial t}\cong-\mathrm{div}(2\vec{J})$$

energetic balance equation

$$-\left(\frac{\vec{m}}{2}\right)(2\vec{J})\cong\vec{\phi}^{rot}\frac{\partial(n\vec{p}^{rot})}{\partial t}+\left(\frac{\vec{m}}{2}\right)\frac{\partial(2\vec{\omega}^{el})}{\partial t}-\mathrm{div}\left(\vec{\phi}^{rot}\wedge\left(\frac{\vec{m}}{2}\right)\right)$$

transverse wave celerity

$$c_t=\sqrt{\frac{K_2+K_3}{mn}}$$

⇔

Maxwell - Ampère equation

$$-\frac{\partial\vec{D}}{\partial t}+\overrightarrow{\mathrm{rot}}\,\vec{H}=\vec{j}$$

Maxwell - Gauss equation

$$\mathrm{div}\,\vec{D}\;=\rho$$

⇔

Maxwell - Faraday equation

$$\frac{\partial\vec{B}}{\partial t}=-\overrightarrow{\mathrm{rot}}\,\vec{E}$$

Maxwell - Thompson equation

$$\mathrm{div}\,\vec{B}\;=0$$

⇔

phenomenology of dielectricity

$$\vec{D}=\varepsilon_0\vec{E}+\vec{P}+\vec{P}_0(t)$$

phenomenology of magnetism

$$\vec{B}=\mu_0\left[\vec{H}+\left(\chi^{para}+\chi^{dia}\right)\vec{H}+\vec{M}\right]$$

⇔

electric charges continuity

$$\frac{\partial\rho}{\partial t}=-\mathrm{div}\,\vec{j}$$

⇔

energetic balance equation

$$-\vec{E}\,\vec{j}\;=\vec{H}\frac{\partial\vec{B}}{\partial t}+\vec{E}\frac{\partial\vec{D}}{\partial t}-\mathrm{div}\left(\vec{H}\wedge\vec{E}\right)$$

⇔

celerity of light

$$c=\sqrt{\frac{1}{\varepsilon_0\mu_0}}$$

Fig. 11. «Maxwellian» formulation of equations of cosmological lattice evolutions in a local frame $Ox_1x_2x_3$ mobile with the lattice, compared with the Maxwell equations of electromagnetism.

When the average volume expansion field is both *homogeneous* and *quasi-constant*, the density of lattice sites can be considered uniform. Newton's equation then reduces to its *purely rotational* part. The full description of the rotational field requires incorporating the *topological equations* for the elastic rotation vector, namely the *geometro-kinetic equation* (Fig. 1—analogous to Maxwell–Ampère), and the *geometro-compatibility equation* (Fig. 2—analogous to Maxwell–Gauss), in the presence of rotation charges.

Exact analogy with Maxwell's equation. In this quasi-constant expansion regime, the set of equations describing shear and rotation in the cosmological lattice is *formally identical* to Maxwell's equations for electromagnetic fields in a continuous medium (Fig. 11). The analogy with electromagnetism offers a direct mapping between lattice quantities and electromagnetic ones:
- *rotation field* $\vec{\omega}^{el}$ of the lattice corresponds to *electric displacement field* $\vec{D}$,
- *rotation torque field* $\vec{m}$ corresponds to *electric field* $\vec{E}$,
- *lattice velocity field* $\vec{\phi}^{rot}$ corresponds to *magnetic field* $\vec{H}$,
- *momentum field* $\eta\vec{p}^{rot}$ corresponds to *magnetic induction field* $\vec{B}$,
- *density of rotation charges* $\boldsymbol{\lambda}$ corresponds to *density of electric charges* $\boldsymbol{\rho}$
- *anelastic rotation field* $\vec{\omega}^{an}$ corresponds to *dielectric polarization* $\vec{P}$ (for which relaxation, resonance and hysteresis behaviors are possible),
- *mass transport in the lattice* corresponds to *magnetic response* of matter (paramagnetic and diamagnetic analogy with atomic concentrations of interstitials and vacancies, magnetization analogy with flux of vacancies and interstitials).

Only the presence of *the vector flexion charge* $\vec{\lambda}^{rot}$ in the Newton's equation of cosmological lattice differs from the Maxwell-Faraday's equation of electromagnetism. But this charge $\vec{\lambda}^{rot}$, which should correspond to a vector electric charge, cannot exist as long as we only consider topological singularities of the loop type.

This correspondence is more than formal: it extends to phenomenological behavior, including relaxation laws, thermal activation effects, and even hysteresis in non-Markovian transport regimes of defects—directly analogous to magnetic hysteresis in ferromagnetic or antiferromagnetic materials.

Lorentz transformation and Special Relativity

Lorentz transformation. In the cosmological lattice approach, the elastic distortion fields generated by moving topological singularities—such as dislocations, disclinations, or rotation charges—propagate at finite speeds through the lattice via transverse waves. When the description is shifted from the local fixed reference frame of the lattice to the local moving frame of the singularity, the transformation laws of the fields reduce exactly to *the Lorentz transformation*. This correspondence reproduces the well-known relativistic effects of length contraction along the direction of motion, time dilation, and invariance of the transverse wave velocity in moving local frames.

To interpret the shortening of the ruler in the direction of movement, we have to imagine the architecture of the cluster as a set of topological singularities linked together by their interactions via their respective fields of rotation (Fig. 12). These singularities of the lattice move relative to the lattice at velocity $\vec{V}$ in the direction Ox_1, and the finiteness of the speed c_t of their interactions via the rotation field requires that the complete architecture of the cluster of singularity contracts in the direction Ox_1.

But this contraction does not affect the lattice, which retains its original volume expansion state, which is shown in Fig. 12 for the case of two clusters of identical singularities which move at two different velocities, $\vec{V}'$ and $\vec{V}''$, measured compared to the lattice by the ***GO*** observer. Thus, the relativistic effects on the rulers of observers ***HS'*** and ***HS''***, associated with the collective movement of singularities with respect to the lattice, have nothing to do with the effects of volume expansion or contraction of the lattice as those illustrated in Fig. 15.

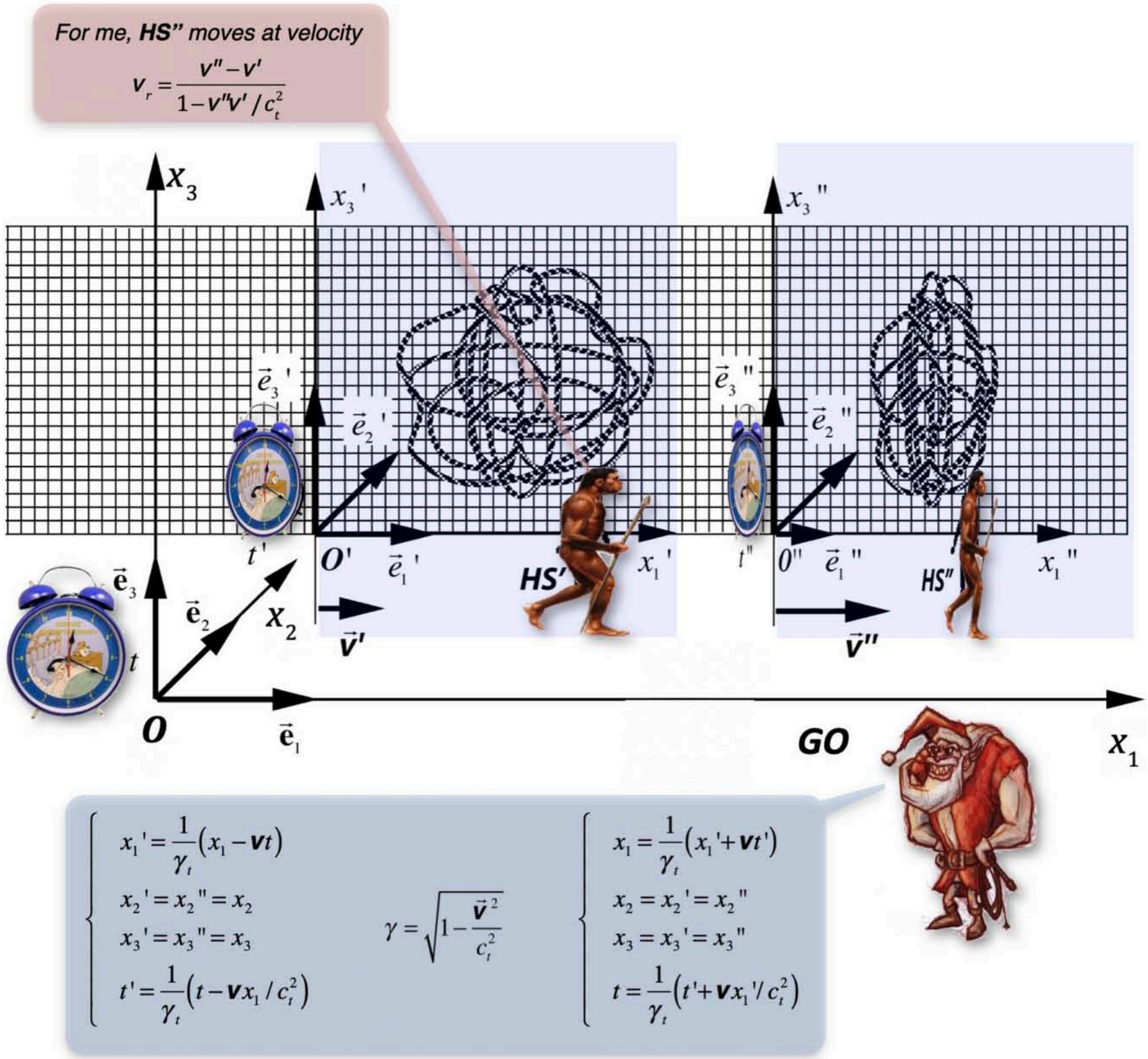


Fig. 12. The mobile Lorentz frames of the moving Homo Sapiens observers **HS'** and **HS"**

Unlike Einstein's formulation, in which the Lorentz transformation is a universal postulate, here it emerges directly from the material structure of the cosmological lattice, which acts as the physical support for all phenomena. This framework privileges the absolute reference frame of the *Grand Observer* ***GO***, capable of measuring absolute velocities and simultaneity. Observers made of singularities—*Homo Sapiens* ***HS'*** and ***HS"***—are limited to relative simultaneity and cannot detect their absolute state of motion inside the lattice.

The relativistic energy of a moving singularity in the lattice follows the exact Einsteinian form $E_0 = mc_t^2$, where c_t is the velocity of transverse waves in the lattice. This result holds for screw and edge dislocations as well as for disclination or dislocation loops. Only spherical rotation charges deviate slightly, producing a situation reminiscent of the classical electromagnetic "electron paradox." The analogy extends further: *the Peach–Koehler force* acting on moving rotation charges plays the same role as *the Lorentz force* in electromagnetism.

In this perspective, the cosmological lattice is *a genuine physical aether*. While the ***GO*** can detect absolute motion and simultaneity, and measures light propagation speed strongly dependent on the value of the lattice expansion, ***HS*** observers always measure a constant light propagation speed in all inertial frames and remain unaware of the underlying absolute frame. Relativistic

effects such as time dilation and length contraction of Fig. 12 coexist with possible local volume variations of the lattice due to expansion or contraction (Fig. 15).

Special relativity. This reinterpretation preserves the predictions of Special Relativity while embedding them in an absolute framework. It offers natural explanations for experimental results, such as the null outcome of *the Michelson–Morley experiment*, the composition of relativistic velocities, and *the classical Doppler–Fizeau formulas*—reinterpreted from the standpoint of the ***GO***.

The twin paradox. Imagine two *Homo Sapiens*, denoted ***HS'*** and ***HS''***, each moving at a different velocity as measured by the external observer, ***GO***. For the two ***HS*** observers themselves—who have no access to these absolute velocities but can only perceive their relative motion, as illustrated in Fig. 12—their principle of relativity corresponds exactly to that of Special Relativity. In particular, when applying the Lorentz transformation, ***HS''*** perceives ***HS'*** as aging more slowly, while ***HS'*** simultaneously perceives ***HS''*** as aging more slowly. At first glance, this symmetrical situation seems paradoxical and is known as the *twin paradox* in Special Relativity. However, within this framework, the paradox finds an elegant resolution. It is the observer ***GO*** who can unambiguously determine that the *Homo sapiens* who traveled at the higher velocity relative to the lattice reference frame will indeed be younger than his twin upon reunion.

Gravitational Field Analogy for the topological singularities

Gravitational Field. In the cosmological lattice framework, topological singularities—localized distortions such as dislocation loops, disclination loops, or rotation charges—generate *external expansion perturbation fields* $\boldsymbol{\tau}$ that behave analogously to *gravitational fields*. Newton's second partial equation shows that these gravitational-like fields consist of three distinct components:
- a dominant term associated with the *energy* (mass-energy term) of the singularity,
- a weaker term linked to the *curvature charge* of the singularity, and
- another weaker term associated with its *rotation charge*.

This threefold decomposition goes beyond Einstein's General Relativity, which accounts only for the mass-energy term.

Static versus dynamic gravitational fields: the quantum decoherence. A central result of the theory, is that the external expansion perturbation fields of a singularity can exist in two fundamentally different regimes:
- *Static regime*: if the energy density or/and rotation charge are *below some critical values*, stable static solutions exist, corresponding to stationary long-range gravitational-like fields.
- *Dynamic regime*: if these quantities *exceed* these critical values, no static solution to Newton's second partial equation exists. The only possible solutions are dynamic, marking a transition to behaviors analogous to *quantum effects*. This threshold defines the *quantum decoherence limit* for the singularity, a topic we will revisit later.

Thus, Fig. 13 maps the domains of existence of static and dynamic solutions, showing that high-energy singularities inevitably enter a time-dependent, potentially quantum-dominated phase.

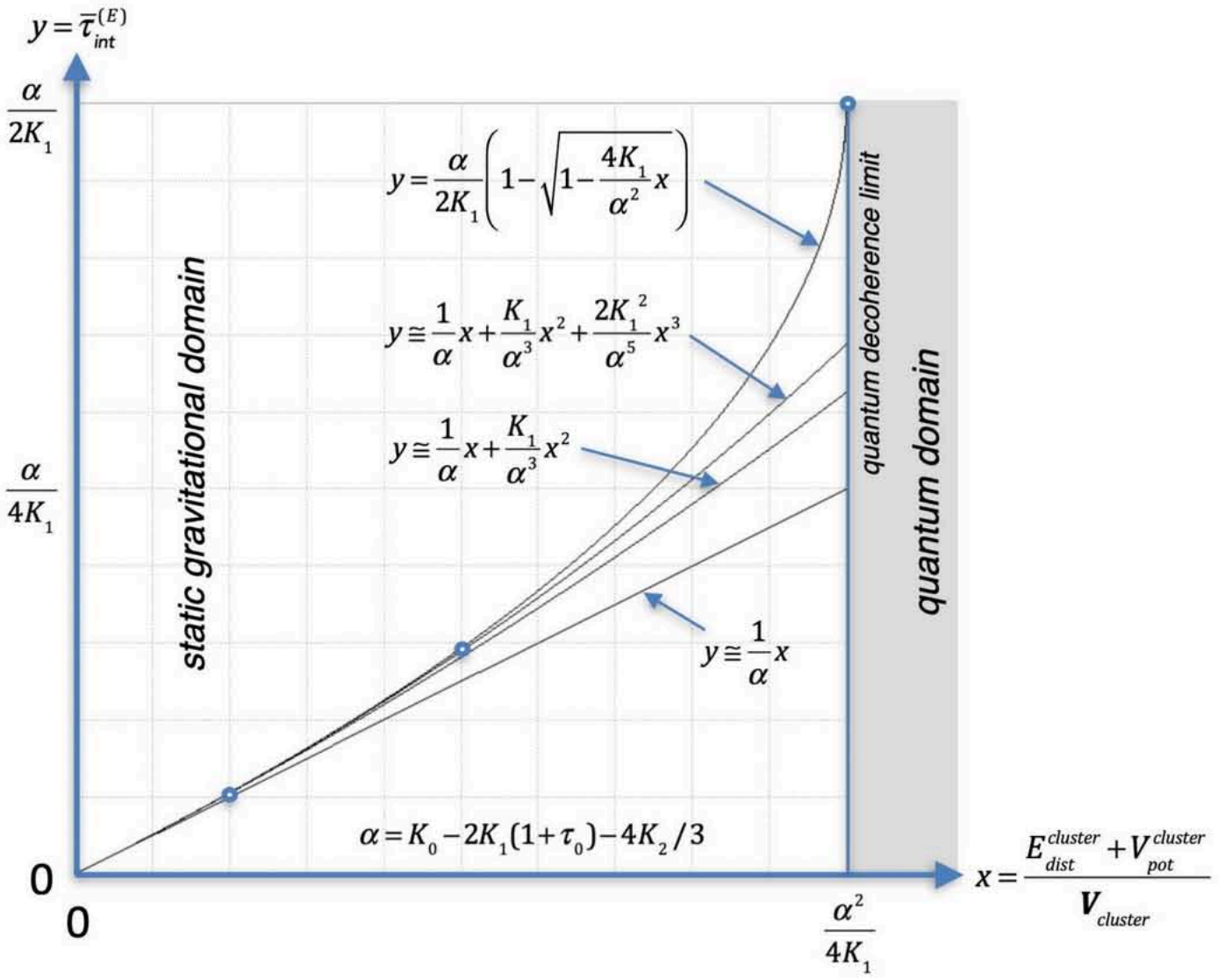


Fig. 13. The mean perturbation field in the static solution domain for energy density values of the singularity below the critical value, and domain of the quantum behaviour for values above the critical value.

Static gravitational fields of loop clusters. Calculations applied to the various types of fundamental loops forming a cluster of loops allow us to determine the static external gravitational fields τ of such clusters with total energy $E_0^{cluster}$, total curvature charge $Q_\theta^{cluster}$, and total rotation charge $Q_\lambda^{cluster}$, as a function of the distance r from the cluster center:

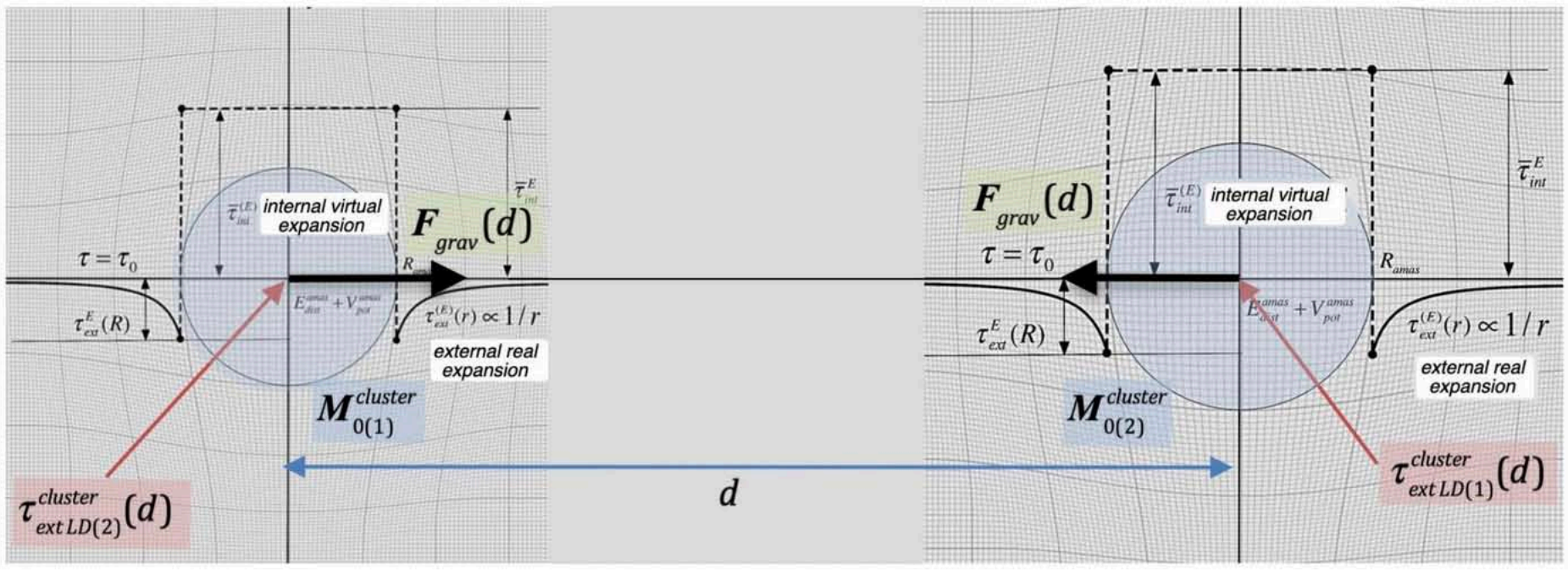
- *for total energy* $E_0^{cluster}$, the cluster generates an external gravitational field proportional to $\tau_{en}(r)\propto -E_0^{cluster}/r\propto -M_0^{cluster}c_t^2/r$,
- *for a total curvature charge* $Q_\theta^{cluster}$, the cluster is responsible for an external gravitational field proportional to $\tau_\theta(r)\propto Q_\theta^{cluster}/r$,
- *for a total rotation charge* $Q_\lambda^{cluster}$, the cluster is responsible for an external gravitational field at long distance proportional to $\tau_\lambda^{LD}(r)\propto -(Q_\lambda^{cluster})^2/r$, but another external gravitational field at short distance proportional to $\tau_\lambda^{SD}(r)\propto (Q_\lambda^{cluster})^2/r^4$ is added to this field.

In all cases, the *energy of the gravitational fields outside the cluster,* for the various fields $\tau_{en}(r)$, $\tau_\theta(r)$, $\tau_\lambda^{LD}(r)$, $\tau_\lambda^{SD}(r)$, is negligible compared to their total energies $E_0^{cluster}$, which means that Einstein's relation $E_0^{amas}=M_0^{amas}c_t^2$ still applies to clusters in the lattice model.

Newtonian Gravitation in the Cosmological Lattice Framework

The long-range gravitational interaction between clusters of twist disclination loops in the cosmological lattice exhibits a strong formal analogy with Newton's law of gravitation. In this framework, the mass of the twist disclination loops—proportional to their energies—dominates over that of the edge or mixed dislocation loops. Consequently, the expansion field perturbations are primarily generated by these twist disclination loops.

When two such clusters, separated by a distance d, interact via their respective perturbations of expansion field, one can calculate the increase in energy $\Delta E_{grav}(d)$ associated with their gravitational interaction and deduce the gravitational interaction force F_{grav} between the two clusters, which depends on their masses $M_{0(1)}^{cluster}$ and $M_{0(2)}^{cluster}$, as shown in Fig. 14.



$$\Delta E_{grav}(d) = M_{0(1)}^{cluster} c_t^2 \left(e^{\tau_{ext\,LD(2)}^{cluster}(d)/8} - 1 \right) + M_{0(2)}^{cluster} c_t^2 \left(e^{\tau_{ext\,LD(1)}^{cluster}(d)/8} - 1 \right)$$

$$F_{grav}(d) = \frac{\partial \Delta E_{grav}(d)}{\partial d} \cong G_{grav} \frac{M_{0(1)}^{cluster} M_{0(2)}^{cluster}}{d^2} \left[1 - \frac{1}{4} \frac{G_{grav}}{c_t^2} \frac{M_{0(1)}^{cluster} + M_{0(2)}^{cluster}}{d} + \ldots\ldots \right]$$

with $$G_{grav} = \frac{c_t^4}{8\pi\left(K_0 - 4K_2/3 - 2K_1(1+\tau_0)\right)R_\infty^2} = \frac{c_{t0}^4}{8\pi\left(K_0 - 4K_2/3 - 2K_1(1+\tau_0)\right)R_{\infty 0}^2} e^{4\tau_0/3} \begin{cases} >0 & if \quad \tau_0 < \tau_{0cr} \\ <0 & if \quad \tau_0 > \tau_{0cr} \end{cases}$$

Fig. 14. The "gravitational" interaction force between two clusters of rotation charge singularities of inertial mass $M_{0(1)}^{cluster}$ and $M_{0(2)}^{cluster}$.

The parameter $G(K_0, K_1, K_2, \tau_0, \ldots)$ plays the role of a gravitational constant, but depends in fact on *the intrinsic lattice parameters* and also on the *local background volume expansion* τ_0. The correction term $\left[1+\ldots\right]$ becomes very close to 1 for low cluster densities and large separation d, recovering *the exact Newtonian form of the gravitational force.*

Unlike the universal constant G of classical gravitation, $G(K_0, K_1, K_2, \tau_0, \ldots)$ *varies with the average state of expansion* τ_0 *of the lattice*, and may even become negative if lattice expansion exceeds a certain critical value. This introduces a potential coupling between cosmological expansion and the effective strength of gravitation, suggesting that gravitational interactions could evolve over cosmic time.

At short ranges, the second-order corrections predict a slight *change* in the force compared with pure Newtonian gravity equation. For planetary motion, these corrections are minimal as in the case of General Gravity

Thus, within the weak-field and large-distance regime, the cosmological lattice approach reproduces Newtonian gravitation exactly, while naturally embedding it into a broader framework in which $G(K_0, K_1, K_2, \tau_0, \ldots)$ becomes a dynamic quantity tied to the lattice's expansion state.

General Relativity analogy

By taking into account the *gravitational effects* on topological singularities composed mainly of *screw disclination loops*, the cosmological lattice model allows us to deduce *how rulers and clocks* of local observers ***HS*** embedded in regions where the lattice's expansion is non-zero behave (Fig. 15).

We show that, for two events separated by *a distance* d_0 and *a time interval* Δt_0 for a local observer (*Homo Sapiens* ***HS***) located in a region of the lattice where the expansion τ is nonzero, the measurement of the same events by *the external observer* ***GO*** yields $d = d_0 \exp(\tau/4)$ and $\Delta t = \Delta t_0 \exp(-\tau/4)$ respectively. Thus, for a local observer placed at a distance r from a cluster of singularities of mass M_0^{amas}, the variation in the expansion field depends on r and is proportional to $\tau_{en}(r) \propto -E_0^{amas}/r \propto -M_0^{amas} c_t^2/r$. Consequently, the distance d measured by the ***GO*** between the two events decreases while the time interval measured by ***GO*** increases. In other words, if an observer ***HS*** is located in the vicinity of a gravitational cluster, the ruler of his reference frame shortens as seen by the ***GO*** while the clock of his reference frame slows down as measured by the ***GO***, and thus the ***HS*** ages more slowly.

Local invariance of Maxwell's equations. A key result is that *Maxwell's equations remain locally invariant* for any local observer ***HS***, regardless of the local value of the lattice's volume expansion. This means that, for each local observer, the *transverse wave velocity*, identified with the speed of light, is constant and equals to c_{t0}. However, when this velocity is measured by the *Great Observer* ***GO*** in his absolute spatial reference frame, this wave velocity equals $c_t = c_{t0} \exp(\tau/2)$ and thus depends exponentially on the local expansion .

This reconciles the invariance of the speed of light in relativity with a deeper mechanical explanation: the constancy of the speed of light is a *local property* of the lattices's dynamics in the local reference frames of ***HS*** observers rather than a fundamental postulate, since the actual speed measured by the external observer ***GO*** depends strongly on the local expansion of the lattice.

Analogies with the equations of General Relativity. The gravitational interactions derived from the expansion field show strong analogies not only with *Newtonian gravitation* in the weak-field limit, but also with the *Einstein's general relativity* in curved space-time descriptions. For example the model reproduces *Schwarzschild-like metrics* at large distances from a massive object, and it predicts *the same deflection of wave trajectories* (light bending) than the General Relativity in strong gravitational fields.

But the Eulerian approach differs slightly from General Relativity, as shown in table 16, and introduces two key refinements compared to General Relativity:

- *Short-range modifications of Schwarzschild's metric*, arising naturally from the lattice structure.
- a finite treatment of black hole horizons: the *radius of the sphere of perturbations* and the *point of no return* are identical, equal to the Schwarzschild radius, and the *limit radius at which gravitational time dilation would become infinite* is reduced to zero, eliminating divergences in the description of the black hole interior. This means that the model does not encounter the *infinite quantities* that often plague black hole solutions in general relativity.

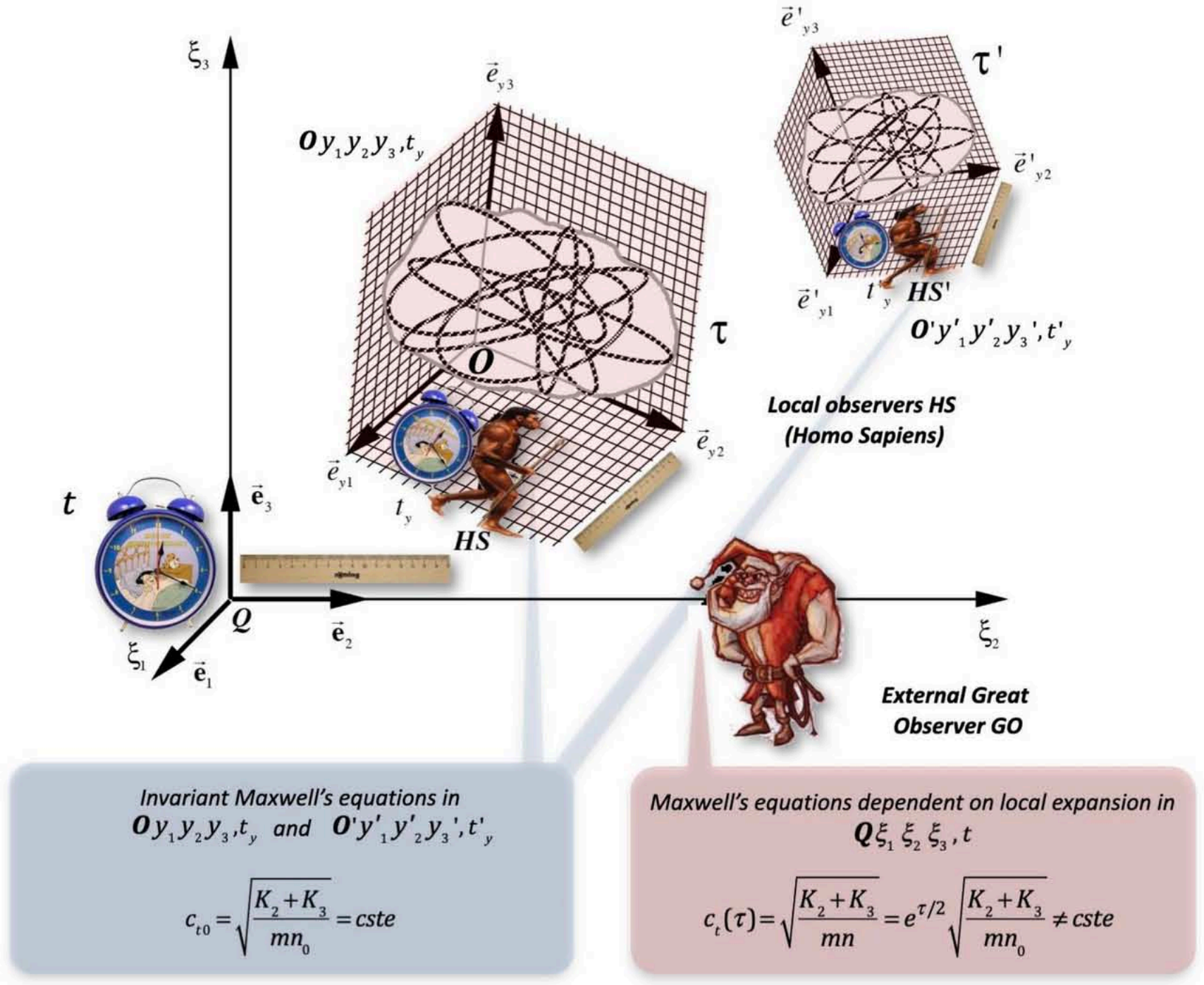


Fig. 15. Local rulers and clocks in the reference frames of the homo sapiens **HS** and **HS'**, and the local invariance of the Maxwell's equations in the **HS** frames.

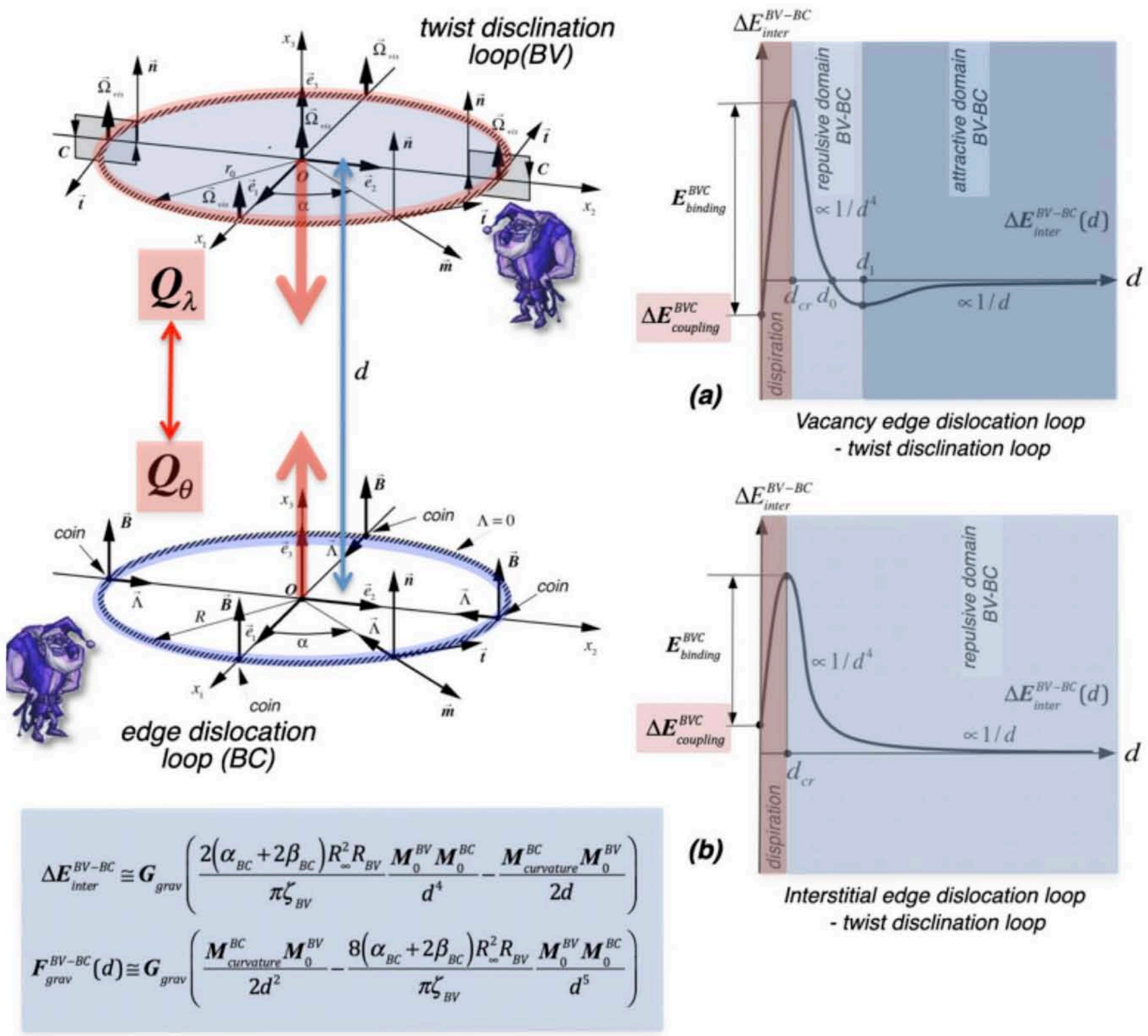
Table 16. Comparative behavior of the perfect cosmological lattice with the General Relativity

Perfect cosmological lattice		*General Relativity*
$\begin{cases} y_i = \mathrm{e}^{\frac{G_{grav}M_0^{cluster}}{c_t^2 r}} x_i \\ t_y = \mathrm{e}^{-\frac{G_{grav}M_0^{cluster}}{c_t^2 r}} t \end{cases}$	*Transformation laws*	$\begin{cases} y_i = \left(1+\frac{G}{c^2}\frac{M_0}{r}+\ldots\right)x_i \\ t_y = \left(1-\frac{G}{c^2}\frac{M_0}{r}\right)t \end{cases}$
$R_{Schwarzschild}=2G_{grav}M_0^{cluster}/c_t^2$	*Schwarzschild radius*	$R_{Schwarzschild}=2G_{grav}M_0^{cluster}/c_t^2$
$R_{photon\,sphere}=2G_{grav}M_0^{cluster}/c_t^2$	*Photon sphere radius*	$R_{photon\,sphere}=3G_{grav}M_0^{cluster}/c_t^2$
$R_{time\,dilation\to\infty}\to 0$	*Radius of infinite dilation of time*	$R_{time\,dilation\to\infty}\cong G_{grav}M_0^{cluster}/c_t^2$
Curvature vector by flexion $\vec{\chi}=-\frac{4K_2/3+2K_1}{2(K_2+K_3)}\overrightarrow{\mathrm{grad}}\,\tau+\frac{1}{2(K_2+K_3)}\left(n\frac{d\vec{p}}{dt}-\overrightarrow{\mathrm{grad}}F^{def}\right)+\frac{K_3}{K_2+K_3}\vec{\lambda}$ *«Gravitational» field* *Energy-momentum vector* *Flexion charge*		*Einstein's curvature tensor* $G=8\pi T$ *Energy-momentum tensor*
Divergence of Newton's equation: equation of motion for "gravitational" distortions $\vec{\nabla}\vec{\chi}=\mathrm{div}\left[\frac{1}{2(K_2+K_3)}\left(n\frac{d\vec{p}}{dt}-\overrightarrow{\mathrm{grad}}F^{def}\right)-\frac{4K_2/3+2K_1}{2(K_2+K_3)}\overrightarrow{\mathrm{grad}}\,\tau+\frac{K_3}{K_2+K_3}\vec{\lambda}\right]=\theta$		*Divergence of the energy-momentum tensor: gravitational motion equation* $\vec{\nabla}\bullet T=0$

These gravitational results not only match Einstein's predictions in the appropriate limits but also extend them, offering new interpretations of relativistic effects as *emergent mechanical phenomena* within the cosmological lattice

Weak Interaction Forces Between Loop Singularities: Particles and Antiparticles

Among the possible *topological loop singularities* in the cosmological lattice, two play a central role in the analogy with particles: the *screw disclination loop* and the *edge dislocation loop*. When a *screw disclination loop* and an *edge dislocation loop* approach each other, their respective rotation and curvature fields interact and attract each other to form a *dispiration loop*. Figure 17 illustrates this phenomenon by plotting the interaction energy curves ΔE_{inter}^{BV-BC} as a function of the distance d between the two loops for edge dislocation loops of interstitial and lacunar nature. This interaction produces a *short-range binding potential*, which corresponds to a *capture force* $F_{grav}^{BV-BC}(d)$ between the loops. Note that these two quantities ΔE_{inter}^{BV-BC} and $F_{grav}^{BV-BC}(d)$ are proportional to G_{grav} and therefore depend on the local expansion state τ of the lattice.



$$\Delta E_{inter}^{BV-BC} \cong G_{grav}\left(\frac{2\left(\alpha_{BC}+2\beta_{BC}\right)R_{\infty}^{2}R_{BV}}{\pi\zeta_{BV}}\frac{M_0^{BV}M_0^{BC}}{d^4}-\frac{M_{curvature}^{BC}M_0^{BV}}{2d}\right)$$

$$F_{grav}^{BV-BC}(d) \cong G_{grav}\left(\frac{M_{curvature}^{BC}M_0^{BV}}{2d^2}-\frac{8\left(\alpha_{BC}+2\beta_{BC}\right)R_{\infty}^{2}R_{BV}}{\pi\zeta_{BV}}\frac{M_0^{BV}M_0^{BC}}{d^5}\right)$$

Fig. 17. Long and short range interactions potential between a twist disclination loop (BV) and an edge dislocation loop (BC), with different dislocation loops nature

Weak interaction force and particles-antiparticles in this lattice formalism. Due to its very limited range, this interaction is directly analogous to the *weak nuclear force* observed in the Standard Model of particles (Fig. 18). The dispiration loop model thus provides a mechanical interpretation of particles bound by the weak force. In this framework:

- *a particle* corresponds to a dispiration loop in which the edge dislocation component is of the *interstitial type* (positive curvature charge),
- *an antiparticle* corresponds to a dispiration loop in which the screw disclination component has the opposite charge and the edge dislocation component is of the *lacunar type* (negative curvature charge).

The screw disclination component provides the *electric charge* of the particle, while the edge dislocation component determines its *curvature charge*. Because of the opposite sign of the curvature mass in these two cases, the interaction energies exhibit quite different behaviors (Fig. 17), which shows that the weak force acts differently in the cases of particles and antiparticles. This point obviously warrants further study.

Mass of Curvature and Deviation from the Equivalence Principle. A key new concept in this model is the *mass of curvature* $M^{BC}_{curvature}$: the equivalent mass associated with the gravitational effects of the *curvature charge*. Unlike inertial mass, curvature mass can be *positive* (vacancy loops) or *negative* (interstitial loops).

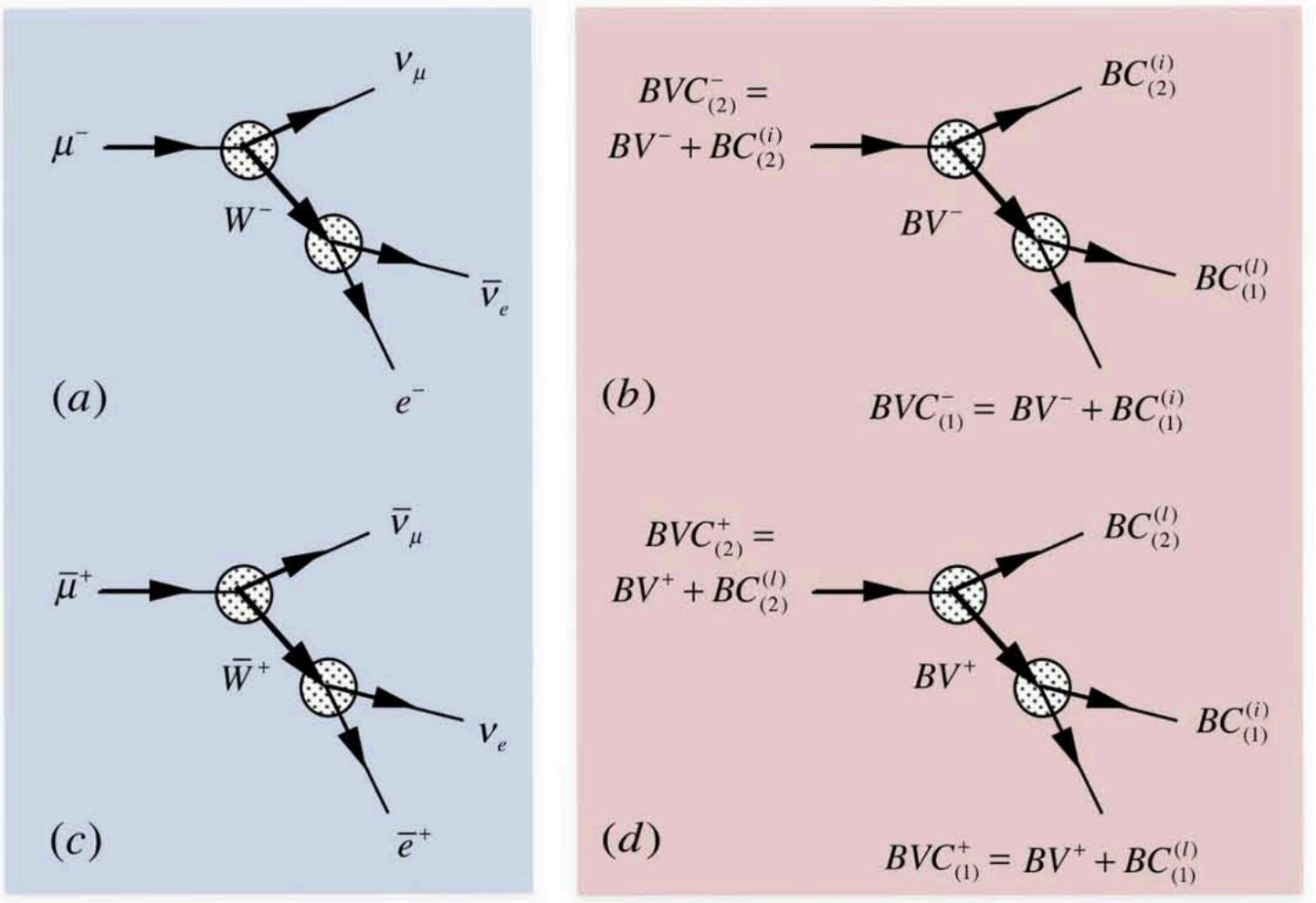


Fig. 18. Analogy between the weak leptonic interaction **(a)** and **(c)** and the decompositions and recompositions of dispiration loops **(b)** and **(d)**

This leads to a *small deviation from the equivalence principle*: particles and antiparticles have identical *inertial masses (related to their energy)*, but their *gravitational masses* (which correspond to the sum of their inertial mass and their curvature mass) differ slightly due to *the opposite signs of their curvature charges*.

For example, in the case of neutrinos and antineutrinos:

- *a neutrino* (pure interstitial edge dislocation loop) has a *negative gravitational mass* (antigravity), because we can show that its negative curvature mass has a greater magnitude than its inertial mass.

- *an antineutrino* (pure vacancy edge dislocation loop) has a *positive gravitational mass* of slightly greater magnitude than the negative gravitational mass of the neutrino.

Cosmological Consequences of Curvature Mass Asymmetry. This asymmetry between the gravitational properties of particles and antiparticles will play a major role in the cosmological evolution of matter and antimatter. It provides a natural mechanism for *matter–antimatter segregation* in the early Universe and offers an explanation for the observed matter dominance in the Universe. In the next sections, we will see that this mechanism also contributes to the formation of *galaxies* and their central *supermassive black holes*, the apparent *disappearance of antimatter* from the observable Universe, and the nature of *dark matter* as a background sea of gravitationally repulsive neutrinos.

Black Holes and Neutron Stars

The cosmological lattice framework allows the introduction of *macroscopic lacunar or interstitial singularities*, which may appear as *a spherical hole* in the lattice of lacunar type (Fig. 19), or *a spherical inclusion* of interstitial type composed of a lattice material embedded within the surrounding lattice (Fig. 20).

For both cases, the behavior of the lattice expansion $\tau_{ext}(r)$ as a function of r is shown. In the case of the spherical hole (Fig. 19), the expansion $\tau_{ext}^{L}(r)$ depends on the radius of the hole R_L and on the baseline expansion of the lattice $\tau_0 + \tau^{external}(R_L)$ at the surface, and the radius of the hole R_L depends on the number N_L of missing sites inside. In the case of the spherical inclusion (Fig. 20), the expansion $\tau_{ext}^{(I)}(r)$ depends on the radius R_I of the inclusion and the baseline expansion of the lattice $\tau_0 + \tau^{external}(R_I)$ at the surface, and the radius of the inclusion R_I depends on the number N_I of sites in the inclusion.

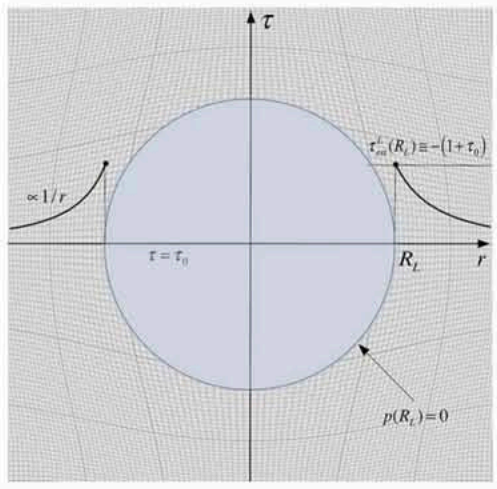
Formation from Gravitational Collapse. Consider a macroscopic object within the cosmological lattice, composed either entirely of *particles* (with interstitial curvature charge) or entirely of *antiparticles* (with vacancy curvature charge).

If the object's mass is sufficiently large, and if it is electrically neutral (composed of electrically neutral atoms), gravitational attraction will eventually cause it to collapse under its own weight:

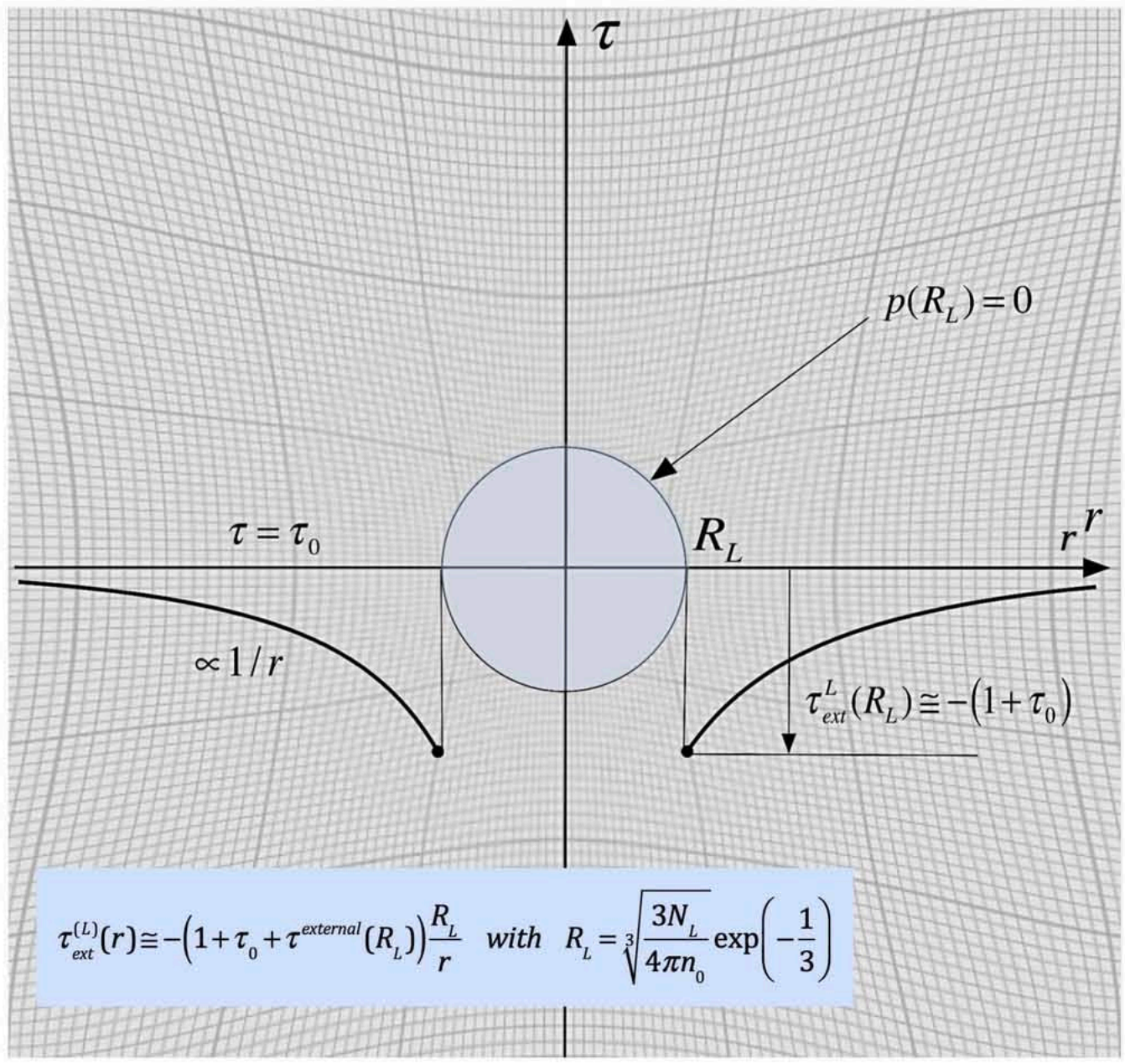
- *Case 1 – Antiparticle-dominated object*: the *twist disclination loops* (electric charges) annihilate in pairs, releasing enormous amounts of energy, and the *edge dislocation loops* of lacunar type merge into a *spherical hole* of N_L missing sites in the lattice. The result is a *macroscopic lacunar singularity* (Fig. 19), becoming a *black hole* in the astrophysical analogy in the case ***(b).***

- *Case 2 – Particle-dominated object:* the *twist disclination loops* (electric charges) also annihilate, again releasing large amounts of energy and the *edge dislocation loops* of interstitial type coalesce into a *spherical inclusion* of N_I reticular material sites. The result is a *macroscopic interstitial singularity* (Fig. 20), a *neutron star (a pulsar)* in the astrophysical analogy.

Neutron Stars and Black Holes as "Particle–Antiparticle" Pairs. In this interpretation, a *black hole* is the macroscopic "antiparticle" of a *neutron star*, if both originate from collapsing objects initially containing equal numbers of curvature-charged loops, as $N_L = N_I$ in this case. Combining a neutron star and a black hole of corresponding magnitudes would then result in *mutual annihilation*, releasing certainly extreme amounts of energy.



(a) $\tau_0 < -\left(1+\tau^{external}(R_I)\right)$



(b) $\tau_0 > -\left(1+\tau^{external}(R_I)\right)$

Fig. 19. The external expansion field of a macroscopic vacancy for two values of the background expansion of the lattice. Case **(b)** may correspond to a black hole.

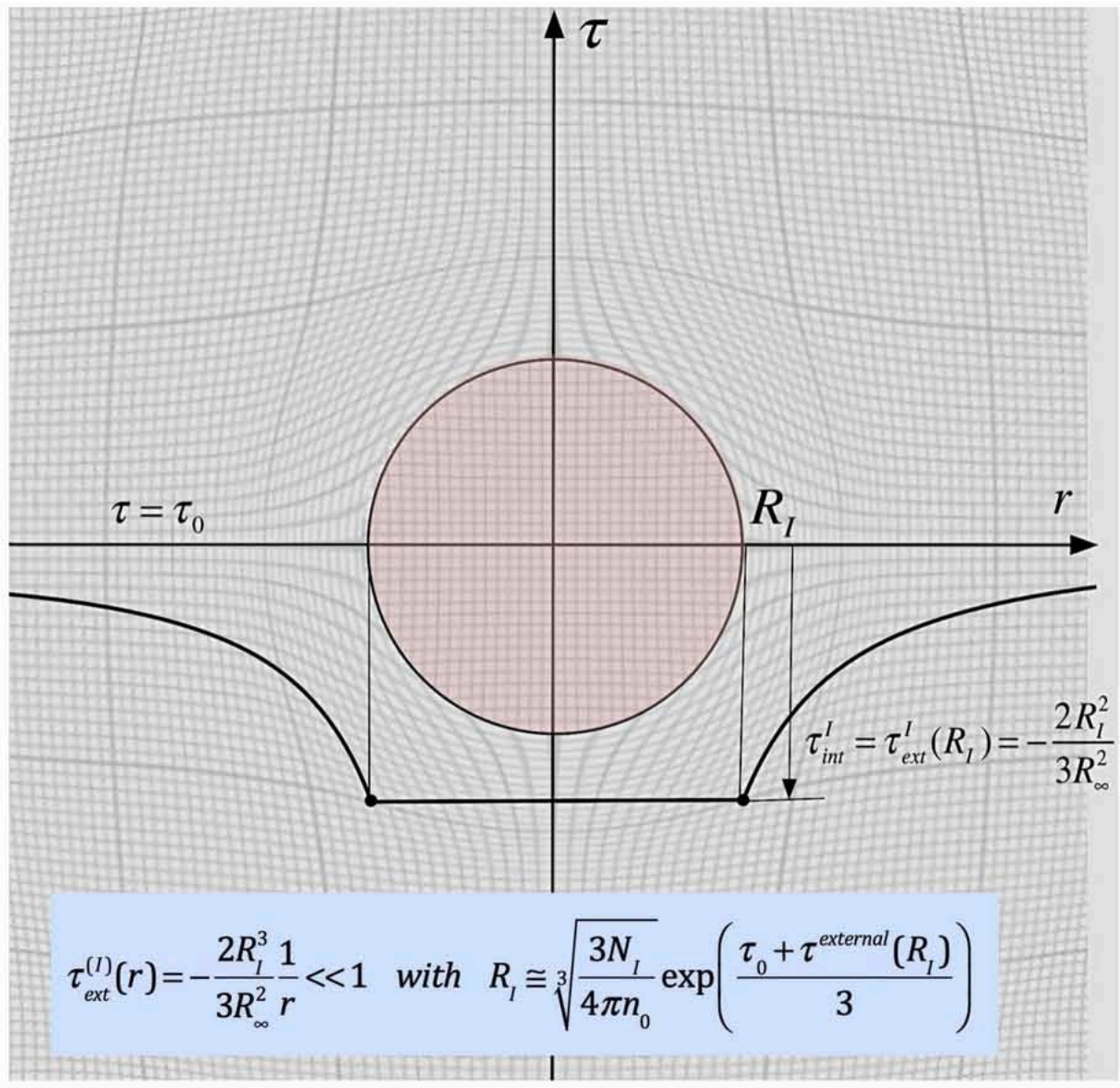


Fig. 20. The internal and external expansion fields of a macroscopic interstitial

Implications for High-Energy Astrophysics. This lattice-based view of compact objects:
- provides a *mechanical analogy* for the nature of black holes and neutron stars,
- suggests new ways to think about *energy release* during collapse.
- links macroscopic astrophysical phenomena directly to the *microscopic topology* of space at the lattice level.

A plausible scenario for the cosmological evolution of the Universe

In standard physics, General Relativity (GR) governs gravitational interactions, while the Standard Model of particle physics describes the properties of elementary particles. However, neither framework satisfactorily explains why our Universe is predominantly matter, how galaxies initially formed, or the nature of the so-called *"dark matter."*

The cosmological lattice theory provides an alternative approach by modeling the fabric of space as an elastic, discrete lattice capable of hosting topological singularities. Particles and antiparticles are not fundamental point-like entities but composite structures made of loops of disclinations and dislocations.

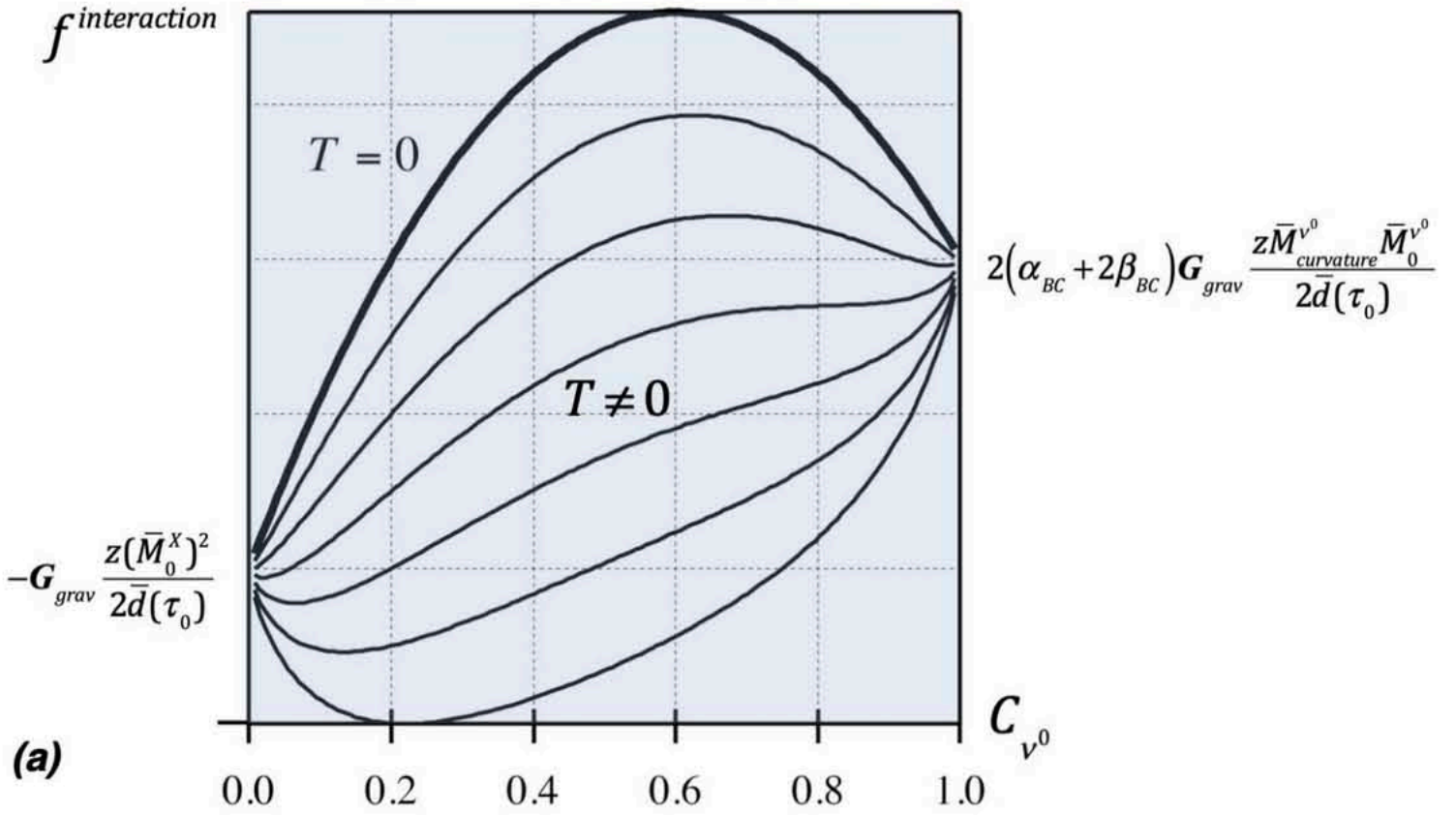
In particular, the theory introduces *the curvature charge*—a property absent from general relativity and the Standard Model—associated with edge dislocation loops. While the gravitational field of the screw disclination loop is largely dominated by *the loop's energy*, producing a long-range gravitational-like field of the 1/r type, the gravitational field of the edge dislocation loop is dominated by *the curvature term*, which also produces a long-range gravitational-like field of the 1/r type. This leads to a difference between the inertial mass and the gravitational mass of the prismatic edge dislocation loop. Furthermore, the equivalent curvature mass can exceed the inertial mass and can even be negative in the case of interstitial-type loops, suggesting the theoretical possibility of repulsive gravity—a phenomenon not predicted by conventional theories.

Particle Composition and Curvature Charge. The model classifies particles according to the nature of their dominant topological singularities:
- *Matter particles* – e.g., electrons, protons, neutrons – contain *twist disclination loops* (giving electrical charge), possible *mixed dislocation loops* (electric dipole moment), and predominantly *interstitial edge loops* with *negative curvature charge*. They are *gravitationally attractive.*
- *Antimatter particles* – e.g., positrons, antiprotons – contain *twist disclination loops*, possible *mixed dislocation loops*, and predominantly *vacancy edge loops* with *positive curvature charge*. They are *gravitationally attractive.*
- *Neutrinos* are *pure interstitial edge loops* with *negative curvature charge*, without disclinations or mixed dislocations. As their equivalent curvature mass is negative and dominate their inertial mass, they are *gravitationally repulsive*.
- *Antineutrinos* are *pure vacancy edge loops* with *positive curvature charge*. They are *gravitationally attractive*.

This structural difference induces *15 possible gravitational interactions* of varying intensities, depending on the type of singularities involved, as particles, antiparticles, neutrinos, antineutrinos, macroscopic vacancy (black holes) or macroscopic interstitial inclusions (neutron stars). In most interactions between particles and/or anti-particles, gravity is attractive but slightly stronger for antiparticles than for particles. In contrast, neutrino–neutrino interactions are repulsive, antineutrino–antineutrino interactions are attractive, and neutrino–antineutrino interactions are extremely weak.

A Plausible Evolutionary Scenario. On the basis of the cosmological expansion-contraction behaviors of the lattice and the gravitational interactions between topological singularities via the local volume expansion of the lattice, we can then imagine a very plausible scenario of cosmological evolution of the topological singularities leading to the current structure of our Universe.

This scenario is entirely based on the fact that, in the case of the simplest edge dislocation loops, analogously similar to neutrinos, the mass of curvature dominates the mass of inertia, so that neutrinos should be the only gravitationally repulsive particles, while anti-neutrinos would be gravitationally attractive. This assertion then allows us to give a simple explanation to several facts that are still very poorly understood in the evolution of matter in the Universe.



$$f^{interaction} \cong \frac{z}{2}\left[-G_{grav}\frac{(\bar{M}^{X}_{0})^2}{\bar{d}(\tau_0)}\left(1-C_{\nu^0}\right)+\frac{1}{2}G_{grav}\frac{\bar{M}^{\nu^0}_{curvature}\bar{M}^{X}_{0}}{\bar{d}(\tau_0)}C_{\nu^0}\left(1-C_{\nu^0}\right)\right]$$
$$-kT_{lattice}\left[C_{\nu^0}\ln C_{\nu^0}+\left(1-C_{\nu^0}\right)\ln\left(1-C_{\nu^0}\right)\right]$$

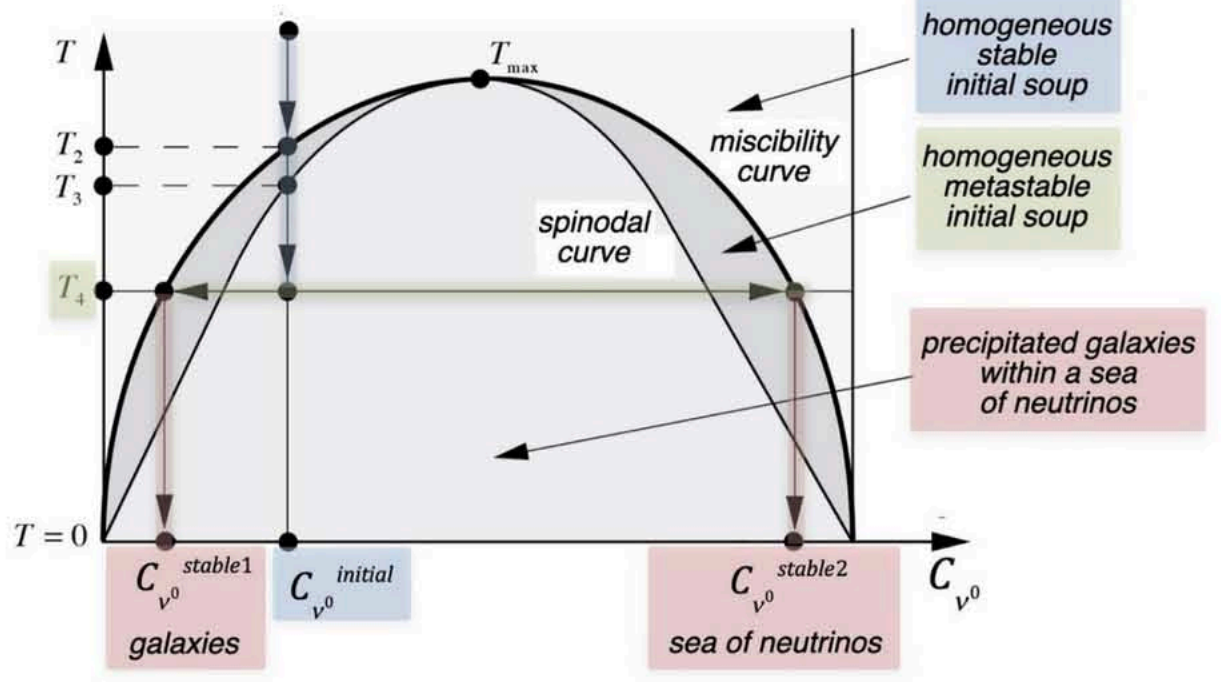


Fig. 21. (a) The particle free interaction energy within the initial hot soup of particles as a function of the concentration of repulsive neutrinos for different lattice temperatures **(b)** Phase diagram of matter in the Universe as a function of lattice temperature

Stage 1 – Big Bounce and Lattice Solidification. At the end of contraction, enormous compression heats the lattice to extreme temperatures, possibly "liquefying" its structure. The rebound initiates cooling, leading to *rapid solidification* into a lattice. As in classical crystallization processes, this transition produces numerous topological defects—dislocations and disclinations, loops, vacancies, interstitials—distributed throughout the lattice space.

Stage 2 – Formation of Elementary Particles. Cooling during inflation causes singularity loops to bind into stable, localized configurations—topological "dispirations"—that correspond to known elementary particles and antiparticles

Stage 3 – Galaxy Formation in a Sea of Repulsive Neutrinos. The initial "hot soup" of particles and anti-particles contains both attractive particles (matter and antimatter) and repulsive neutrinos. As temperature decreases, the system undergoes a *phase separation* (Fig. 21): attractive particles and anti-particles precipitate, while neutrinos form an expansive surrounding medium. This phase transition naturally yields *proto-galaxies* embedded in a *neutrino "ocean."* This mechanism, absent in *classical cosmology*, makes neutrino repulsion the *driver* of galaxy formation.

Stage 4 – Matter–Antimatter Segregation within Galaxies. Gravitational asymmetry between matter and antimatter leads antiparticles to migrate inward toward galactic centers, while matter remains in the periphery. The central zones experience intense annihilation matter-antimatter (producing gamma radiation).

Stage 5 – Disappearance of Antimatter via Black Hole Formation. The antimatter-rich galactic cores undergo *gravitational collapse*, producing macroscopic vacancies that, beyond a certain expansion threshold, behave as *supermassive black holes*. This process explains both the *absence of antimatter* in today's Universe and the observed ubiquity of *massive central black holes in galaxies*.

Stage 6 – Star and Planetary System Formation. With antimatter gone, residual matter coalesces into gas clouds, igniting star formation and generating planetary systems.

Stage 7 – Stellar Collapse and Neutron Stars. Most massive matter stars in galaxies can also undergo gravitational collapse into *macroscopic interstitial singularities*, corresponding to *neutron stars or pulsars*—never into vacancy-type black holes, since they lack the structural composition of antimatter.

Stage 8 – Future Evolution. The Universe continues expanding at an accelerating rate. Approaching a critical expansion value will invert the gravitational constant's sign and eliminate localized quantum modes in favor of the appearance of longitudinal waves, leading to a cataclysmic evolution of the Universe. This stage could be followed by a contraction phase (Fig. 8) and, eventually, another big bounce.

Dark Matter. The pervasive neutrino sea exerts a compressive effect on galaxies, which counterbalances rotational and tidal forces, and which naturally explains the high velocities of peripheral stars. This mechanism directly links the concept of curvature charge in neutrinos to the dark matter problem*, removing the need for dark matter* (unseen exotic mass).

Reinterpretation of Key Cosmological Observations. The cosmological lattice model provides a unified reinterpretation of key cosmological phenomena and their present-day consequences:

- *Matter–Antimatter Asymmetry* – The introduction of curvature charge in dislocation loops provides a single mechanism that explains both the observed asymmetry and the subsequent disappearance of antimatter. This same property drives the segregation of matter and antimatter during galaxy formation.

- *Supermassive Black Holes* – Their universal presence at galactic centers is naturally explained by the gravitational collapse of segregated antimatter, linking the antimatter problem to one of the most striking large-scale structures in the Universe.
- *Neutron Stars* – The collapse of massive stars in the matter-dominated arms of galaxies produces compact stellar remnants (neutron star), whose density and rotation reflect the specific curvature charges and rotation of the initial star.
- *Large-Scale Galaxy Distribution* – The combined effects of matter clustering, antimatter collapse into central black holes, and the compressive action of the neutrino sea shape the hierarchical structure of galaxies, clusters, and filaments observed today.
- *Hubble Constant* – instead of being a universal constant, it emerges as a direct measure of the lattice expansion rate, and therefore varies with cosmological epoch. This connects the large-scale dynamics of the Universe with the microscopic structure of the lattice.
- *Galaxy Redshift* – the observed spectral shifts arise from lattice expansion during photon travel, rather than from Doppler motion. In this framework, no speed-of-light limit applies in the *GO* frame, thereby reconciling observed redshifts at extreme distances.
- *Cosmic microwave background (CMB)* – when the temperature drops to ~3000 K, matter and antimatter become electrically neutral (via atom formation), allowing photons to decouple and propagate freely, producing *the cosmic microwave background (CMB)*. The observed "cooling" of the *CMB* to 2.7 K is explained as a direct effect of lattice expansion altering rulers and clocks *in local HS reference frames*, while in the *GO* frame photon frequency remains constant and only the wavelength stretches.

Conclusion. *The formation of galaxies* could correspond to *a phenomenon of precipitation* of matter and antimatter within a sea of repulsive neutrinos. *The disappearance of antimatter* could correspond to *a phenomenon of segregation* of particles and antiparticles within galaxies, due to their slight difference in gravitational properties, a segregation during which antiparticles would gather in the center of galaxies to finally collapse and form *gigantic black holes in the heart of galaxies*, a phenomenon that perfectly explains *the disappearance of anti-matter from the Universe*.

The cosmological lattice theory unifies aspects of particle physics, gravitation, and cosmology in a coherent framework rooted in topological singularities. Its predictions—particularly regarding neutrino gravitational behavior and the evolution of curvature charge—offer multiple avenues for observational verification. If confirmed, this model would provide a physically grounded alternative to both dark matter and inflationary cosmology, while opening new perspectives on the cyclic nature of the Universe.

Quantum physics

Quantum mechanics, despite its extraordinary predictive power, remains conceptually opaque. The central object of the theory—the wave function—is a mathematical tool without an agreed-upon physical interpretation. Attempts to restore physical meaning, such as de Broglie's pilot-wave theory or Bohm's stochastic mechanics, illustrate the enduring unease about the completeness of the quantum formalism.

From Static to Dynamic Perturbations. In Fig. 13 of the lattice model, a singularity's mass density defines whether expansion perturbations $\tau^{(p)}$ remain static or dynamic. Below the critical threshold, internal distortions balance elastically, producing *a static perturbation field corresponding to a gravitational field*. Above it, equilibrium becomes impossible, and perturbations

$\tau^{(p)}$ of the expansion must oscillate dynamically. This threshold must be identified with the *quantum decoherence limit*, the boundary between classical-like static states and dynamical states fully corresponding to quantum behavior.

These dynamic perturbations obey Newton's second partial equation for lattice expansion (Fig. 22). At first order, localized perturbation solutions exist in the form of exponentially decaying oscillations. These represent stable, bounded fluctuations whose amplitude diminishes with distance but oscillates with a pulsation dependent on the singularity's energy. In effect, singularities become sources of oscillatory gravitational waves confined within the lattice.

Partial Newton's equation for gravitational fluctuations

$$\frac{\partial^2 \tau^{(p)}}{\partial t^2} \cong -c_t^2 \Delta\left[\tau^{(p)} - \frac{K_1}{K_0}\left(\tau^{(p)}\right)^2 - \frac{1}{K_0}\left(F_{dist}^{ch}(\vec{r},t) + F_{pot}^{ch}(\vec{r},t)\right)\right]$$

Isolated gravitational fluctuations

$$\begin{cases} \underline{\tau}_{localisée}^{(p)} \cong \underbrace{\underline{\psi}_0 e^{-\frac{|x_1|}{\delta_1}} e^{-\frac{|x_2|}{\delta_2}} e^{-\frac{|x_3|}{\delta_3}}}_{\underline{\psi}_{localisée}(\vec{r})} e^{(\pm) i\omega_f t} \\ \frac{1}{\delta_1^2} + \frac{1}{\delta_2^2} + \frac{1}{\delta_3^2} = \frac{\omega_f^2}{c_t^2} \end{cases}$$

Gravitational fluctuations associated to a mobile topological singularity

$$\underline{\tau}^{(p)}(\vec{r},t) \cong \hbar^2 \underline{\psi}(\vec{r},t) e^{(\pm) i \underline{\omega}_f(\vec{r},t) t}$$

$$\underline{\omega}_f(\vec{r},t) \cong \underline{\omega}_f\left(E_v(\vec{r},t), \vec{P}_v(\vec{r},t)\right)$$

$$\hbar^2 \frac{\partial^2 \underline{\psi}}{\partial t^2}(\pm) 2\left(\hbar \underline{\omega}_f(\vec{r},t)\right) i\hbar \frac{\partial \underline{\psi}}{\partial t} - \left(\hbar \underline{\omega}_f(\vec{r},t)\right)^2 \underline{\psi} \cong -c_t^2 \hbar^2 \Delta \underline{\psi}$$

Conjecture: *there are two operators which, applied to the wave function of a mobile singularity in the lattice, allow to measure the relativistic energy and momentum of it*

$$\begin{cases} \frac{\partial^2}{\partial t^2}(\hbar^2 \underline{\psi}) \to -\frac{E_v^2}{\hbar^2}(\hbar^2 \underline{\psi}) \\ \Delta(\hbar^2 \underline{\psi}) \to -\frac{\vec{P}_v^{\,2}}{\hbar^2}(\hbar^2 \underline{\psi}) \end{cases} \Rightarrow \begin{cases} i\hbar \frac{\partial}{\partial t} \underline{\psi} \to E_v \underline{\psi} \\ -i\hbar \frac{\partial}{\partial x_i} \underline{\psi} \to P_{vi} \underline{\psi} \end{cases}$$

$$E_v(\vec{r},t)(\mp)\hbar \underline{\omega}_f(\vec{r},t) \cong [\pm] i \sqrt{c_t^2 \vec{P}_v^{\,2}(\vec{r},t)}$$

Relativistic relations

$$E_v^2 = M_0^2 c_t^4 + \vec{P}_v^{\,2} c_t^2 \qquad \gamma = \sqrt{1 - \frac{\vec{v}^2}{c_t^2}}$$

$$\begin{cases} E_v = \frac{M_0 c_t^2}{\gamma} = \frac{E_0^{dist} + V(\vec{r},t)}{\gamma} \\ M_0 c_t^2 = E_0^{dist} + V(\vec{r},t) \\ \vec{P}_v = \frac{M_0}{\gamma} \vec{v} = \frac{E_0^{dist} + V(\vec{r},t)}{\gamma c_t^2} \vec{v} \end{cases}$$

$$\begin{cases} \underline{\omega}_f(\vec{r},t) = (\pm)\frac{E_v}{\hbar}\left(1[+] i\frac{\boldsymbol{v}}{c_t}\right) = (\pm)\frac{1}{\hbar}\frac{E_0^{dist} + V(\vec{r},t)}{\gamma}\left(1[+] i\frac{\boldsymbol{v}}{c_t}\right) \\ \underline{\omega}_f^*(\vec{r},t) = (\pm)\frac{E_v}{\hbar}\left(1[-] i\frac{\boldsymbol{v}}{c_t}\right) = (\pm)\frac{1}{\hbar}\frac{E_0^{dist} + V(\vec{r},t)}{\gamma}\left(1[-] i\frac{\boldsymbol{v}}{c_t}\right) \end{cases}$$

$$\left|\underline{\omega}_f\right|(\vec{r},t) = \sqrt{\underline{\omega}_f \underline{\omega}_f^*} = \frac{1}{\hbar} E_v \sqrt{1 + \frac{\vec{v}^2}{c_t^2}} = \frac{1}{\hbar}\sqrt{E_v^2 + c_t^2 \vec{P}_v^{\,2}}$$

Relativistic wave equation for gravitational fluctuations

$$\hbar^2 \frac{\partial^2 \underline{\psi}}{\partial t^2} + 2E_v\left(1[\pm] i\frac{\boldsymbol{v}}{c_t}\right) i\hbar \frac{\partial \underline{\psi}}{\partial t} - E_v^2\left(1[\pm] i\frac{\boldsymbol{v}}{c_t}\right)^2 \underline{\psi} \cong -c_t^2 \hbar^2 \Delta \underline{\psi}$$

Fig. 22. From Newton's partial equation for gravitational fluctuations to the relativistic wave equation for the fluctuations associated with a moving singularity

To connect these fluctuations with measurable quantities, *a conjecture* has to be made, which postulates a correspondence between derivatives of the wave function and physical observables:
- the *second time derivative* correlates with the square of relativistic energy,
- the *spatial Laplacian* correlates with the square of relativistic momentum.

Introducing a universal scaling constant—identified with *Planck's constant*—aligns these relations with the canonical operators of quantum mechanics. This conjecture is not arbitrary: it arises naturally from the dynamics of lattice fluctuations and thus provides a physical grounding for the operator formalism of quantum mechanics.

Relativistic Regime. For a massive singularity moving at relativistic speeds, the relativistic wave equation predicts (Fig. 23):
- *Temporal oscillations* with frequency increasing with energy and diverging as velocity approaches the speed of light.
- *Spatial oscillations* whose wavelength contracts with velocity, reproducing Lorentz contraction.
- *Envelope decay* narrowing with increasing energy, meaning fluctuations become more localized for massive or fast-moving singularities.

$$\underline{\psi}(\vec{r},t) \cong \psi_0 \, e^{i\underline{k}(\vec{r},t)x_2} \rightarrow \hbar^2 \frac{\partial^2 \underline{\psi}}{\partial t^2} + 2E_{\mathbf{v}}\left(1[\pm]i\frac{\mathbf{v}}{c_t}\right)i\hbar\frac{\partial \underline{\psi}}{\partial t} - E_{\mathbf{v}}^2\left(1[\pm]i\frac{\mathbf{v}}{c_t}\right)^2 \underline{\psi} \cong -c_t^2\hbar^2\Delta\underline{\psi}$$

$$\underline{k}(\vec{r},t) \cong \{\pm\} i\frac{E_{\mathbf{v}}}{\hbar c_t}\left(1[\pm]i\frac{\mathbf{v}}{c_t}\right) \rightarrow \underline{\tau}^{(p)}(\vec{r},t) \cong \hbar^2\psi_0 \, e^{\{-\}\frac{E_{\mathbf{v}}}{\hbar c_t}\left|x_2[\mp]\mathbf{v}t\right|} e^{i\frac{E_{\mathbf{v}}}{\hbar}\left(t[\pm]\frac{\mathbf{v}}{c_t^2}x_2\right)}$$

$$\tau_{réel}^{(p)}(\vec{r},t) \cong \hbar^2\psi_0 \, e^{(-)\frac{E_{\mathbf{v}}}{\hbar c_t}\left|x_2[\mp]\mathbf{v}t\right|} \cos\left[\frac{E_{\mathbf{v}}}{\hbar}\left(t[\pm]\frac{\mathbf{v}\,x_2}{c_t^2}\right)\right]$$

Relativistic gravitational perturbations

$$f = \frac{E_{\mathbf{v}}}{2\pi\hbar} = \frac{E_0^{dist} + V(\vec{r},t)}{2\pi\hbar\gamma} = \frac{E_0^{dist} + V(\vec{r},t)}{2\pi\hbar\sqrt{1-\frac{\vec{\mathbf{v}}^{\,2}}{c_t^2}}} \quad \textit{(frequency of perturbations)}$$

$$\lambda = \frac{2\pi\hbar c_t^2}{E_{\mathbf{v}}\mathbf{v}} = \frac{2\pi\hbar c_t^2\gamma}{\left(E_0^{dist} + V(\vec{r},t)\right)\mathbf{v}} = \frac{2\pi\hbar c_t^2}{\left(E_0^{dist} + V(\vec{r},t)\right)\mathbf{v}}\sqrt{1-\frac{\vec{\mathbf{v}}^{\,2}}{c_t^2}} \quad \textit{(wave length of perturbations)}$$

$$\delta = \frac{\hbar c_t}{E_{\mathbf{v}}} = \frac{\hbar c_t\gamma}{E_0^{dist} + V(\vec{r},t)} = \frac{\hbar c_t}{E_0^{dist} + V(\vec{r},t)}\sqrt{1-\frac{\vec{\mathbf{v}}^{\,2}}{c_t^2}} \quad \textit{(spatial range of perturbations)}$$

Fig. 23. Associated gravitational perturbations
to a massive singularity moving at relativistic speed

These predictions echo relativistic effects described in special relativity, but here they are derived from lattice dynamics rather than spacetime geometry.

The wave function is no longer abstract. It is the *mathematical representation of oscillatory gravitational fluctuations* coupled to singularities. Regions where the amplitude vanishes correspond to zones with negligible gravitational oscillations—hence negligible probability of finding a singularity. Conversely, zones of high amplitude correspond to a high likelihood of presence.

Non-Relativistic Limit. When motion is slow and a potential dominates, the relativistic wave equation reduces to a *non-relativistic form* identical to *Schrödinger's equation* (Fig. 24)

$$\hbar^2\frac{\partial^2\underline{\psi}}{\partial t^2}+2E_{\mathbf{v}}\left(1[\pm]i\frac{\mathbf{v}}{c_t}\right)i\hbar\frac{\partial\underline{\psi}}{\partial t}-E_{\mathbf{v}}^2\left(1[\pm]i\frac{\mathbf{v}}{c_t}\right)^2\underline{\psi}\cong-c_t^2\hbar^2\Delta\underline{\psi}$$

Relativistic wave equation

non-relativistic speeds ← $|\mathbf{v}|\ll c_t$

$$\hbar^2\frac{\partial^2\underline{\psi}}{\partial t^2}+2E_{\mathbf{v}}\,i\hbar\frac{\partial\underline{\psi}}{\partial t}-E_{\mathbf{v}}^2\underline{\psi}\cong-c_t^2\hbar^2\Delta\underline{\psi}$$

conjecture 10 ← $-\hbar^2\frac{\partial^2\underline{\psi}}{\partial t^2}\to E_{\mathbf{v}}^2\underline{\psi}$

$$i\hbar\frac{\partial\underline{\psi}}{\partial t}\cong-\frac{c_t^2\hbar^2}{2E_{\mathbf{v}}}\Delta\underline{\psi}+E_{\mathbf{v}}\underline{\psi}$$

non-relativistic speeds ← $E_{\mathbf{v}}=\frac{M_0c_t^2}{\gamma}=\frac{E_0^{dist}+V(\vec{r},t)}{\gamma}\underset{|\mathbf{v}|\ll c_t}{\cong}\begin{cases}M_0c_t^2\\E_0^{dist}+V(\vec{r},t)\end{cases}$

$$i\hbar\frac{\partial\underline{\psi}}{\partial t}\cong-\frac{\hbar^2}{2M_0}\Delta\underline{\psi}+\left(E_0^{dist}+V(\vec{r},t)\right)\underline{\psi}$$

Non-relativistic wave equation and associated gravitational perturbations

$$\underline{\tau}^{(p)}\cong\hbar^2\underline{\psi}\,e^{\pm i\omega_f t}\cong\hbar^2\underline{\psi}(\vec{r},t)e^{\pm i\frac{E_{\mathbf{v}}}{\hbar}t}\cong\hbar^2\underline{\psi}(\vec{r},t)e^{\pm i\frac{E_0^{dist}+T+V(\vec{r},t)}{\hbar}t}$$

change of fonction ← $\underline{\psi}\left(\vec{r},t\right)=\underline{\psi}_H\left(\vec{r},t\right)e^{-i\frac{E_0^{dist}}{\hbar}t}$

$$i\hbar\frac{\partial\underline{\psi}_H}{\partial t}\cong-\frac{\hbar^2}{2M_0}\Delta\underline{\psi}_H+V(\vec{r},t)\underline{\psi}_H\left(\vec{r},t\right)$$

Classical Schrödinger's equation and associated gravitational perturbations

$$\underline{\tau}^{(p)}\cong\hbar^2\underline{\psi}\,e^{-i\omega_f t}\cong\hbar^2\underline{\psi}\,e^{-i\frac{E_0^{dist}+T+V(\vec{r},t)}{\hbar}t}=\hbar^2\underline{\psi}_H\left(\vec{r},t\right)e^{-i\frac{H}{\hbar}t}$$

Fig. 24. Non-relativistic wave equation and Schrödinger's equation in the case of gravitational perturbations associated to a massive singularity moving at non-relativistic speed

The Hamiltonian $H=T+V(\vec{r},t)$ emerges as the sum of kinetic and potential energies of the singularity. Stationary solutions correspond to eigenstates with quantized energies, just as in standard quantum theory.

The last one relation for $\underline{\tau}^{(p)}$ in Fig. 24 allows us *for the first time* to give a comprehensible interpretation to quantum mechanics by saying that:

"The Schrödinger equation is an equation deduced from the second partial equation of Newton of a perfect cosmological lattice, which allows us *to calculate the wave function* $\underline{\psi}_H(\vec{r},t)$ of a topological singularity, representing *the amplitude and phase of the dynamic gravitational fluctuations of pulsation* $\omega = H/\hbar$ associated with its Hamiltonian H".

Stationary Case. In static potentials, the wave equation reduces further to the *time-independent Schrödinger equation*, leading to discrete eigenvalues and eigenfunctions. Physically, this describes standing gravitational oscillations modulated by the potential landscape (Fig. 25).

$$i\hbar\frac{\partial\underline{\psi}}{\partial t} \cong -\frac{\hbar^2}{2M_0}\Delta\underline{\psi} + \left(E_0^{dist} + V(\vec{r})\right)\underline{\psi}$$ ***Non-relativistic wave equation***

conjecture 10 ← $i\hbar\frac{\partial}{\partial t}\underline{\psi} \to E_v\underline{\psi}$

$$-\frac{\hbar^2}{2M_0}\Delta\underline{\psi} + V(\vec{r})\underline{\psi} = \left(E_v - E_0^{dist}\right)\underline{\psi} = \left(E^{cin} + V\right)\underline{\psi} = H\underline{\psi}$$ *Wave equation independent of time*

eigen values of the energy ← $H = H_n$

$$-\frac{\hbar^2}{2M_0}\Delta\underline{\psi}_n + V(\vec{r})\underline{\psi}_n = H_n\underline{\psi}_n$$ ***Stationary Schrödinger's equation***

stationnary wave function ← $\underline{\psi}_n$

$$\underline{\tau}_n^{(p)}(\vec{r},t) \cong \hbar^2\underline{\psi}_n(\vec{r})\,\mathrm{e}^{\pm i\frac{E_0+H_n}{\hbar}t}$$ ***Stationary gravitational perturbations***

Fig. 25. Schrödinger's standing wave equation with eigenvalues for a massive singularity placed in a static potential

Quantum Phenomena Reinterpreted. This approach naturally explains the emergence of wave–particle duality, Heisenberg's uncertainty principle, bosons and fermions, Pauli's exclusion principle, and quantum entanglement:

- *Wave–Particle Duality:* In this model, the *singularity is the particle* and the *gravitational fluctuation field is the wave*. Their coexistence makes wave–particle duality a straightforward consequence rather than a paradox**.**
- *Double-Slit Experiment*. A singularity passes through one slit, but its fluctuation field spans both. Interference arises when fields recombine, guiding the trajectory of the singularity and producing the observed statistical pattern.
- *Uncertainty Principle.* Non-commutativity of operators derived from the conjecture in Fig. 22 yields Heisenberg's uncertainty relations. Measurement imprecision reflects the inherent coupling between position and momentum encoded in gravitational fluctuations, not an intrinsic randomness of nature.

- *Entanglement and Decoherence.* When two singularities share a common fluctuation field, they become *entangled***:** perturbing one modifies the shared field, immediately affecting the other. Decoherence occurs when the shared field is disrupted, decoupling the singularities.

- *Bosons, Fermions, and the Exclusion Principle.* When two singularities coexist in the same potential, *symmetric superpositions (bosons)* allow them to share states without destructive interference of fluctuations of pulsation $\omega=\left(2E_0+H_n+H_m\right)/\hbar$, and *antisymmetric superpositions (fermions)* annihilate fluctuations of pulsation $\omega=\left|H_n-H_m\right|/\hbar$ if states coincide, embodying *Pauli's exclusion principle.* This distinction emerges directly from the behavior of lattice perturbations, not as an imposed axiom, as shown in Fig. 26.

$$\begin{cases} -\dfrac{\hbar^2}{2M_0}\Delta\underline{\psi}_n(\vec{r}_a)+V(\vec{r}_a)\underline{\psi}_n(\vec{r}_a)=H_n\underline{\psi}_n(\vec{r}_a) & \times\ \underline{\psi}_m(\vec{r}_b) \\ -\dfrac{\hbar^2}{2M_0}\Delta\underline{\psi}_m(\vec{r}_b)+V(\vec{r}_b)\underline{\psi}_m(\vec{r}_b)=H_m\underline{\psi}_m(\vec{r}_b) & \times\ \underline{\psi}_n(\vec{r}_a) \end{cases} \quad \Sigma$$

$$-\frac{\hbar^2}{2M_0}\Delta\left[\underline{\psi}_n(\vec{r}_a)\underline{\psi}_m(\vec{r}_b)\right]+\left[V(\vec{r}_a)+V(\vec{r}_b)\right]\underline{\psi}_n(\vec{r}_a)\underline{\psi}_m(\vec{r}_b)=\left(H_n+H_m\right)\underline{\psi}_n(\vec{r}_a)\underline{\psi}_m(\vec{r}_b)$$

$$\underline{\tau}\left(\vec{r}_a,\vec{r}_b,t\right)=\hbar^2\underline{\psi}_n(\vec{r}_a)\mathrm{e}^{\left(\pm\right)i\frac{E_0+H_n}{\hbar}t}\underline{\psi}_m(\vec{r}_b)\mathrm{e}^{\left[\pm\right]i\frac{E_0+H_m}{\hbar}t}$$

$$\begin{cases} \underline{\tau}_{boson}\left(\vec{r}_a,\vec{r}_b,t\right)=\hbar^2\underline{\psi}_n(\vec{r}_a)\underline{\psi}_m(\vec{r}_b)\mathrm{e}^{\left(\pm\right)i\frac{1}{\hbar}\left(2E_0+H_n+H_m\right)t} \\ \underline{\tau}_{fermion}\left(\vec{r}_a,\vec{r}_b,t\right)=\hbar^2\underline{\psi}_n(\vec{r}_a)\underline{\psi}_m(\vec{r}_b)\mathrm{e}^{\left(\pm\right)i\frac{1}{\hbar}\left(H_n-H_m\right)t} \end{cases}$$

symmetric wave function for a superposition of bosons

$$\underline{\Psi}_{sym}=\alpha\sum_{a,b,\ldots,N}\psi_n(\vec{r}_a)\psi_m(\vec{r}_b)\ldots\psi_k(\vec{r}_N)$$

antisymmetric wave function for a superposition of fermions

$$\underline{\Psi}_{anti}=\beta\begin{vmatrix}\psi_n(\vec{r}_a) & \psi_n(\vec{r}_b) & \ldots\\ \psi_m(\vec{r}_a) & \psi_m(\vec{r}_b) & \ldots\\ \ldots & \ldots & \ldots\end{vmatrix}$$

Fig. 26. Stationary equation for the superposition of topological singularities, gravitational fluctuations of bosons and fermions and symmetrical and anti-symmetrical wave functions

- *Relation to Bohmian Mechanics*. The approach parallels Bohm's pilot-wave theory but grounds the guiding wave in the *real physical substrate* of lattice fluctuations. Unlike purely formal pilot waves, these fluctuations have measurable energetic content and obey Newtonian equations.

- *Reconciling Einstein and Quantum Mechanics,* Einstein's critique of quantum theory—that it lacked completeness—finds validation here. The probabilistic nature of quantum outcomes is not fundamental but arises from stochastic dynamics of singularities, akin to Brownian motion or walking droplets experiments. Hidden variables exist, but they are *non-local gravitational fluctuations*, consistent with Bell's theorems.

- *The Role of Planck's Constant*. Planck's constant enters naturally as the scaling factor between wave function derivatives and energetic terms. This raises the possibility that Planck's constant is not fundamental but derivable from lattice parameters, offering a deeper origin of quantization

Conclusion. We have established a coherent framework where quantum mechanics emerges as the *microscopic manifestation of gravitational fluctuations* in a cosmological lattice. Schrödinger's equations, uncertainty principles, and particle statistics all follow directly from Newton's second partial equation of the lattice once the quantum decoherence limit is surpassed.

This approach demystifies the wave function, explains quantum probabilities as expressions of fluctuating gravitational fields, and unifies classical and quantum descriptions under a single lattice-based mechanics. If correct, this framework implies that *quantum physics is already a gravitational theory*, rendering unnecessary attempts to "quantize gravitation" in the traditional sense.

Topological and Classical Interpretation of Quantum Spin

Spin is a cornerstone of modern quantum mechanics, yet its physical meaning remains enigmatic. In the standard view, spin is treated as an intrinsic quantum number without classical analogue. Attempts by early quantum theorists to interpret spin as the self-rotation of a particle were abandoned because the equatorial velocity of such a rotation would exceed the speed of light. However, within the cosmological lattice framework—where space is modeled as an elastic medium populated by topological singularities—this objection disappears. Near the core of singularity loops, static expansion is extremely high, raising the effective local speed of light and allowing rotational motions that would otherwise be forbidden. This reinterpretation opens the possibility that spin is, in fact, a quantized rotational motion of loops of topological defects.

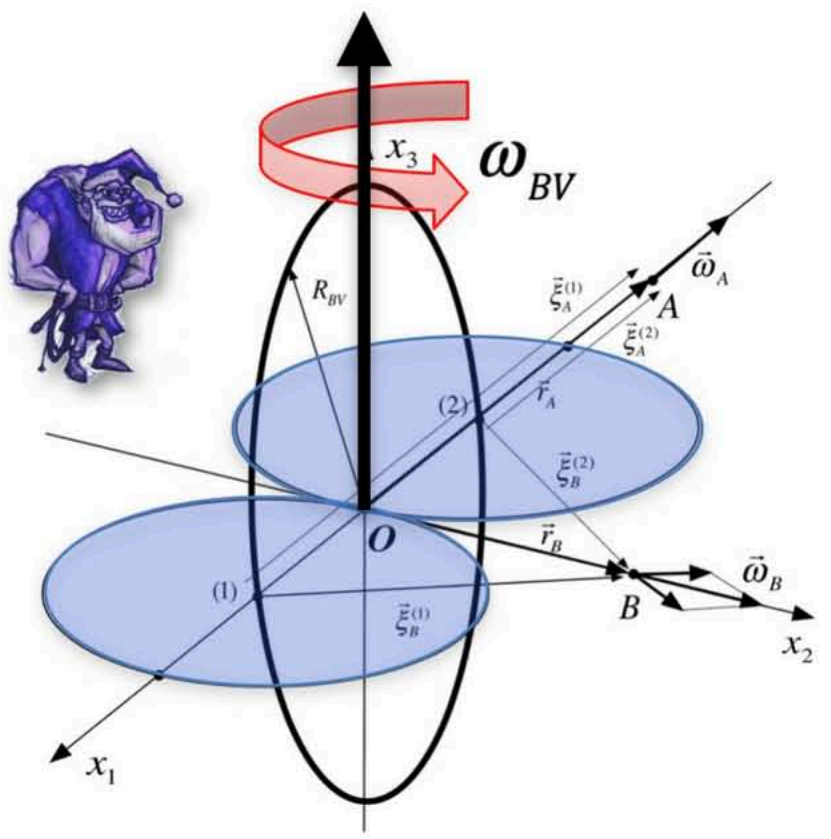
As a matter of fact, using a simplified form of Newton's second partial equation applied within the torus surrounding a *twist disclination loop*, one finds that static solutions require unrealistic constraints on elastic moduli. Numerical estimates, using analogies with electron parameters, confirm that these conditions cannot be met. Therefore, the internal field of gravitational perturbations inside the loop cannot remain static. This leads to the conjecture that, in the perfect cosmological lattice, the loop must adopt a dynamic state.

Classic treatment of the loop rotation. The only possible dynamic solution is a confined rotation of the loop on itself. Treating the loop as a classic rotating toroidal object with distributed mass yields expressions for its moment of inertia, angular momentum and kinetic energy (Fig. 27).

Because the loop carries a rotation charge (analogous to electric charge), its rotation induces a *magnetic moment*. The ratio of magnetic moment to angular momentum, i.e. *the gyromagnetic ratio*, emerges naturally and is approximately equal to 2, recovering the *Bohr magneton* for electrons.

Quantization*:* Assuming that the twist disclination loop actually turns on itself, this microscopic movement of rotation will induce a field of gravitational fluctuations in the vicinity of the loop, depending on the second partial Newton equation.

Now we saw in the previous part that, in the absence of a time-varying potential, Newton's second partial equation leads to the stationary Schrödinger equation, illustrated in Fig. 25. The treatment of the rotation movement of a microscopic object around an axis by the stationary Schrödinger equation is succinctly summarized in Fig. 28.



Angular momentum $(\delta_1 \cong 1)$

$$\vec{L}_{BV} = \delta_1 \oint \vec{r} \wedge \vec{v}\, dm = \delta_1 \vec{e}_{axe} \int_0^{R_{BV}} 4 \int_0^{\pi/2} \underbrace{r\cos\theta}_{|\vec{r}|} \underbrace{r\cos\theta\, \omega_{BV}}_{|\vec{v}|} \underbrace{\frac{\delta_1 M_0^{BV}}{\pi R_{BV}^2} r d\theta dr}_{dm} = \delta_1 \frac{M_0^{BV} R_{BV}^2}{4} \omega_{BV} \vec{e}_{axis} \cong I_{BV} \omega_{BV} \vec{e}_{axis}$$

$$\rightarrow \quad I_{BV} = \delta_1 \frac{M_0^{BV} R_{BV}^2}{4} \quad \textit{(moment of inertia)}$$

Magnetic moment $(\delta_2 \cong 1)$

$$\vec{\mu}_{BV} = \delta_2 \frac{1}{2} \oint \vec{r} \wedge \vec{v}\, d\boldsymbol{q} = \delta_2 \vec{e}_{axis} 2 \int_0^{\pi/2} \underbrace{R_{BV}\cos\theta}_{|\vec{r}|} \underbrace{R_{BV}\cos\theta\, \omega_{BV}}_{|\vec{v}|} \underbrace{\frac{\boldsymbol{q}_{\lambda BV}}{2\pi} d\theta}_{d\mathbf{q}} = \delta_2 \frac{R_{BV}^2 \boldsymbol{q}_{\lambda BV}}{4} \omega_{BV} \vec{e}_{axis} \cong g_{BV} \frac{\boldsymbol{q}_{\lambda BV}}{2M_0^{BV}} \vec{L}_{BV}$$

$$\rightarrow \quad g_{BV} = 2\frac{\delta_2}{\delta_1} \cong 2 \quad \textit{(gyromagnetic ratio)}$$

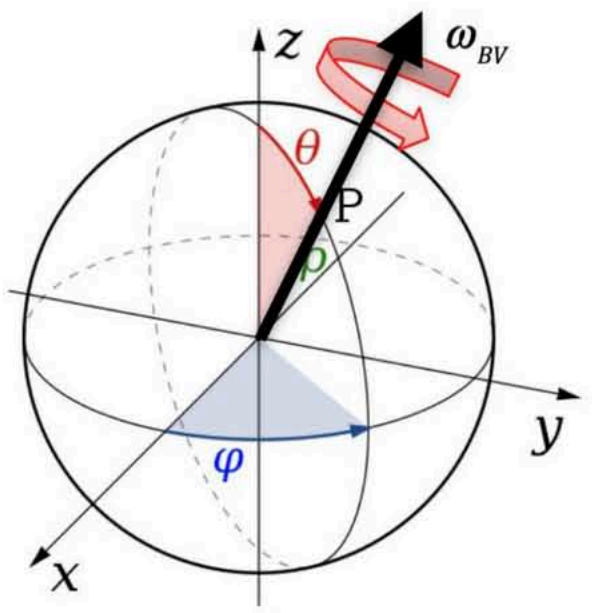
Kinetic energy

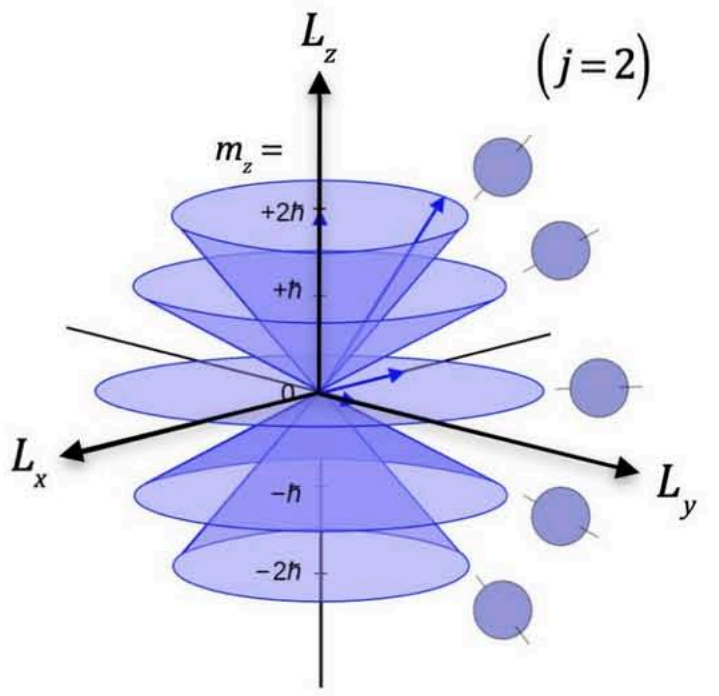
$$E_{rotation\,BV}^{cin} = \delta_1 \frac{1}{2} \oint \vec{v}^2\, dm = \delta_1 \int_0^{R_{BV}} 2 \int_0^{\pi/2} \underbrace{r^2\cos^2\theta\, \omega^2}_{\vec{v}^2} \underbrace{\frac{M_0^{BV}}{\pi R_{BV}^2} r d\theta dr}_{dm} = \delta_1 \frac{M_0^{BV} R_{BV}^2}{8} \omega_{BV}^2 \cong \frac{2\vec{L}_{BV}^2}{\delta_1 M_0^{BV} R_{BV}^2} \cong \frac{\vec{L}_{BV}^2}{2I_{BV}}$$

Fig. 27. Classic solution of rotation of the twist disclination loop: angular momentum, magnetic moment and kinetic energy.

For a particle subject to rotation, it is preferable to describe the operator $\hat{H}$ linked to the classical Hamiltonian in spherical coordinates (θ,φ). In the absence of a potential, this operator $\hat{H}$ is linked to the square operator of the angular momentum $\hat{L}^2$ by the last relation obtained in Fig. 27. With the expression of this operator in spherical coordinates, we deduce the stationary Schrödinger's equation in spherical coordinates, whose stationary solutions have quantified energy levels $\varepsilon_j = \hbar^2\, j(j+1)/2I_{BV}$ of rotation.

For each value of the energy ε_j corresponding to a given angular speed, there are $2j+1$ different eigenstates corresponding conventionally to different orientations of the axis of rotation. It is said that the energy state ε_j has a degeneracy of $2j+1$.





Square angular momentum operator in spherical coordinates

$$\hat{L}^2 = -\hbar^2\left[\frac{1}{r^2\sin\theta}\frac{\partial}{\partial\theta}\left(\sin\theta\frac{\partial}{\partial\theta}\right)+\frac{1}{r^2\sin^2\theta}\frac{\partial^2}{\partial\varphi^2}\right]$$

Stationary Schrödinger's equation in spherical coordinates

$$\hat{H}\underline{\psi}_n = \frac{\hat{L}^2}{2I_{BV}}\underline{\psi}_n(\theta,\varphi) = \varepsilon_n\underline{\psi}_n(\theta,\varphi)$$

Stationary gravitational fluctuations in spherical coordinates

$$\underline{\tau}_n^{(p)}(\theta,\varphi) \cong \hbar^2\underline{\psi}_n(\theta,\varphi)\exp\left(\pm i(E_0+\varepsilon_n)t/\hbar\right)$$

The spin of a twist disclination loop

$$E^{cin}_{rotationBV} = \varepsilon_n = \frac{\hbar^2}{2I_{BV}}j(j+1) \qquad (j=0,1,2,\ldots)$$

$$\vec{L}^2_{BV} = 2I_{BV}E^{cin}_{rotationBV} = \hbar^2\, j(j+1)$$

$$\left|\vec{L}_{BV}\right| = \hbar\sqrt{j(j+1)}$$

$$L_z = \hbar m_z \qquad (m_z = j, j-1, \ldots, 1-j, -j)$$

$$\vec{\mu}_{BV\,z} \cong g_{BV}\frac{\boldsymbol{q}_{\lambda BV}}{2M_0^{BV}}L_z\vec{e}_z = g_{BV}\frac{\hbar\boldsymbol{q}_{\lambda BV}}{2M_0^{BV}}m_z\vec{e}_z$$

$$\omega_{BV} \cong \pm\left(\frac{8E^{cin}_{rotationBV}}{\delta_1 M_0^{BV}R_{BV}^2}\right)^{1/2} = \pm\frac{4\hbar}{\delta_1 M_0^{BV}R_{BV}^2}\sqrt{j(j+1)}$$

$$v_{equatorial} = R_{BV}\omega_{BV} = \pm\frac{4\hbar}{\delta_1 M_0^{BV}R_{BV}}\sqrt{j(j+1)}$$

Fig. 28. Quantum solution of rotation of the twist disclination loop: quantified rotational energy levels and magnetic quantum number

It is *the magnetic quantum number* $\boldsymbol{m_z}$ that characterizes the quantification of the projection of the angular momentum along a certain axis $\boldsymbol{z}$. It can take the $\boldsymbol{2j+1}$ following values $\boldsymbol{m_z = j, j-1, \ldots, 1-j, -j}$, so that the projection $\boldsymbol{L_z}$ of the angular momentum on an axis $\boldsymbol{Oz}$ takes the values $L_z = \hbar m_z$.

Apart from the kinetic energy and the kinetic momentum of the loop, we still deduce *the quantized magnetic moment* of the loop along the axis $\boldsymbol{Oz}$, which depends directly on the magnetic quantum number $\boldsymbol{m_z}$, which also depends on *the Landé factor* $\boldsymbol{g_{BV}}$ of the screw loop, which is roughly equal to 2 in the case of the twist disclination loop, but which would depend on the distribution of mass and charge in the case of other types of topological singularities. We note that, in the expression of the quantified momentum, we then find the value of the famous *Bohr magneton*, namely $\hbar\boldsymbol{q}_{\lambda BV}/2M_0^{BV}$.

Finally, the resolution of the stationary Schrödinger equation in this case makes it possible to deduce the eigen wave functions $\underline{\psi}_n(\theta,\varphi)$ correlated to the different energy levels ε_j, and to use them to obtain the stationary gravitational perturbations $\underline{\tau}_n^{(p)}$ in the immediate vicinity of the loop under the form $\underline{\tau}_n^{(p)}(\theta,\varphi) \cong \hbar^2 \underline{\psi}_n(\theta,\varphi)\exp\left(\pm i(E_0+\varepsilon_n)t/\hbar\right)$.

Conclusion. A longstanding objection to the "classical rotation" interpretation of spin is that the equatorial velocity would exceed the light velocity. Within this framework, however, the *local speed of light* is enhanced by the enormous static expansion near the loop core. Explicit calculations show that the condition $v_{equatoriale} = R_{BV}\omega_{BV} < c$ is satisfied, making the rotational motion both possible and necessary. Hence, spin can be regarded as a *real, relativistically consistent rotation.*

In this reinterpretation, *spin is not an abstract intrinsic property* but a real, quantized rotational motion of topological loops within the cosmological lattice.

This model reproduces all known features of spin—discrete angular momentum, degeneracy, magnetic moments—while resolving the apparent conflict with relativity. It also bridges the gap between fermions and bosons as topological manifestations of different rotational states. At the cosmological scale, it has also been shown that the existence of spin enforces constraints on the dynamics of the Universe, linking microscopic loop structure to macroscopic cosmic evolution.

Attempt to explain the Standard Model with a "Colored" FCC Cosmological Lattice

We present here an *hypothetical reinterpretation of the Standard Model* of particle physics based on the concept of a *colored face-centered cubic (FCC) cosmological lattice*. In this framework, fundamental particles are identified with *topological singularities* such as screw disclination loops and edge dislocation loops, embedded in the lattice. The quantization of charges, the origin of color, the emergence of baryons and mesons, the structure of weak and strong interactions, and the replication of particle families are explained as direct consequences of the mechanical and topological constraints of the lattice. The model also introduces the concept of *curvature charge*, which provides a physical origin for the matter–antimatter asymmetry and clarifies the distinction between fermions and bosons.

Emergence of "colors". The foundation of this hypothetical model is a *face-centered cubic lattice* in which the densest crystallographic planes are assigned cyclic colors *(R, G, B)*. This coloring reflects in fact the existence of *preferred orientations of planes* and enforces three strict *stacking rules*:

- *Rule 1*: the *RGB* alternation of the dense planes cannot be disrupted without introducing *stacking faults* that cost very high *stacking fault surface energies*,
- *Rule 2*: connections between misaligned planes perpendicular to the dense planes generate a *connecting fault plane* perpendicular to the dense planes, with a non-zero *connecting surface fault energy* γ_0,
- *Rule 3*: rotations of a lattice plane with an angle of $\pm\pi/3$ or $\pm 2\pi/3$ *permute its color assignment*.

Quarks as Dispirations. These simple geometrical rules already encode the possibility of *fractional quantization of charge*: screw disclination loops inserted in this structure naturally carry charges in multiples of 1/3, reproducing the charge spectrum of quarks.

Quarks are modeled as *dispirations*, i.e., coupled entities formed from screw disclination loops and edge dislocation loops (Fig. 29). As already discussed, the *weak interaction* is interpreted as a short-range coupling between screw disclination loops and edge dislocation loops, and this association reduces strongly the formation energy of quarks by allowing to respect the first stacking rules.

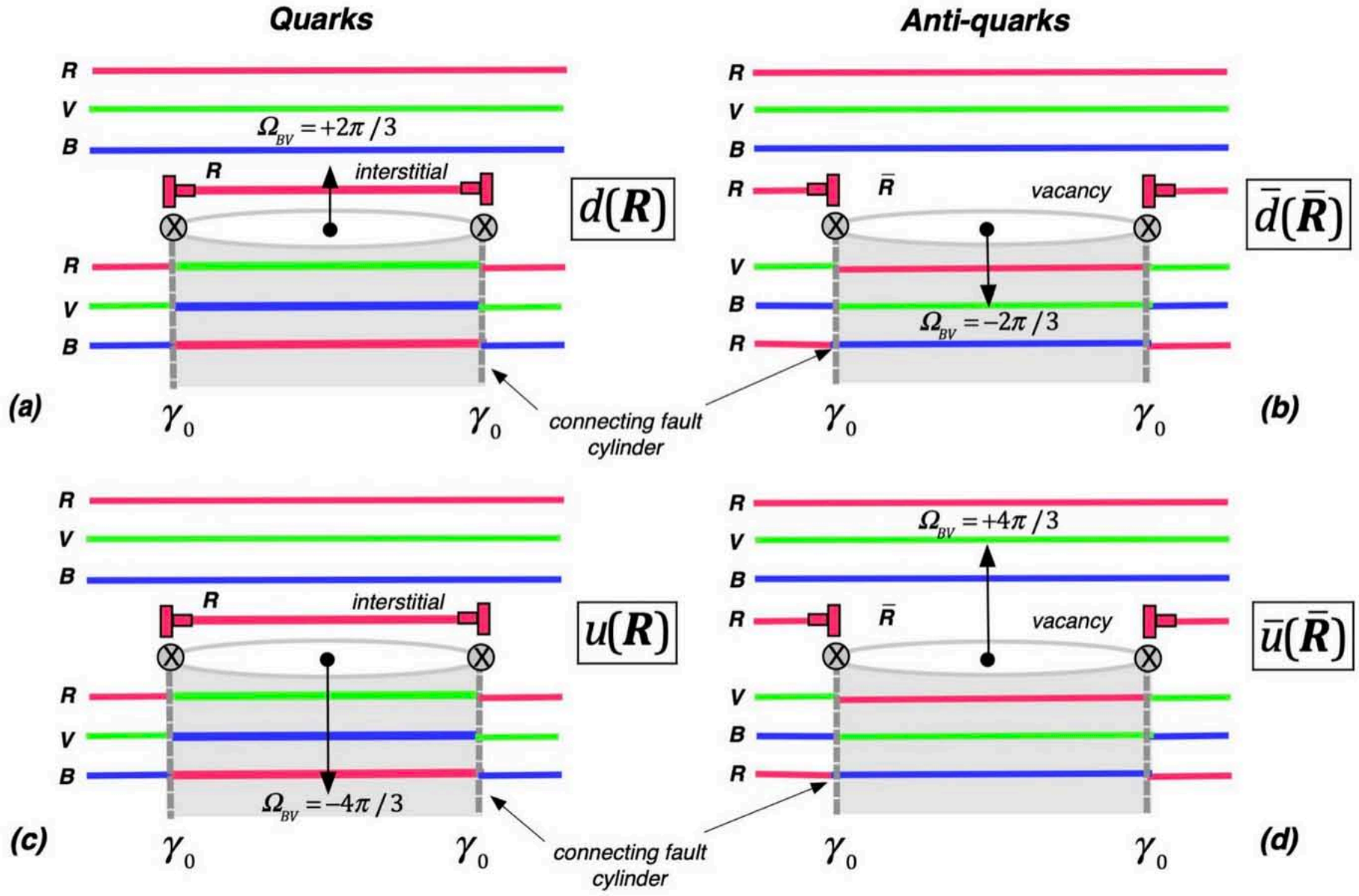


Fig. 29. Quarks and antiquarks formed by combinations of screw disclination loops of quantized angles with edge dislocation loops which ensure the continuity of succession of planes **R,B,V.**

Table 30. The four quarks composed of a screw disclination loop combined with an interstitial or lacunar edge dislocation loops

name	Ω_{BV}	$q_{\lambda BV}$	edge loop	$q_{\theta BC}$	color
d	$+2\pi/3$	$-2\pi^2 R_{BV}^2/3$	interstitial	$-2\pi a$	**R**, **V** ou **B**
u	$-4\pi/3$	$+4\pi^2 R_{BV}^2/3$	interstitial	$-2\pi a$	**R**, **V** ou **B**
$\bar{d}$	$-2\pi/3$	$+2\pi^2 R_{BV}^2/3$	vacancy	$+2\pi a$	$\bar{\boldsymbol{R}}$, $\bar{\boldsymbol{V}}$ ou $\bar{\boldsymbol{B}}$
$\bar{u}$	$+4\pi/3$	$-4\pi^2 R_{BV}^2/3$	vacancy	$+2\pi a$	$\bar{\boldsymbol{R}}$, $\bar{\boldsymbol{V}}$ ou $\bar{\boldsymbol{B}}$

Their fractional rotation charges $q_{\lambda BV}$ ($\pm 2\pi^2 R_{BV}^2/3, \pm 4\pi^2 R_{BV}^2/3$) emerge from the rotation Ω_{BV} ($\pm\pi/3$ or $\pm 2\pi/3$) carried by the screw disclination, while the *color charge (R, G, B)* corresponds to the cyclic *RGB* orientation of the lattice planes disturbed by the defect. The three colors of quarks (red, green, blue) are therefore not abstract quantum numbers but *geometric properties of the*

lattice. Antiquarks correspond to the complementary defects of the quark. The edge dislocation loops associated in the disclination loops can be of *interstitial or vacancy type*, and carry a curvature charge $q_{\theta BC}$ (Table 30).

Gluons are particles allowing to exchange the "color orientation" of the quarks they connect. They correspond well to pairs of edge dislocation loops propagating between quarks, and they are massless due to their lattice symmetries (Fig. 31).

This approach offers a *mechanical analog* of Yang–Mills fields, but rooted in the geometry of the cosmological lattice.

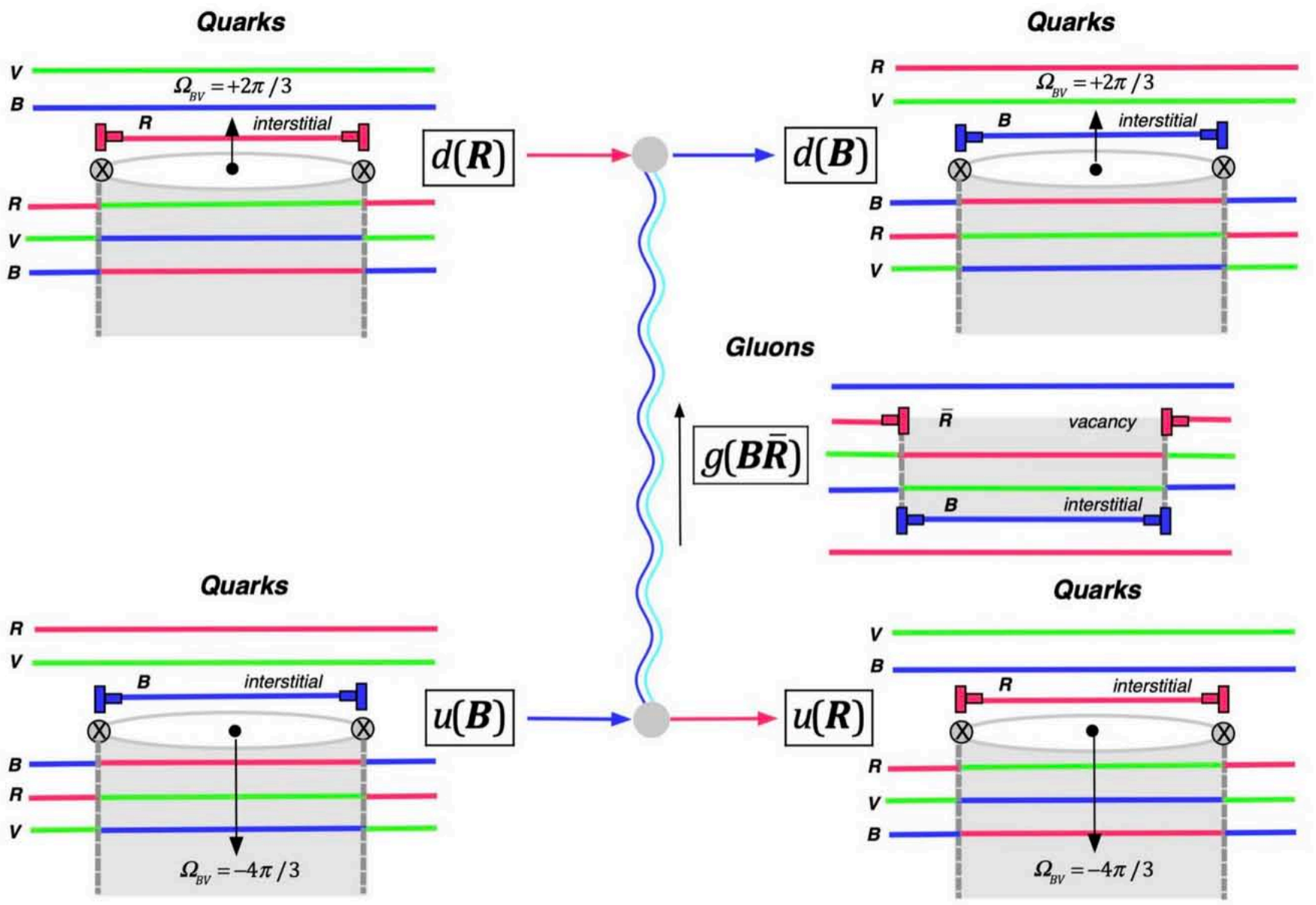


Fig. 31. Feynman diagram of the color exchange of two quarks by the exchange of a bicolor gluon

Strong Interaction, Confinement and Asymptotic Freedom. The *strong interaction* arises because dispirations composing the quarks cannot exist freely without violating stacking rules: they must be confined in color-neutral combinations (triplets or pairs), in which each quark is connected to the others by a *cylinder of connecting fault of surface fault energy* γ_0. This naturally explains why free quarks are unobservable.

At long separation distances, the energy stored in these connecting fault cylinders *increases linearly with the separation distance*, leading finally to a *quark confinement* with a constant force of interaction, as experimentally proved by the *Jefferson Lab Data* [38]. When trying to separate quarks, the energy stored in the *cylinder of connecting fault* increases to the point where it creates new quark–antiquark pairs: isolating a quark without hadronization is then impossible. At short separation distances, the interaction weakens, producing an *asymptotic freedom* effect, fully consistent with *QCD* phenomenology.

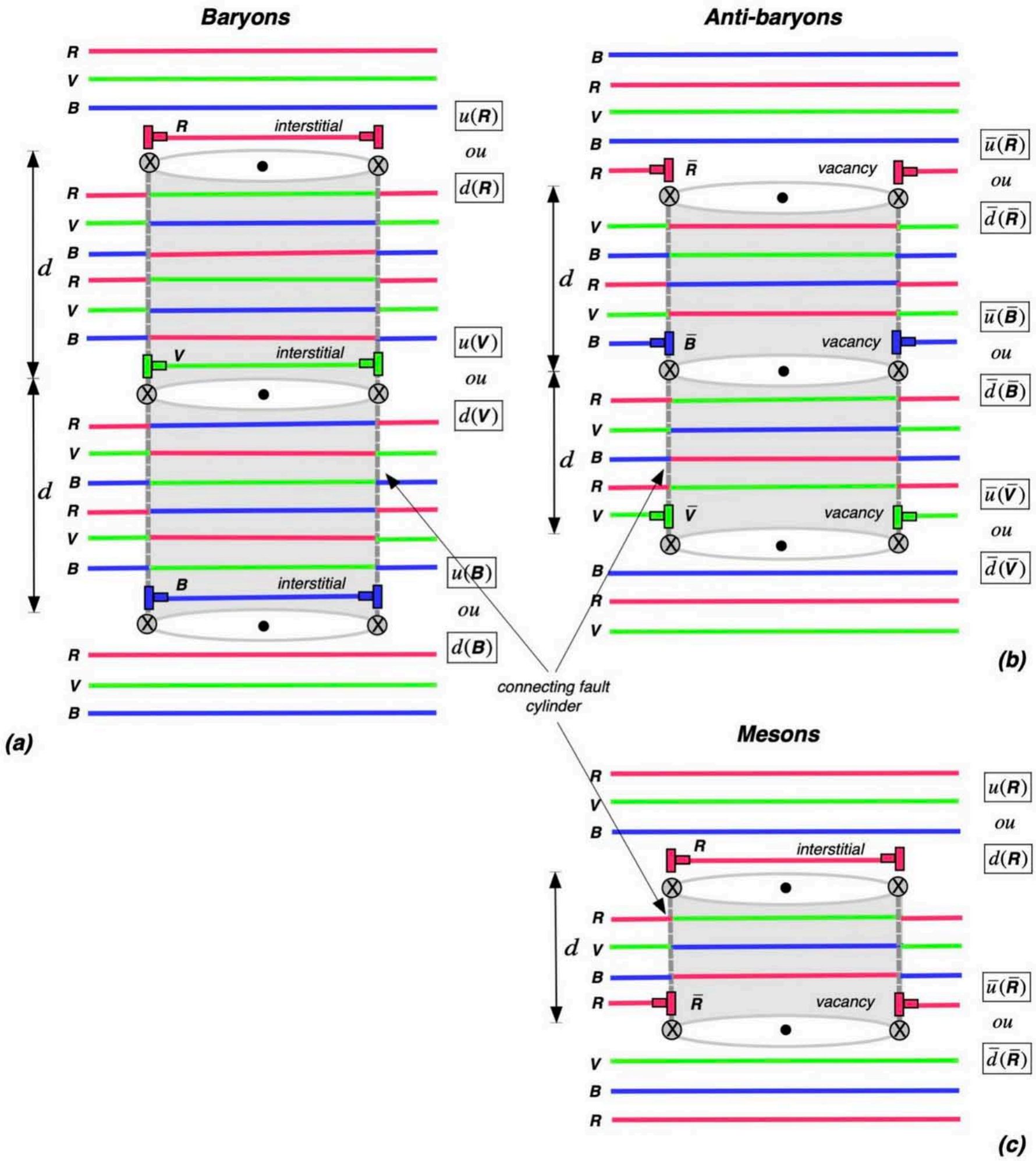


Fig. 32. The three possible combinations of 2 or 3 dispirations (quarks) allowing to form perfectly localized topological singularities: the baryons **(a)** and **(b)**, and the mesons **(c)**.

Baryons, Mesons, and Composite Particles. The necessary confinement of quarks lead to two types of stable particles: the *baryons* and the *mesons* (Fig. 32).

- *Baryons* of table 33, which are formed from triplets of dispirations (quarks) whose combined colors sum to neutrality *(R+G+B)*. The fractional charges add up to integer values (e.g., proton, neutron). Spin and magnetic moments emerge from the collective rotation of the loops.

- *Mesons* of table 34, which correspond to quark–antiquark pairs, color-neutral due to cancellation of *RGB* with *anti-RGB*.

Table 33. The "white" baryons formed by 3 quarks, and the four "leptons" obtained by collapsing combinations of three same quarks.

combina-tions	*symbol spin 1/2*	*symbol spin 3/2*	Ω_{BV}	$q_{\lambda BV}$	*edge loop*	$q_{\theta BC}$
$d\,d\,d$	e^- (?) *electron*	Δ^-	$+2\pi$	$-2\pi^2 R_{BV}^2$	*interstitial*	$-6\pi a$
$d\,u\,d$	n *neutron*	Δ^0	0	0	*interstitial*	$-6\pi a$
$u\,d\,u$	p *proton*	Δ^+	-2π	$+2\pi^2 R_{BV}^2$	*interstitial*	$-6\pi a$
$u\,u\,u$	e^{++} (???) *lepton ?*	Δ^{++}	-4π	$+4\pi^2 R_{BV}^2$	*interstitial*	$-6\pi a$
$\bar{d}\,\bar{d}\,\bar{d}$	$\bar{e}^+$ (?) *positron*	$\bar{\Delta}^+$	-2π	$+2\pi^2 R_{BV}^2$	*vacancy*	$6\pi a$
$\bar{d}\,\bar{u}\,\bar{d}$	$\bar{n}$ *antineutron*	$\bar{\Delta}^0$	0	0	*vacancy*	$6\pi a$
$\bar{u}\,\bar{d}\,\bar{u}$	$\bar{p}$ *antiproton*	$\bar{\Delta}^-$	$+2\pi$	$-2\pi^2 R_{BV}^2$	*vacancy*	$6\pi a$
$\bar{u}\,\bar{u}\,\bar{u}$	$\bar{e}^{--}$ (???) *anti-lepton ?*	$\bar{\Delta}^{--}$	$+4\pi$	$-4\pi^2 R_{BV}^2$	*vacancy*	$6\pi a$

Table 34. The "white" mesons formed by a quark and an anti-quark.

combina-tions	*symbol spin 0*	*symbol spin 1*	Ω_{BV}	$q_{\lambda BV}$	*edge loop*	$q_{\theta BC}$
$d\,\bar{d}$	π^0	ρ^0	0	0	-	0
$d\,\bar{u}$	π^-	ρ^-	$+2\pi$	$-2\pi^2 R_{BV}^2$	-	0
$\bar{d}\,u$	π^+	ρ^+	-2π	$+2\pi^2 R_{BV}^2$	-	0
$u\,\bar{u}$	η^0	ω^0	0	0	-	0

This construction reproduces completely the observed *hadronic spectrum*, including the spin composition leading to the difference between spin ½ baryons (proton, neutron) and spin 3/2 baryons (Δ baryons), and the spin 0 mesons (π and η mesons) and the spin 1 mesons (ρ and ω mesons). In the case of the triplet combinations of Fig. 32, it appears that the triplets composed of three identical quarks or anti-quarks with total spin ½ do not correspond to existing baryons, but could correspond to leptons of different electrical charges. This surprising point is discussed in detail in references [10,11].

Leptons. Leptons arise from simpler loop configurations (Fig. 35 and Table 36):

- *Neutrinos and anti-neutrinos* correspond to pure edge dislocation loops inserting or removing three consecutive colored planes (*RGB* or *anti-RGB*) in order to respect the first stacking rule. Their *helicity (left-handed helicity of neutrino* versus *right-handed helicity of anti-neutrino)* follows directly from the geometry of these insertions and the stacking rules of the colored cosmological lattice. The fact that neutrinos and anti-neutrinos are always respectively left-handed and right-handed is very important, because it explains *the phenomenon of parity violation in the weak interaction*.

- *Electrons and positrons* are modeled as screw disclination loops with angle of rotation Ω_{BV} of $\pm 2\pi$, combined with triple edge dislocation loops, and bounded by *the weak interaction force* (Fig. 18).

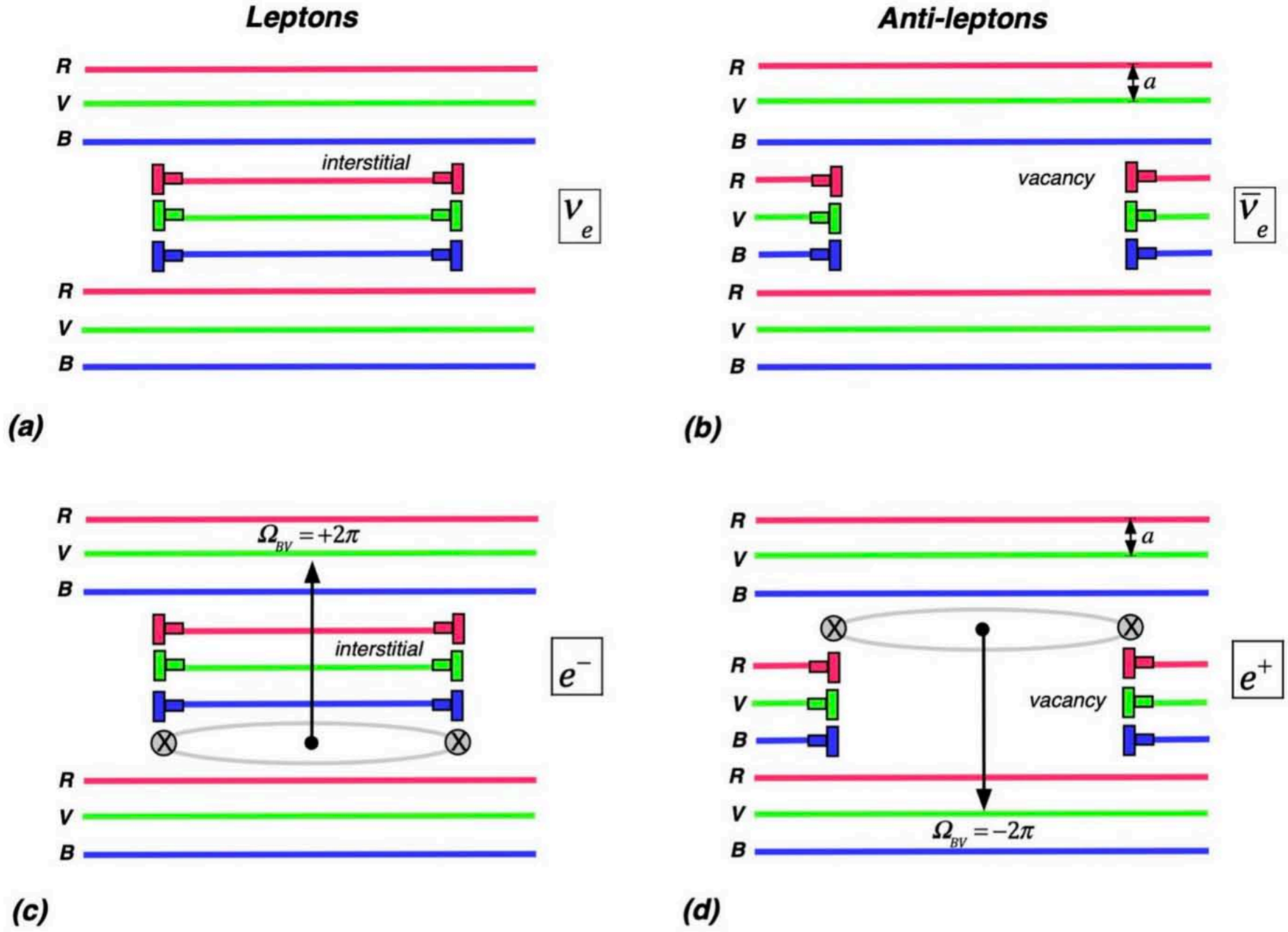


Fig. 35. Structure of the neutrino, the anti-neutrino, the electron and the positron, as assemblies of edge dislocation loops and screw disclination loops.

Table 36. The leptons of the first family and the intermediate gauge bosons.

symbol	Ω_{BV}	$q_{\lambda BV}$	*edge loop*	$q_{\theta BC}$
ν_e	0	0	*interstitial*	$-6\pi a$
e^-	$+2\pi$	$-2\pi^2 R_{BV}^2$	*interstitial*	$-6\pi a$
$\bar{\nu}_e$	0	0	*vacancy*	$6\pi a$
e^+	-2π	$+2\pi^2 R_{BV}^2$	*vacancy*	$6\pi a$
W^-	$+2\pi$	$-2\pi^2 R_{BV}^2$	-	0
W^+	-2π	$+2\pi^2 R_{BV}^2$	-	0
Z^0	$(+2\pi)+(-2\pi)$	0	-	0

Massive Bosons. Other configurations are produced when the angle of rotation Ω_{BV} of the screw disclination loop is $\pm 2\pi$, but without combination with edge dislocation loops, corresponding to the *W and Z bosons* (Table 36). The high mass of the *W* charged bosons results from the concentration of a screw disclination of angle $\pm 2\pi$ within extremely small distances, due to the absence of edge dislocation loops which are not necessary to respect the stacking rules in this case. And the *Z* boson of neutral charge could correspond to a particle composed of two pure screw disclination loops of rotation angle $+2\pi$ and -2π bounded by their opposed electrical charges. These massive bosons allow the weak interaction to operate not only in the case of *weak leptonic interactions* as in Fig. 18, but also between quarks.

Attempt to explain the three families of quarks and leptons of the Standard Model

In the Standard Model, there are not only the quarks and leptons just described, but there are also two additional families of quarks and leptons, distinguished mainly by the much higher masses observed experimentally each time one moves from one family to the next.

The fact that there are two additional families with much higher energies could perhaps be attributed to the appearance of stacking faults between dense axial planes, faults that were initially eliminated by rule 1. In fact, we constructed the first family of particles taking this rule into account, i.e., by ensuring that the ***R, V, B*** sequence of dense planes is never violated. To do this, we had to introduce edge dislocation loops of the correct color to describe quarks, and introduce a triple edge loop of three colors to describe leptons.

Let us imagine that there could be stacking faults between the dense planes of the lattice. There are only two types of stacking faults that are possible: either a faulty alternation of planes of the type ***X-Y-X***, or a faulty alternation of the type ***X-X***.

Let us assume that the defect energies associated with these two types of stacking faults are essentially due to the axial properties of these planes, and therefore have axial surface defect energies γ_{1a} and γ_{1b} respectively. The defect energy γ_{1a} is associated with an ***X-Y-X*** type stacking

fault, while the defect energy γ_{1b} is due to an ***X-X*** type stacking fault. The fault energy γ_{1a} is therefore related to a stacking error with the second neighboring plane, while γ_{1b} is related to a stacking error with the first neighboring plane. There is therefore a strong possibility that the energy γ_{1b} will be significantly higher than the energy γ_{1a}, and therefore that $\gamma_{1b} >> \gamma_{1a}$.

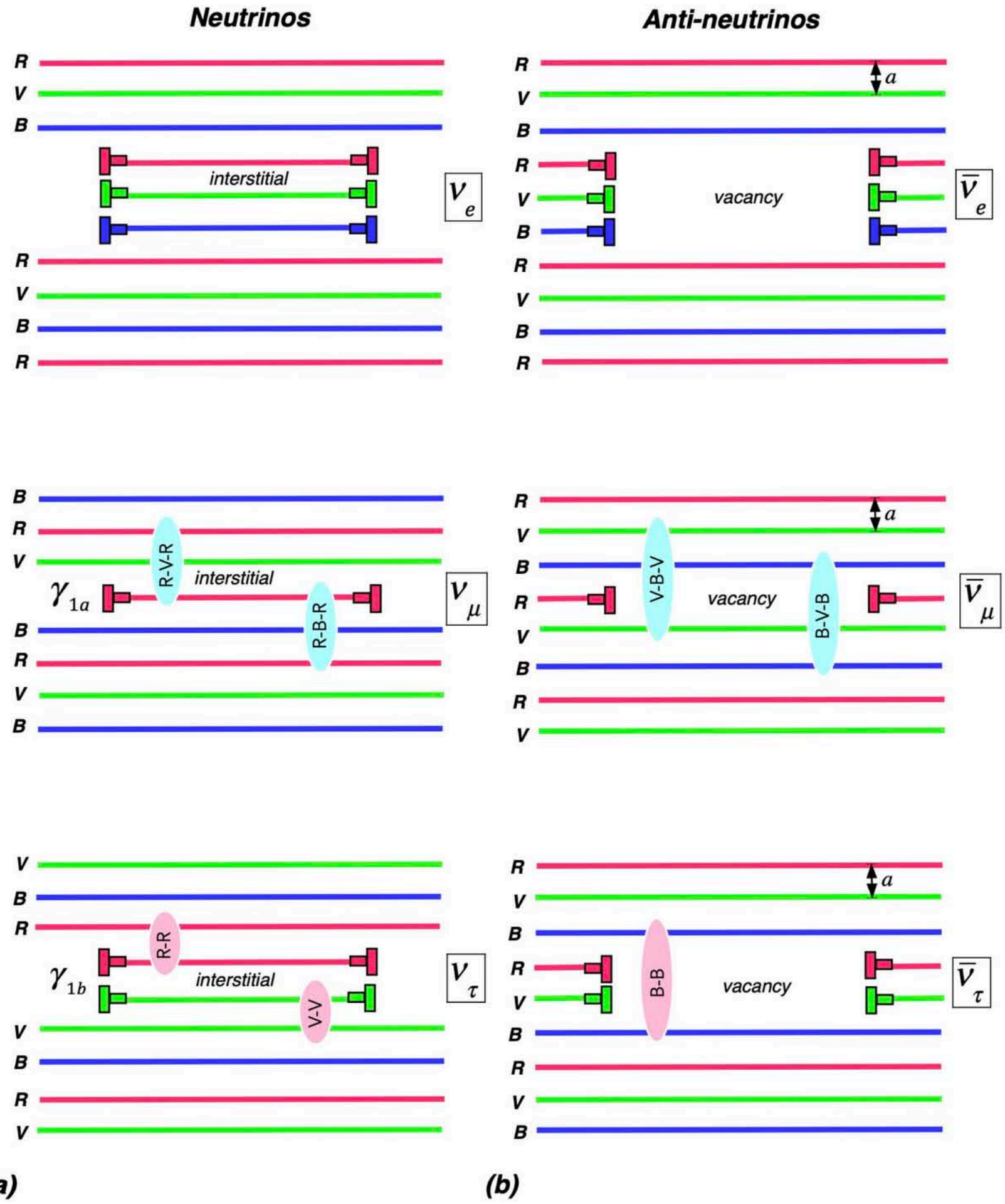


Fig. 37. The three families of neutrinos and anti-neutrinos obtained by removing or adding one or two dense planes, with the appearance of stacking faults of type **X-Y-X** and **X-X**.

On the possible constitution of neutrino families. Let's take the case of neutrinos, which we know exist in three different states or three "flavors," as physicists say: electron, muon, and tau. By removing or adding one or two planes to the electron neutrino and antineutrino in Fig. 35, we can construct the six neutral leptons shown in Fig. 37.

On the possible constitution of electron families. In the case of electrons and anti-electrons in Fig. 38, it suffices to add to the neutrinos in Fig. 35 the screw disclination loops with a rotation angle Ω_{BV} of $\pm 2\pi$ respectively. In these cases, we obtain the electrons and anti-electrons of the first

family, the muons and anti-muons of the second family, and the taus and anti-taus of the third family shown in Fig. 37.

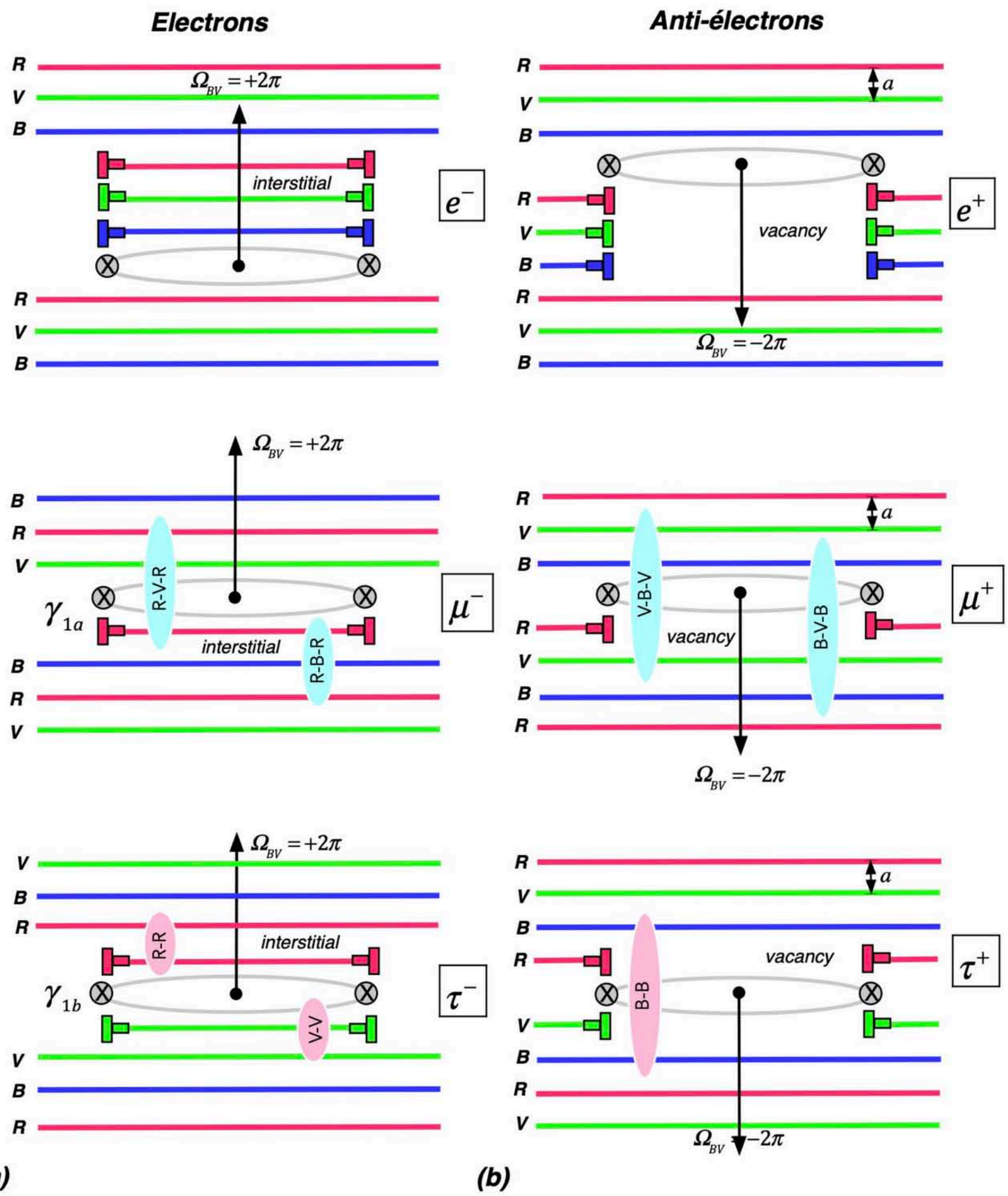


Fig. 38. The three families of electrons and anti-electrons obtained by removing or adding two or one dense plane, in combination with a screw disclination loop.

On the possible constitution of quark families. In the case of quarks, we can add or subtract 1 or 2 axial dense planes to quarks u and d and/or anti-quarks $\bar{u}$ and $\bar{d}$, so as to reveal stacking faults in the axial dense planes with energies γ_{1a} or γ_{1b}.

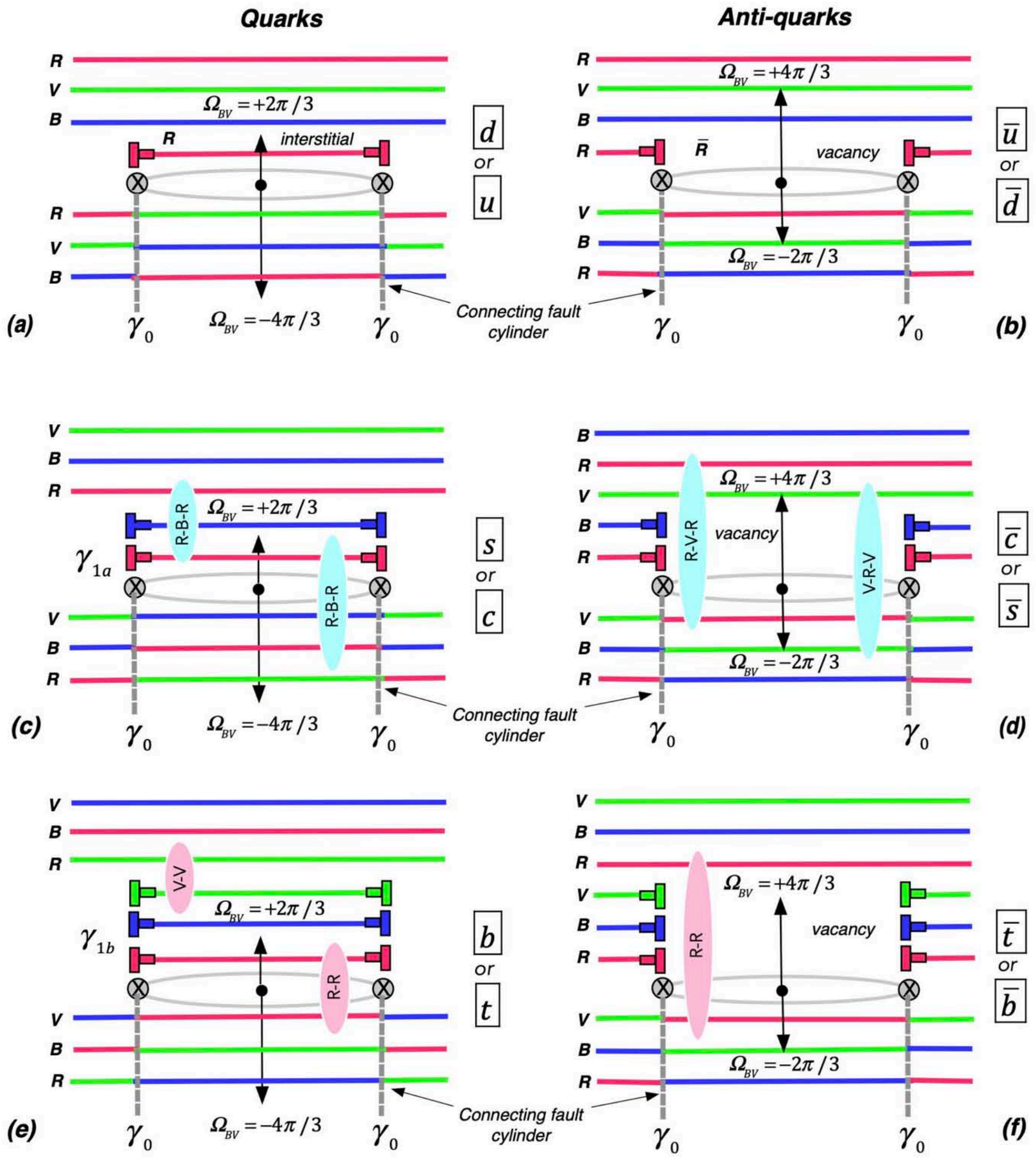


Fig. 39. The three families of quarks and anti-quarks obtained by adding or removing one or two dense planes, in combination with a screw disclination loop.

This gives us the family of *quarks* shown in Fig. 39, which is also composed of three generations of two types of electrically charged particles: the first generation consists of *down* (***d***) and *up* (***u***) quarks, with electric charges of -1/3 and +2/3 of the electric charge of the electron, respectively; a second generation composed of *strange* (***s***) and *charm* (***c***) quarks, with electric charges of -1/3 and +2/3 of the electric charge of the electron, respectively, and a third generation composed of *bottom* (***b***) and *top* (***t***) quarks, with electric charges of -1/3 and +2/3 of the electric charge of the electron, respectively.

Each quark also has its own antiparticle with the opposite electric charge ($\bar{d}, \bar{u}, \bar{s}, \bar{c}, \bar{b}, \bar{t}$).

Quark decay via weak interaction. According to this hypothetical model describing the three families of quarks and their respective flavors *d, u, s, c, b,* and *t*, based on the existence of ***X-Y-X*** and ***X-X*** stacking faults between dense planes, we can deduce the pathways through which quarks should decay. The diagram of possible decays is shown in Fig. 40.

With this hypothetical model, we find the usual pure decays via weak interaction during the transformations *u->d, c->s*, and *t->b* within the same family. On the other hand, the decays from one family to another *c->d, s->u, t->s, b->c, t->d*, and *b->u* do not correspond exactly to the decays described in the literature since, in addition to the emission of a usual boson W^+ or W^-, *the emission of a lepton* ν_μ *ou* ν_τ *must be added to respect the number of axial planes during the decay.* This discrepancy with the usual theory of the standard model should make it possible to experimentally verify or refute the idea that the existence of three families of elementary particles could be due to energies γ_{1a} and γ_{1b} of stacking faults of dense planes in a "colored" *FCC* lattice.

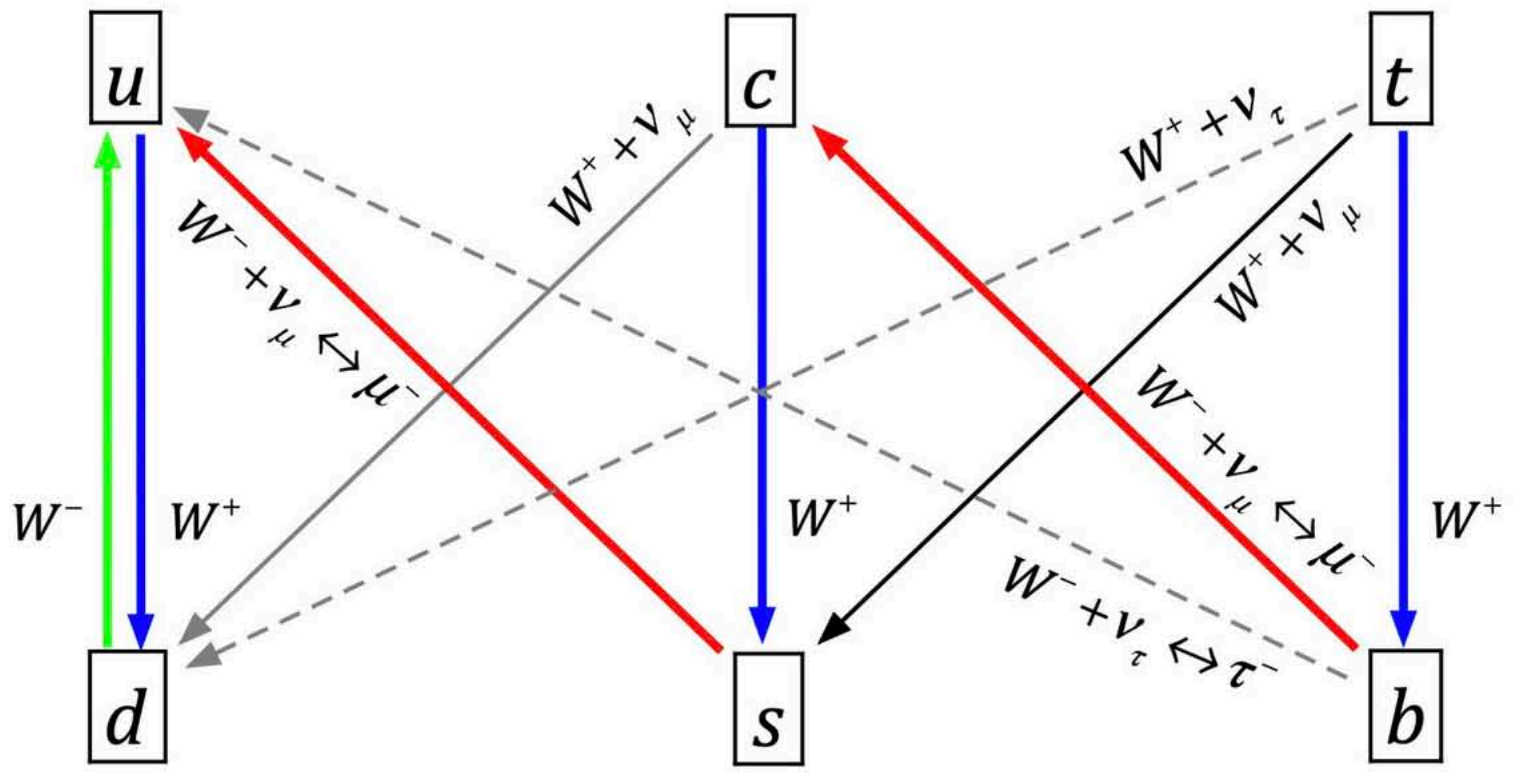


Fig. 40. Diagram of possible quark decays via weak interaction, with particles produced according to each decay pathway.

Conclusion. This hypothetical *colored FCC cosmological lattice* provides a topological reinterpretation of the Standard Model, unifying quarks, leptons, and bosons as manifestations of screw disclination loops and edge dislocation loops. Fractional charge, color, confinement, weak parity violation, and family replication all emerge naturally from the geometry and stacking rules of the lattice. The introduction of *curvature charge* offers a physical explanation for matter–antimatter asymmetry and the fermion–boson distinction. While open questions remain, this model suggests a possible *mechanical and geometrical foundation of particle physics*, connecting the Standard Model to the deeper structure of the cosmological lattice.

Quantum fluctuations of the vacuum, cosmological theory of multiverses and gravitons

It is still possible to deduce some *very hypothetical consequences* of the perfect cosmological lattice associated with *pure gravitational fluctuations (fluctuations of the scalar lattice expansion).*

One can imagine the existence of pure longitudinal fluctuations within the cosmological lattice that can be treated either as random gravitational fluctuations that could have an analogy with *the quantum fluctuations of the vacuum*, or as stable gravitational fluctuations, which could lead at the

macroscopic scale to *a cosmological theory of Multiverses*, and at the microscopic scale to the existence of a form of *stable quasi-particles that could be called gravitons*, by analogy with photons, but which in fact have nothing in common with the gravitons usually postulated in the framework of General Relativity.

General Conclusion

This paper does not claim to present a fully developed *Theory of Everything*, but rather to show that a rigorous approach to elastic solid lattices using Eulerian coordinates provides a framework for investigation that is much simpler than differential geometries—such as those used, for example, in general relativity—and that is potentially very rich and fruitful, since it has been shown quite simply that it is possible to reveal very strong and often perfect analogies with all the major physical theories of the macrocosm and the microcosm.

In this approach, *Newton's equation* presented in Fig. 7 plays a central and crucial role, as it underlies most of the astonishing properties of the cosmological lattice. It also introduces the perfectly novel concept of *the curvature charge of edge dislocation loops*, which is an unavoidable consequence of treating a solid lattice and its topological singularities in Euler coordinates. This concept, which is entirely absent from all modern theories of physics, provides explanations for numerous obscure points in modern theories. As for the structure of the cosmological lattice, it also plays a dominant role in the analogies we have developed. Indeed, it was necessary to imagine *a face-centered cubic lattice with an axial property of the dense planes*—imaginatively "colored" red, green, and blue—satisfying certain simple rules regarding their arrangement, in order to find topological loops surprisingly analogous to all the particles—leptons, quarks, intermediate bosons, and gluons—of the Standard Model.

However, it is clear that this cosmological lattice, despite its undeniable successes, still contains many unclear points that deserve to be studied and, if possible, clarified. But despite these unclear points, it appears that this *Theory of the Crystalline Ether* contains many strong analogies with all the major theories of modern physics, and that in this respect it possesses enormous unifying power. And this approach to the Universe via a cosmological lattice is very simple, unlike the superstring theories or M-theory proposed by theorists to "forcefully" unify physical theories, which leads to extremely complicated mathematics in very complex n-dimensional spaces (n=11 for M-theory) and which to date have shown no predictive power.

It is interesting to note here that modern theories rely on strings and branes in complicated multidimensional spaces to quantize gravity, whereas our approach also relies on strings, loops, and membranes, but which are then simple topological singularities of a purely three-dimensional lattice, with an additional dimension of absolute time completely decoupled from the spatial dimensions, since time can be measured there by the universal clock of a ***GO*** outside the lattice in absolute space.

And if the quasi-static volumetric expansion of this cosmological lattice on the macroscopic scale is the manifestation of phenomena attributed to *gravity*, the dynamic fluctuations in the expansion of this lattice on the microscopic scale are nothing other than the manifestation of phenomena attributed to *quantum physics*. It is therefore erroneous to seek to quantify the theory of gravity, since quantum physics in the *Theory of the Crystalline Ether* is precisely the expression of the dynamic fluctuations of gravity on the microscopic scale.

Ultimately, in this approach of the Universe, nothing comes yet to give a definitive explanation to *the existence of the Universe*, to *the deep cause of the big-bang*, and to *the real composition of the crystalline ether*, i.e. of the solid, massive and elastic cosmological lattice. These points remain, at least for the moment, within the scope of individual philosophy or beliefs. But, *from an epistemological point of view*, this approach shows that it is perfectly possible to find a very simple framework to understand, explain and unify the different theories of modern physics, a framework in which there would no longer be many mysterious phenomena other than the *"raison d'être"* of the Universe.

References

[1] G. Ross, Grand Unified Theories. Westview Press, 1984, ISBN 978-0-8053-6968-7.

[2] C. Kiefer, Quantum gravity, International series of monographs on physics (3rd ed.), Oxford University Press, 2012, pp. *1*–4, ISBN 978-0-19-958520-5.

[3] M. Dine, Supersymmetry and String Theory: Beyond the Standard Model, Cambridge University Press, 2007, p. 169, ISBN 978-0-521-[3] 85841-0

[4] K. Becker, M. Becker, J. Schwarz, (2007). String theory and M-theory: A modern introduction. Cambridge University Press, 2007, ISBN 978-0-521-86069-7.

[5] D. Rickles, (2014). A Brief History of String Theory: From Dual Models to M-Theory, Springer, 2014, p. 104, ISBN 978-3-642-45128-7

[6] Alexander Unzicker and Sheilla Jones, «Bankrupting Physics», Palgrave McMillan, New York, 2013, ISBN 978-1-137-27823-4.
Alexander Unzicker, «The Higgs Fake», amazon.co.uk, 2013, ISBN 978-1492176244

[7] Lee Smolin, «The trouble with Physics», Penguin Books 2008, London, ISBN 978-1-137-27823-4.
Lee Smolin, «La révolution inachevée d'Einstein, au-delà du quantique», Dunod 2019, ISBN 978-2-10-079553-6.
Lee Smolin, «Rien ne va plus en physique., L'échec de la théorie des cordes», Dunod 2007, ISBN 978-2-7578-1278-5

[8] Peter Woit, «Not Even Wrong, the failure of String Theory and the continuing challenge to unify the laws of physics», Vintage Books 2007, ISBN 9780099488644

[9] Sabine Hossenfelder, «Lost in Maths», Les Belles Lettres 2019, ISBN978-2-251-44931-9

[10] G. Gremaud, Theory of The Crystalline Ether — Universe and Matter conjectured as a 3-dimensional Lattice with Topological Singularities, Amazon, Charleston (USA), 2025, 662 pages, ISBN 979-8883393982.
G. Gremaud, Théorie de l'Ether Cristallin — Univers et Matière conjecturés comme un Réseau Tridimensionel avec des Singularités Topologiques, Amazon, Charleston (USA), 2025, 642 pages, ISBN 979-8880376872

[11] G. Gremaud, The Crystalline Ether — What if the Universe was a lattice and we were its topological singularities?, Amazon, Charleston (USA), 2025, 318 pages, ISBN 979-8883536273.
G. Gremaud, L'Ether Cristallin — Et si l'Univers était un réseau et que nous en étions des singularités topologiques?, Amazon, Charleston (USA), 2025, ISBN 979-8883513656

[12] G. Gremaud, Théorie eulérienne des milieux déformables — charges de dislocation et désinclinaison dans les solides, Presses polytechniques et universitaires romandes (PPUR), Lausanne (Switzerland), 2013, 751 pages, ISBN 978-2-88074-964-4

[13] G. Gremaud, Eulerian theory of newtonian deformable lattices — dislocation and disclination charges in solids", Amazon, Charleston (USA), 2016, 312 pages, ISBN 978-2-8399-1943-2

[14] G. Gremaud, "On local space-time of loop topological defects in a newtonian lattice", arXiv:1407.1227(2014)

[15] G. Gremaud, "Maxwell's equations as a special case of deformation of a solid lattice in Euler's coordinates", arXiv :1610.00753 (2016)

[16] G. Gremaud, "Universe and Matter conjectured as a 3-dimensional Lattice with Topological Singularities", Journal of Modern Physics, 7, 1389-1399 (2016)

[17] G. Gremaud, "In Search of a Theory of Everything — What if the Universe was an elastic and massive lattice and we were its topological singularities?", Journal of Advances in Physics, 17, 282-285 (2020)

[18] G. Gremaud, "The Crystalline Ether", European Journal of Applied Sciences, Vol.11, No.3 (2023)

[19] J.F. Nye, Acta Metall.,vol. 1, p.153, 1953

[20] K. Kondo, RAAG Memoirs of the unifying study of the basic problems in physics and engeneering science by means of geometry, volume 1. Gakujutsu Bunken Fukyu- Kay, Tokyo, 1952

[21] B.A. Bilby, R. Bullough and E. Smith, «Continous distributions of dislocations: a new application of the methods of non-riemanian geometry», Proc. Roy. Soc. London, Ser. A 231, p. 263–273, 1955

[22] E. Cartan, C.R. Akad. Sci., 174, p. 593, 1922 & C.R. Akad. Sci., 174, p.734, 1922

[23] E. Kröner, «Allgemeine Kontinuumstheorie der Versetzungen und Eigenspannungen», Arch. Rat. Mech. Anal., 4, p. 273-313, 1960

[24] E. Kröner, «Continuum theory of defects», in «physics of defects», ed. by R. Balian et al., Les Houches, Session 35, p. 215–315. North Holland, Amsterdam, 1980.

[25] M. Zorawski, «Théorie mathématique des dislocations», Dunod, Paris, 1967.

[26] J.-P. Hirth, «A Brief History of Dislocation Theory», Metallurgical Transactions A, vol. 16A, p. 2085, 1985

[27] V. Volterra, «L'équilibre des corps élastiques», Ann. Ec. Norm. (3), XXIV, Paris, 1907

[28] E. Orowan, Z. Phys., vol. 89, p. 605,614 et 634, 1934

[29] M. Polanyi, Z. Phys., vol.89, p. 660, 1934

[30] G.I. Taylor, Proc. Roy. Soc. London, vol. A145, p. 362, 1934

[31] J.M. Burgers, Proc. Kon. Ned. Akad. Weten schap., vol.42, p. 293, 378, 1939

[32] P.B. Hirsch, R.W. Horne, M.J. Whelan, Phil. Mag., vol. 1, p. 667, 1956

[33] W. Bollmann, Phys. Rev., vol. 103, p. 1588, 1956

[34] O. Lehmann, «Flussige Kristalle», Engelman, Leibzig, 1904

[35] G. Friedel, Ann. Physique, vol. 18, p. 273, 1922

[36] S.E. Whittaker, «A History of the Theory of Aether and Electricity», Dover reprint, vol. 1, p. 142, 1951.

[37] A. Unzicker, «What can Physics learn from Continuum Mechanics?», arXiv:gr-qc/0011064, 2000

[38] S.J. Brodky, A. Deur, C.D. Roberts, «The Secret to the Strongest Force in the Universe», Scientific American Magazine, Vol.330, No.5, May 2024